Petroleum Systems and Geologic Assessment of Oil and Gas in the San Joaquin Basin Province, California

Chapter 7

The Three-Dimensional Geologic Model Used for the 2003 National Oil and Gas Assessment of the San Joaquin Basin Province, California

By Allegra Hosford Scheirer[1]

Contents

Abstract 1
Introduction 2
Toward a Three-Dimensional Model for Petroleum Assessment 3
  Modeling Tool 3
  Approach 4
  Data Collection and Synthesis 5
  Model Drawbacks 6
Three-Dimensional Geologic Model of the San Joaquin Basin 7
  Basement Composite Surface 7
  Cretaceous Rocks 9
    Forbes Composite Surface/Forbes Unit 10
    Sacramento Composite Surface/Sacramento Unit 10
    Lathrop Composite Surface/Lathrop Unit 10
    Sawtooth Composite Surface/Sawtooth Unit 11
    Tracy Composite Surface/Tracy Unit 11
    Ragged Valley Composite Surface/Ragged Valley Unit 11
    Moreno Composite Surface/Moreno Unit 12
    Summary of Cretaceous Rocks 12
  Paleocene-Eocene Rocks 12
    Domengine Composite Surface/Domengine Unit 12
    Kreyenhagen Composite Surface/Kreyenhagen Unit 13
  Eocene-Oligocene-Miocene Rocks 13
    Temblor Composite Surface/Temblor Unit 13
    Monterey Composite Surface/Monterey Unit 14
  Pliocene and Younger Rocks 14
    Etchegoin Composite Surface/Etchegoin Unit 14
    San Joaquin Composite Surface/San Joaquin Unit 15
    Tulare Composite Surface/Tulare Unit 15
  Summary of Cenozoic Rocks 15
Applications of Three-Dimensional Model 15
  Definition and Visualization of Assessment Units 16
  Resource Potential at Depth 16
  Petroleum System Modeling 16
  Data Archive 16
Conclusions 16
Acknowledgments 17
References Cited 18
Figures 7.1 through 7.23 25

Appendix 7.1—Digital file of the three-dimensional geologic model of the San Joaquin Basin, provided in EarthVision viewing software by Dynamic Graphics, Inc

Appendix 7.2—Database of well picks for formations in the San Joaquin Basin Province, California

Abstract

We present a three-dimensional geologic model of the San Joaquin Basin (SJB) that may be the first compilation of subsurface data spanning the entire basin. The model volume spans 200 × 90 miles, oriented along the basin axis, and extends to ~11 miles depth, for a total of more than 1 million grid nodes. This model supported the 2003 U.S. Geological Survey assessment of future additions to reserves of oil and gas in the SJB. Data sources include well-top picks from more than 3,200 wildcat and production wells, published cross sections, regional seismic grids, and fault maps. The model consists of 15 chronostratigraphic horizons ranging from the Mesozoic crystalline basement to the topographic surface. Many of the model units are hydrocarbon reservoir rocks and three—the Cretaceous Moreno Formation, the Eocene Kreyenhagen Formation, and the Miocene Monterey Formation—are

[1]Now at Department of Geological and Environmental Sciences, Stanford University, *allegras@stanford.edu*.

hydrocarbon source rocks. The White Wolf Fault near the southern end of the basin divides the map volume into 2 separate fault blocks. The construction of a three-dimensional model of the entire SJB encountered many challenges, including complex and inconsistent stratigraphic nomenclature, significant facies changes across and along the basin axis, time-transgressive formation tops, uncertain correlation of outcrops with their subsurface equivalents, and contradictory formation top data. Although some areas of the model are better resolved than others, the model facilitated the 2003 resource assessment in several ways, including forming the basis of a petroleum system model and allowing a precise definition of assessment unit volumes.

Introduction

The San Joaquin Basin is a prolific source of petroleum in the United States—four oil fields each with cumulative production of more than 1 billion barrels and 21 fields each with cumulative production of more than 1 million barrels of oil lie within the basin's borders (CDOGGR, 2003). Accordingly, this basin is one of the most thoroughly explored petroleum-producing provinces in the country, containing greater than 100,000 oil and gas wells and thousands of miles of industry-acquired seismic lines (Curtis Conway, PacSeis, Inc., written commun., 2008). Consequently, abundant data exist, some in the public domain, for mapping the extent and geometry of petroleum source and reservoir rocks within the basin. A team of scientists from the U.S. Geological Survey (USGS) set out to make such maps in support of the 2003 assessment of future additions to reserves of oil and gas in the San Joaquin Basin Province of California (Gautier and others, 2004; San Joaquin Basin Province Assessment Team, this volume, chapter 1).

The abundance of surface and subsurface data in the San Joaquin Basin Province presents challenges because a comprehensive synthesis of this data within a short time period requires an efficient method for data organization and analysis, as well as sophisticated tools for interpretation and visualization. Previous geologic- and petroleum-oriented studies of this basin attempted to solve parts of the subsurface geologic puzzle; these efforts included the preparation of cross sections (for example, Bloch, 1991a), structure contour maps of various stratigraphic horizons (for example, Webb, 1981), paleogeography maps for significant depositional sequences (for example, Reid, 1995), and surface geologic maps (for example, Dibblee, 1968). Such representations are useful for characterizing relationships between rock units and two-dimensional structure in the subsurface, but force the scientific reader to make decisions about the validity of the geology between control points on cross sections, to resolve data inconsistencies or gaps on contour maps, and to imagine changing depositional systems between paleogeographic time-slices. Studies such as these also tend to concentrate on particular geographic areas, stratigraphic horizons, or tectonic events, rather than investigate the basin as a whole.

An additional limitation common to the graphical products mentioned above is that they are essentially flat representations of subsurface geology; cross sections provide a subsurface view within a single two-dimensional plane, whereas structure contour maps lack information about the geometry of the contoured horizon relative to that of the underlying or overlying horizon. Surface geologic maps can be considered as "two-and-a-half" dimensional products, because they display the age, distribution, and structural orientation of geologic units at the Earth's surface, while speculating on the geometry of those components at depth by using stratigraphic relationships and structural orientation symbols. The use of cross sections, structure contour maps, and geologic maps, therefore, provides useful but limited access to the third dimension within a study area.

This chapter describes the database and interpretation methods used to construct a three-dimensional geologic model that formed the backbone of the 2003 National Oil and Gas Assessment of the San Joaquin Basin Province (Gautier and others, 2004). Three-dimensional geologic models differ from the geologic graphical products described above because of the explicit inclusion of the depth dimension—these models retain the fundamental relationships between geologic structures at the Earth's surface evident in surface maps, while extending those relationships into the subsurface. This model of the entire province, the first of its kind within the National Oil and Gas Assessment Project (NOGA) of the U.S. Geological Survey, incorporates 15 chronostratigraphic horizons and one major fault, mapped from abundant subsurface data made available to us from the petroleum industry and from the California Division of Oil, Gas, and Geothermal Resources.

The three-dimensional model of the San Joaquin Basin Province facilitated the 2003 resource assessment in several ways. First, the model required a compilation of comprehensive rock unit information from exploratory well data; this allowed determination of the frequency that strata were penetrated (Hosford Scheirer and Magoon, this volume, chapter 5) and provided control on strata thickness, distribution, and geometry basin wide. Second, the model utilized regional grids of industry seismic data for five key rock units in the basin, allowing a province-wide, digital representation of those units for the first time. This representation was used as input for a petroleum system model. Third, the model provided a visual means for the assessment team to evaluate statistical quantities such as drilling density, petroleum accumulation size and distribution, reservoir depth, and so on, within assessment units. The three-dimensional model also provided a volumetric treatment of assessment units for the first time; for example, double assessment of stacked assessment units could be rigorously avoided by investigating the model visually and querying it numerically. Finally, the model provided valuable graphic representation of regional geologic information for publications related to the 2003 assessment (for example, Gautier and Hosford Scheirer, this volume, chapter 13, chapter 14, and chapter 19; Hosford Scheirer and Magoon, this volume, chapter 21 and chapter 22).

It is important to note that this chapter documents the specific model realization used for the 2003 resource assessment. NOGA requires that assessment products be "frozen" in time, so that statistical determinations of future additions to reserves in the studied province are thoroughly documented and repeatable.

Toward a Three-Dimensional Model for Petroleum Assessment

To characterize and visualize subsurface geology in a given study area, the USGS recently began building three-dimensional geologic models of several regions and features in California, including the Santa Clara Valley (Jachens and others, 2005), the Hayward Fault Zone (Graymer and others, 2005; Phelps and others, 2008), the Santa Rosa Plain (McCabe and others, 2004), and the Quaternary sequence in the Dominguez Gap region of Long Beach (Ponti and others, 2007). These products typically use as their starting point surface geologic maps (for example, Phelps and others, 2009), and may incorporate features modeled from gravity and magnetic inversions and seismic tomography, as well as use conventional depth information such as that available from water, oil, and gas wells.

In contrast, the three-dimensional geologic model of the San Joaquin Basin Province described in this chapter supported the USGS 2003 assessment of future additions to reserves of oil and gas in the basin (Gautier and others, 2004; San Joaquin Basin Province Assessment Team, this volume, chapter 1). As such, this model differs from others produced by the USGS in that it relies almost exclusively on digital depth data from wells and seismic experiments. In this way, the model incorporates key petroleum source and reservoir rocks throughout the basin but ignores complex structural elements such as decollement surfaces and thrust faults. We also omitted surface geology and structural information implied by surface geometry on the complex western edge of the basin because of a lack of time.

This model, built in 2003, is more closely related to other modeling efforts in the San Joaquin Basin in which three-dimensional models were constructed to investigate questions related to petroleum exploration. A very early such example is that of Grender and others (1974), who describe a quantitative model of subsurface structure, lithology, and oil occurrence within a 1,000 square mile × 25,000 foot volume centered on Bakersfield, California. This model served as a quantitative tool that allowed management personnel to visualize and analyze both existing and prospective petroleum deposits—much as our effort attempted to do 30 years later. A much more recent treatment in a region of similar size and location is documented by Wagoner (2009); this three-dimensional model incorporated 15 stratigraphic horizons and numerous faults and may eventually be used to simulate the fate of injected carbon dioxide in the vicinity of a power plant. Still other treatments of subsurface geology in the San Joaquin Basin consider much smaller areas. Typically such models contain millions of computational nodes to represent the geology within specific exploration targets (for example, Ponek and others, 2000; Harness and Tran, 2004).

The model presented in this chapter may be the first, digital compilation of subsurface geologic data spanning the entire San Joaquin Basin Province. The external border of the model corresponds to the official province boundary defined by the USGS Energy Resources Program in previous assessments (for example, Beyer and Bartow, 1987; Gautier and others, 1996). Generally, the boundary follows the contact of basement rocks with alluvium at the foothills of the Tehachapi-San Emigdio Mountains in the south, the surface trace of the San Andreas Fault and outcrops of Franciscan Complex rocks in the Diablo Range in the west, the Stanislaus county line in the north, and the alluvium-basement contact in the Sierra Nevada foothills in the east (heavy black line, fig. 7.1).

Modeling Tool

In contrast to the preparation of a surface geologic map, the preparation of a three-dimensional geologic model is fundamentally a digital, but interpretive, process. The spatial relationships of all geologic elements in the model must be determined by synthesizing subsurface data quantitatively, instead of determined in the field at well-exposed outcrops. This numerical synthesis requires the modeler to establish, in advance or iteratively during model development, a set of rules that govern the relationships between geologic elements. These rules may include, for example, whether the contacts between strata are conformable or unconformable and whether faults offset strata in a reverse or normal sense.

The three-dimensional model of the San Joaquin Basin Province was constructed with EarthVision®, a software package by Dynamic Graphics, Inc.®, that allows the integration of different types of data and the display of that data in an interactive, three-dimensional environment. Conceptually, EarthVision® partitions the model volume into smaller, fault-bounded volumes (called fault blocks). Each fault block is assigned to one or more geologic units. Relationships between strata are calculated within each fault block alone and then assembled into the full model volume.

The technical aspects of modeling using EarthVision® consist of a well-defined sequence of three main operations. First, point data of discrete locations in space are compiled for all geologic elements (strata and faults). These points are then interpolated to a two-dimensional or three-dimensional regular grid, which represents a surface, with a horizontal range that spans the rectangular model area. Next, the grids (surfaces) that represent faults are assigned an order of precedence, to determine which surface should be truncated when two surfaces cross. Similarly, the grids (surfaces) that represent the tops of geologic units or unconformities are assigned rules that determine whether the surface adds material to the top

of surfaces below (geologic unit top) or whether the surface subtracts material from the top of surfaces below (unconformity). Finally, all elements are assembled into the model volume according to the defined rules. The model is then inspected quantitatively and visually, and iteratively refined to test differing scenarios (geologic rules) or to incorporate additional data. The 2003 realization of this modeling workflow is provided digitally in appendix 7.1 in the EarthVision® three-dimensional viewer.

One aspect of this modeling process that contrasts with the preparation of surface geologic maps is that computer-prepared, three-dimensional models require all space in the study area to be filled with geologic elements. Regions of uncertainty due to absence of data or structural complexity must be resolved, either by the modeler or automatically by the computer, to produce the final model. Traditional geologic maps, of course, allow the mapper to indicate less well-known areas with dotted or queried contacts; the scientist can visit these regions again during subsequent field sessions to improve the map. Similar indications of uncertainty in three-dimensional models are difficult to make with currently available technology. The stricter convention that all space must be filled in a three-dimensional model forces the scientist to make decisions about layer or fault geometries in regions of the model that are sparsely-populated by data. One advantage of this strict requirement is that the modeler can test competing scenarios for resolving uncertain regions of the model, which is readily accomplished with fast computers. One disadvantage is that less-certain regions of the three-dimensional model appear as well understood in the final model as regions that are much better resolved by data.

Approach

The preparation of a three-dimensional geologic model requires the identification of the critical geologic elements (faults and tops of geologic units) that are included in the model volume. Because the primary purpose of this model is to support the USGS 2003 assessment of future additions to petroleum reserves in the San Joaquin Basin, we paid particular attention to the essential elements of the petroleum system (after Magoon and Dow, 1994), that is, the source, reservoir, seal, and overburden rocks in the basin. To consistently model these rock units throughout the San Joaquin Basin, stratigraphic correlation charts were developed for the southern, central, and northern sections of the basin (fig. 7.2; for more, see Hosford Scheirer and Magoon, this volume, chapter 5).

The creation of an integrated stratigraphic framework for the entire basin is problematic in a depositional and structural setting as complex as the San Joaquin Basin but needs to be done to create a three-dimensional model. Perhaps most challenging is correlating key rock units possessing pronounced facies variations across the basin; in some locations the variations occur over short distances, whereas at other places the variations are gradual—the result of multiple and shifting depocenters. Rocks mapped as Temblor Formation, for example, include nonmarine, shallow-marine, and deep-marine deposits (Graham, 1985). Similarly, the top of the Monterey Formation is locally siliceous shale, clay, porcelanite, diatomite, and diatomaceous shale or chert (Graham and Williams, 1985).

Additional complexity arises from the basin's long tectonic history; tectonic regimes range from convergent margin-forearc environment to transform-margin environment, resulting in varying emergent and subsiding terranes. Different tectonic and sedimentary environments bordering the western and eastern margins of the basin also affected basin inputs—whereas the eastern basin experienced relatively "quiet" conditions characterized by relatively simple marine shelf-slope geometry, the western margin was greatly affected by changes in slab subduction angle, transition to transform tectonics, episodes of deformation and nondeposition, and rapid changes in water depth (for example, Graham and others, 1984; Bartow, 1991).

Inconsistent nomenclature for stratigraphic units further complicates the data synthesis process. Typically, terms applied to both surface and subsurface rock units consist of a combination of formal names used by the USGS and academia and informal names used by the petroleum industry. Indeed, in our well database of (stratigraphic) tops of units (provided in appendix 7.2), nearly 600 unique geologic names are used to refer to more than 13,000 well picks. Nomenclatural issues also arise because of pronounced facies variations within a given package of strata and from a mixture of biostratigraphic and lithostratigraphic classification (Graham, 1985).

Finally, in addition to addressing the dramatic facies variations, structural complexities, and inconsistent nomenclature, there is the requirement that the top of each rock unit be the same age (where possible) within the three-dimensional geologic model. That is, the spatial representation of each rock unit is a series of x,y,z coordinates—longitude, latitude, and depth—such that each z value represents the same age. Comprehensive treatments of stratigraphic sequences within the valley (Callaway, 1990; Bloch, 1991b; Hosford Scheirer and Magoon, this volume, chapter 5; Johnson and Graham, this volume, chapter 6) as well as more focused studies of specific units (Bent, 1985; Graham and Williams, 1985) guided the identification and combination of time-equivalent rocks, so that, for example, depositionally coeval submarine and shelfal sands, and basinal, slope, and shelfal shales were combined into a single unit bearing the name of the major upper member (fig. 7.2*B*). This methodology insures, in theory, that mapped layers stay within stratigraphic sequence boundaries and can be properly depicted in the three-dimensional model.

For example, to establish the 5.5 Ma surface, we combined an industry-supplied seismic grid with well picks for the tops of the Monterey Formation, its Reef Ridge Shale Member, and the top of the Miocene. Generally the top of these units dates to 5.5 Ma (Hosford Scheirer and Magoon, this volume, chapter 5). This surface is referred to as the Monterey Composite Surface (hereafter referred to as Monterey CS), and the Monterey Unit extends from the Monterey CS to the

underlying composite surface. The decision to explicitly retain certain rock unit names in the model, rather than renaming each unit by time interval (such as late Miocene in this example), explicitly grounds the model in petroleum source and reservoir rock terminology for ease of use by the petroleum geologist or geophysicist.

Data Collection and Synthesis

In 2002 and 2003, the modeling effort centered on mining multiple sources of existing data held by both the public and private sectors. Because we relied solely on the collection of existing data rather than on the acquisition of new data, we focused substantial effort on data collection and synthesis.

Depth data of two primary types form the backbone of the three-dimensional geologic model of the San Joaquin Basin Province—well top picks and seismic grids. We combed the literature to compile a database of depth picks for the horizons of interest. More than 95 percent of the depth picks in the final database derive from well picks available in the annual reports of the California Division of Oil, Gas, and Geothermal Resources and in a compilation of drilled wells (CDOG, 1982). However, these publications exist primarily in paper or nonsearchable Portable Document Format (PDF) format rather than as an electronic database. Thus, we made these data electronic through a combination of electronic optical character recognition and manual entry. The final database includes 100 percent of the records for prospect wells from the years 1966 to 1999, as well as selected additional wells from all of the counties that lie entirely or partly within the province boundary. Because only one major fault is included in the 2003-vintage model presented in this chapter, picks in wells that list repeated strata (indicating thrust faulting) were excluded below the first occurrence of the repeated section. In contrast, wells that may have crossed normal faults, inferred by missing formation picks, were entered into the database as presented. We also excluded wells with nonvertical well paths, which preclude the reconstruction of true depth to formation tops, because we lacked well trajectories.

Additional well-top data supplemented the records from the California Division of Oil, Gas, and Geothermal Resources. These data were obtained from studies by Applied Earth Technology, Inc. (1990) for early Paleocene and older rocks in the northern San Joaquin Basin; by Reid (1988) for Eocene and older rocks on the basin's east side; and by both Imperato (1995) and Johnson and Graham (this volume, chapter 6) for Tertiary rocks in the central and southern San Joaquin Basin. The entire well-top database, excluding records obtained through proprietary agreement (such as those from Applied Earth Technology, 1990), is presented in appendix 7.2. A location map of all wells in the database is shown in figure 7.3.

Initial three-dimensional modeling of strata in the San Joaquin Basin using well-top data alone showed that subsurface geology was well represented throughout most of the basin, except in the region of extensive folding on the basin's west side ("west side fold belt"). To better map important petroleum-bearing anticlines within the west side fold belt, we incorporated into the model seismic interpretations of several stratigraphic horizons. Rather than obtaining raw seismic travel time data, these data from industry came as processed seismic-depth grids. The processing scheme used by our industry contact included identifying formation tops on seismic lines, using picks in 10 deep wells as guides; creating grids in units of seismic travel time for each horizon; constructing regional velocity grids using check-shot surveys and sonic logs; and multiplying the time grids by the velocity grids to obtain structural depth grids. Original seismic-line spacing averaged 1 mile in the east-west direction and 3 miles north-south, with some dip-oriented lines on the west side for additional control. We received grids of five horizons at about 0.5-mile (0.8 kilometer, km) grid spacing. These were for the basement surface, and the Kreyenhagen, Temblor, Monterey, and Etchegoin Formations.

The topographic surface truncates all subsurface geologic horizons in the three-dimensional geologic model. This surface derives from a 1-km resolution, GTOPO30 topography grid (U.S. Geological Survey, 2012).

One fault is incorporated into the three-dimensional geologic model of the San Joaquin Basin, the White Wolf Fault. Located near the southeastern portion of the province boundary (fig. 7.1), the fault isolates a small block called the Tejon embayment, which has a unique tectonic and depositional history compared to the rest of the San Joaquin Basin (Goodman and Malin, 1992). Numerous studies document a complicated evolution for the White Wolf Fault, with conflicting conclusions regarding the fault's geometry and sense of motion through time (Davis and Lagoe, 1988; Bartow, 1991; Goodman and Malin, 1992). The resolution of such complexity is beyond the scope of this modeling effort, especially because the three-dimensional model of the San Joaquin Basin represents only the present-day geology of the basin.

The fault structure map of Goodman and Malin (1992) for the Southern San Joaquin Basin shows the White Wolf Fault as composed of three segments—a western and central segment, which are buried but whose projected surface traces appear essentially colinear, and an exposed eastern segment that is parallel to the other segments but displaced several kilometers to the south. A digital representation of the White Wolf Fault has been used in at least two previous studies. Stein and Thatcher (1981) studied seismic and aseismic deformation associated with the 1952 M_w 7.3 Arvin-Tehachapi earthquake by modeling the fault as three 25-km long segments, each with unique fault slip, dip, orientation, and elevation. In contrast, Bawden (2001) investigated the faulting geometry and slip history during the earthquake by inverting coseismic triangulation and geodetic observations. Satisfactory model fit was achieved with two uniformly dipping fault segments. For the sake of simplicity, this 2003-vintage model uses the fault parameters of Bawden (2001) to model the White Wolf Fault in three dimensions: two fault segments that each strike 51° and dip 75° to the southeast.

Model Drawbacks

A single three-dimensional geologic model is unable to encapsulate every known facet of the geometry within a volume, nor can the model capture geologic detail across a broad range of spatial scales. Accordingly, before discussing the specifics of the three-dimensional geologic model of the San Joaquin Basin, it is important to recognize its limitations.

Arguably the single most important modeling decision in any such undertaking, at least initially, is the identification of the model's physical boundaries. A model should be spatially large enough to capture the region of interest but small enough to optimize computer calculation speeds. Typically, a rectangular grid defines the model domain. Because this particular modeling effort supported a USGS assessment of petroleum resources, the model domain was prescribed to be the San Joaquin Basin Province outline from previous assessments (fig. 7.1), which was determined on the basis of surface geology (fig. 7.1; Beyer and Bartow, 1987; Beyer, 1996). This boundary, however, incorporates regions of limited relevance for a subsurface resource assessment. For example, Cretaceous outcrops (and the volume of rock below them in the subsurface) in the northwest part of the province (green polygons, fig. 7.1) are unprospective for petroleum source or reservoir rocks, but we were required by the preexisting province boundary to include them in the model.

A second weakness of the model is the requirement that coeval strata be merged into a single, time-equivalent rock unit. The stratigraphic compilation of the San Joaquin Basin by Hosford Scheirer and Magoon (this volume, chapter 5), shown in figure 7.2, postdated the combination of coeval strata into the composite surfaces and units described above. We now recognize inconsistencies in how several composite surfaces in the three-dimensional geologic model were defined. For example, the tops of several of the most important units are time transgressive; the top of the Temblor Formation is two million years younger in the central part of the basin than in the southern region (fig. 7.2). Similarly, the top of the Kreyenhagen Formation has been eroded in the northern part of the basin, but is conformably overlain by the Tumey formation of Atwill (1935) in the central part. In other instances, we inadvertently included multiple depositional sequences into one composite surface (CS). For example, the Moreno CS in this model includes picks for the "top Cretaceous" and for the Cima Sandstone Lentil, both deposited at about 65 Ma (Callaway, 1990), but the top of the Moreno Formation extends into the Paleocene (61 Ma). In this case, however, those erroneously included well picks represent a small percentage of the total amount of data available for the top of the Moreno Formation, and are located among densely spaced data. Thus, they contribute very little to the numerical surface calculated to represent the Moreno CS. Finally, combining multiple formation tops into a single time-equivalent surface results, in some cases, in an amalgamation of multiple units spanning a time of deposition greater than that implied by the explicit model unit name. For example, the Temblor Unit extends to the base of the Tumey formation of Atwill (1935) (fig. 7.2*B*), or to late Eocene, whereas the base of the Temblor Formation itself dates to early Miocene or possibly Oligocene times.

The scale of the three-dimensional model may also limit its applicability. The internal architecture of individual sand bodies, such as the Stevens sand of Eckis (1940) within the Monterey Formation and the Point of Rocks Sandstone Member of the Kreyenhagen Formation, fail to appear as distinct layers in the model. Instead, the model portrays just the upper surfaces of the Monterey and Kreyenhagen Formations (fig. 7.2*B*) (or more accurately, their composite surfaces), although the depth and structure of those particular sand bodies are incorporated into the petroleum system model of the San Joaquin Basin by Peters, Magoon, Lampe, and others (this volume, chapter 12). Similarly, although facies variations at a given geologic time are combined into a single layer in the model, and thus essentially eliminated from the 2003-vintage geologic model, those variations do appear explicitly in the petroleum system model through a series of two-dimensional grids.

Small-offset faults are absent in the 2003-realization of the three-dimensional model of the San Joaquin Basin. These would be essential in a geologic framework model for unraveling the history of folding and deformation in the basin's subsurface, but are less essential for a petroleum system model of the basin. In part, the regional scale of the model explains this notable absence; many of the faults that help trap petroleum at individual oil and gas fields would appear quite small at the resolution of this model. The absence of faults in the stable northern part and the eastern margin of the province, both of which lack notable fault structures (Bartow, 1991), is not too problematic for the purposes of oil and gas resource assessment. In the southern part of the basin, north of the White Wolf Fault and south of the Bakersfield Arch, a case could be made for the inclusion of the Greeley Fault system, but maximum offset is only about 600 m at the basement surface, decreasing to zero at the level of late Miocene-aged strata (Bartow, 1991). Similarly, there are major structural lineaments near the northwestern boundary of the San Joaquin Basin Province such as the Tesla-Ortigalita Fault and the San Joaquin Fault zone (Raymond, 1973), but neither plays a role in the trapping of petroleum nor are they well understood. It is the deformed west side fold belt on the basin's southwest margin that perhaps suffers most from the conspicuous absence of faults in the 2003-vintage three-dimensional model. However, the incorporation of numerous faults on the basin's west side would have required numerous man hours for correlating fault picks in well, seismic, and surface data. Such an effort was not possible within the scope of the 2003 resource assessment.

A problem common to any quantitative analysis that uses numerous sources of data is inconsistency. Because seismic data and well logs sample rock volumes at inherently different scales of resolution (for example, Liu and others, 2004), depth values obtained from seismic grids at the locations of drilled wells typically disagree with depths identified on the logs from those wells. Further, seismic depth

grids are derivative products dependent on a complicated workflow; reconciliation of the two types of data is difficult in this case because of varying sources of seismic and well data. To adequately integrate formation depths derived from both well logs and seismic data into the 2003-vintage three-dimensional geologic model of the San Joaquin Basin, we performed a series of calculations to examine the differences between gridded maps based on each type of data alone. We calculated the difference between regional seismic grids and well picks, producing a sparsely sampled point data set of difference values. We then interpolated these values using default gridding routines in EarthVision® software to produce a grid of the estimated difference. We then corrected the seismic grid using the difference grid.

Finally, the model presented in this chapter is not a "geologic framework model," such as those prepared by other USGS authors and others for the Edwards aquifer (Pantea and others, 2008), California's Central Valley (Faunt and others, 2009), and the Arbuckle-Simpson Aquifer (Faith and others, 2010). Rather, it is a model whose purpose in 2003 was to define volumes of rock that could be quantitatively assessed for oil and gas resources. Although the inclusion of surface geologic maps in the three-dimensional model may have expanded its applicability in the wider geology community, as well as aided in unraveling geology on the San Joaquin Basin's structurally complex west side, such an effort was not possible due to limited time. Moreover, petroleum is chiefly trapped in the subsurface; surface seeps contribute volumetrically insignificant sums to the total petroleum resource in a province. Our efforts thus were focused on obtaining high-quality, province-wide subsurface data for petroleum source and reservoir rocks rather than on incorporating surface geology into the model. Workers wishing to incorporate surficial geology into a model of the San Joaquin Basin should consult regional-scale geologic maps by Graham and others (1999), Wagner and others (2002), and Wentworth and others (1999).

Because we did not use surface geologic data in this iteration of the model of the San Joaquin Basin, the geometry of model layers in the subsurface is highly inaccurate on the basin's west side. To indicate this graphically, we define the "area of correspondence" in the model as that region where subsurface and surface geology correspond (east of heavy gray line in figure 7.1) and the "area of unresolved complexity" that region where model geometry is known to conflict with subsurface and surface geology (west of heavy gray line in figure 7.1). Similarly, we use blue polygons on figures of model output for Cretaceous-aged units to indicate the region of confidence for each layer.

The three-dimensional geologic model presented here is the one used for the 2003 National Oil and Gas Assessment project (Gautier and others, 2004). Revisions of the model cannot be considered in this paper, as assessment results are predicated in part on this particular choice of input data and modeling parameters. Despite the limitations described above, the construction of a fully three-dimensional, self-consistent geologic model that could be queried as a rock volume before, during, and after the assessment process proved valuable to all the geologists involved.

Three-Dimensional Geologic Model of the San Joaquin Basin

The fundamental architecture of the three-dimensional geologic model of the San Joaquin Basin Province consists of 15 geologic units and two fault blocks separated by the White Wolf Fault. Figure 7.2*B* shows these 15 units (by name and color) by recasting the stratigraphic columns for the southern, central, and northern San Joaquin Basin, shown in figure 7.2*A*, into the corresponding composite surface in the three-dimensional geologic model. The model itself measures ~200 miles long at its longest point along the basin axis and ~90 miles at its widest point across axis. Table 7.1 provides additional quantitative information about the model, and figure 7.2*C* summarizes key geographic features in the model.

The three-dimensional model is calculated in a rectangular space oriented 30° west of north, aligned with the trend of the province (fig. 7.3). Because valid data in the model exist only within the province boundary itself, all three-dimensional views of the geologic model appear cut by the province boundary polygon. We use feet for units of length throughout this work because the English system is widely used by the energy industry in California. All spatial positions use California State Plane Zone 3 coordinates. Input data for each model surface were gridded by EarthVision® at either 0.5 mile or 1 mile spacing (table 7.1); model features larger than these values that lie within the area of correspondence are reliable.

Basement Composite Surface

The basement unit is the oldest and deepest modeled layer in the three-dimensional geologic model of the San Joaquin Basin. Although the inclusion of a deep basement unit may appear at odds with the goal of assessing undiscovered petroleum resources within much younger and shallower units, accurate modeling of basement rocks beneath the San Joaquin Basin is essential for this effort for several reasons. First, the basement unit essentially acts as a boundary condition at depth: it is the foundation on which younger rocks are deposited, it is the deepest unit for which well data exists, and it is the deepest unit represented in the model. All younger rocks must overlie basement unless fault or fold relationships indicate otherwise. Second, one of the units that forms the basement unit, fractured schist, acts as both a petroleum reservoir and seal in the Edison and Mountain View fields (White, 1955; and Park, 1966, respectively) on the east side of the basin (see fig. 7.4 for location of fields labeled "E" and "MV"). Thus, future additions to reserves could be from a reservoir rock within basement rocks on the basin's east side.

Table 7.1. Top age, number of control points, and grid dimension for the composite surface for each unit in the three-dimensional digital model of the San Joaquin Basin Province.

Composite Surface (CS)[1]	Age (Ma)[2]	Number of data points defining top of layer[3]	Grid spacing (mile)
15 Tulare CS	0	87,721	0.5 × 0.5
14 San Joaquin CS	2.5	7,061	1 × 1
13 Etchegoin CS	4.5	32,683	0.5 × 0.5
12 Monterey CS	5.5	36,997	0.5 × 0.5
11 Temblor CS	14/16	31,122	0.5 × 0.5
10 Kreyenhagen CS	37	27,536	0.5 × 0.5
9 Domengine CS	48.5	642	1 × 1
8 Moreno CS	61	410	1 × 1
7 Ragged Valley CS	71.5	264	1 × 1
6 Tracy CS	72	142	1 × 1
5 Sawtooth CS	73	194	1 × 1
4 Lathrop CS	73.5	169	1 × 1
3 Sacramento CS	77	52	1 × 1
2 Forbes CS	78	46	1 × 1
1 Basement CS	120/160	27,667	0.5 × 0.5

[1]Numbers refer to the rock units in figure 7.2*B*.

[2]See Hosford Scheirer and Magoon (this volume, chapter 5) for more information.

[3]Values greater than 1,000 indicate that both seismic data and well picks are used to model the surface, whereas values less than 1,000 indicate that only well picks are used. Reported number of observations lie solely within the San Joaquin Basin Province, although well picks north of the province boundary may have been used to characterize the surface.

Rocks commonly termed "basement" in the San Joaquin Basin include at least three units that are in unconformable, conformable, or fault contact with the Upper Jurassic to Paleocene Great Valley Sequence—Sierran Nevadan batholithic rocks, Coast Range ophiolite, and Franciscan Complex, respectively (Bartow, 1983). The entire eastern and probably much of the central San Joaquin Basin is underlain by Sierran metamorphic and plutonic rocks (Chen and Moore, 1982). In contrast, the western margin of the San Joaquin Basin is underlain by Coast Range ophiolite, except where rocks of the Franciscan Complex and fragments of ophiolite underlie Great Valley Sequence in the Diablo Range and elsewhere (Bartow, 1983). The relative geometries of all three types of basement rocks, particularly on the western margin of the San Joaquin Basin, is a topic of longstanding study (Wentworth and others, 1984; Jachens and others, 1995; Dickinson, 2002) and is beyond the scope of this investigation.

The most complete compilation of elevation data for the basement unconformity in the San Joaquin Basin, the database of Wentworth and others (1995), incorporates drillhole data and seismic interpretations of all three types of basement rock; they subsequently interpolated the elevation values to a 2-km regular grid. Where well penetrations of the basement unconformity are absent in the central basin, we used the results of previous magnetic modeling (Jachens and others, 1995), which suggests that the top of magnetic basement beneath the San Joaquin Basin lies at depths of 15 to 20 km (specifically, see profile GJ in their figure 4). Finally, we supplemented well penetrations and magnetic-inversion derived basement depths with industry seismic estimations of

basement depth (stippling in figure 7.5*B*) to achieve the final basement surface (figs. 7.5*A*, *C*).

We did not incorporate into the model of the composite basement surface known outcrops of Franciscan Complex or Coast Range ophiolite on the basin's west side. Thus, basement geometries in the area of unresolved complexity must be more intricate than depicted here.

Features on the Basement CS approximately fall into four general corridors (white labels and dashed lines, fig. 7.5*C*). The easternmost margin of the basement surface—east of the northern gas fields and central oil fields—forms a near-flat featureless plain. Depths average about 5,000 feet below sea level. The central corridor, by contrast, is marked by several basement highs and lows—essentially ridges and intervening valleys (figure 7.5*A*) on the order of 1,000 feet of relief. These ridges, at least 3 of them, are spaced several miles apart, are well resolved by this model, and were previously noted by Reid (1988) from well data alone. Speculation on the cause of these relatively low-amplitude basement features is beyond the scope of this paper; however, these features are absent in overlying Cretaceous, Paleogene, and Neogene units, possibly indicating that basement deformation predated Cretaceous times. Reid (1988) suggests that these eastern basement valleys may record erosion from ancestral streams draining the Sierra Nevada.

The southern corridor in the Basement CS features the Bakersfield Arch, a broad dome that trends east-west near the south end of the basin (Bartow, 1991), and the Maricopa deep, a depocenter filled with about 10 kilometers of Cenozoic strata (Bartow, 1991) (fig. 7.5*A*). The trace of the White Wolf Fault is also visible in the basement surface in figure 7.5*A*. The fourth basement corridor lies within the area of unresolved complexity, which in this 2003-vintage model is largely schematic and should not be interpreted geologically.

Cretaceous Rocks

Although much is known about Jurassic and Early Cretaceous rocks of the Great Valley Sequence in outcrop on the western margin of the San Joaquin Basin (Dibblee, 1981; Bartow and Nilsen, 1990), far less is known about those same units in the adjacent subsurface (Ingersoll, 1978; Cherven, 1983). Comprehensive treatments of Late Cretaceous units in the San Joaquin Basin focus mainly on outcrop stratigraphy and sequence stratigraphic architecture (Callaway, 1964; Bishop, 1970; Cherven, 1981; McGuire, 1988a; Reid, 1988; Nilsen and Moore, 1997) and faunal assemblages and classification (Goudkoff, 1945; Almgren, 1986). In general, Late Cretaceous rocks in the San Joaquin Basin—and indeed, in all of the Great Valley—record a regressive sequence of submarine fan, slope, and shelf deposits whose provenance is the Sierra Nevada to the east. These units generally form a westward-thickening wedge of strata that lap onto the Sierran basement surface, where they pinch out. Because the northern San Joaquin Basin is relatively free of folds and faults (Hoffman, 1964; Bartow, 1991), the environment of deposition for all of the Cretaceous units appears to have been stable over long periods of time with only minor disruptions by tectonic deformation.

Initial attempts at incorporating Cretaceous-aged units into the three-dimensional model of the basin used just the Moreno and Panoche Formations. This was problematic, however, because these names refer more accurately to outcrop units rather than to units in the subsurface (see Hosford Scheirer and Magoon, this volume, chapter 5, for more on this topic), and direct correlation of outcrop sections (both on the western and eastern margins of the basin) to the deep subsurface remains difficult due to inadequate well control, pronounced facies variations, and diachroneity (Bishop, 1970). Further, the inclusion of just two Cretaceous units oversimplified the stratigraphy in the northern part of the San Joaquin Basin, where the bulk of the strata is Cretaceous in age.

To satisfactorily incorporate units of Late Cretaceous age into the model, we therefore adopted a stratigraphic section comprised of seven layers (fig. 7.2*B*); these are the units that appear most frequently in publicly available well records and are summarized by Nilsen and Moore (1990; fig. 7.6). The units were modeled using a proprietary database provided by Applied Earth Technology (1990). This approach provided enough detail to assess undiscovered resources in the gas-rich northern San Joaquin Basin (Hosford Scheirer and Magoon, this volume, chapter 21), and allowed for an analysis of the effect of Cretaceous strata on the overlying Tertiary section.

Compared to the wealth of information available for the northern San Joaquin Basin, much less data exists for Cretaceous-aged rocks south of about Coalinga oil field ("C," fig. 7.4). In part this situation results from the absence of Cretaceous outcrops in the Temblor Range on the basin's west side (Bartow, 1991). Perhaps more fundamentally, relatively little is known about Cretaceous-aged rocks within the southern two-thirds of the basin because of increasingly greater burial depths from north to south; at San Joaquin Northwest field ("SNJW," fig. 7.4), the southernmost gas field in the northern San Joaquin Basin, the top of Cretaceous strata is more than 8,000 feet deep whereas at Elk Hills field ("EH," fig. 7.4) Cretaceous rocks are more than 20,000 feet deep. Furthermore, in contrast to the alternating sand and shale layers that characterize Cretaceous strata in the northern part of the basin (for example, fig. 7.6), the Cretaceous section appears to be undifferentiated on well logs from the central and southern portions of the San Joaquin Basin (Reid, 1988), so Cretaceous-aged rocks south of about Coalinga field are poorly subdivided.

The Cretaceous section south of Coalinga field was constructed in two ways. In the area of unresolved complexity, Cretaceous layers in the model were smoothly interpolated southward, which we know to be largely incorrect on the basis of surface geologic maps. In the area of correspondence, we extended the seven Cretaceous units southward by adding control points at known oil fields where data is lacking. To emphasize where surfaces in the model are best controlled by data, we indicate coverage polygons on the *B*, *C*, and *D* panels of figures 7.7 to 7.12.

Forbes Composite Surface/Forbes Unit

The next-oldest unit in the three-dimensional model is the Forbes Unit, which is defined by the Forbes Composite Surface (top) and named to indicate that its upper constituent is the Forbes formation of Kirby (1943; hereafter referred to as Forbes formation). The Forbes formation is generally the deepest and oldest rock layer identified in wells in the northern San Joaquin Basin, and is thus the first stratigraphic surface above basement for which sufficient data existed. However, the unit as we have defined it incorporates older, deeper units such as the G-zone Dobbins shale of Hoffman (1964) and even older Cretaceous and Late Jurassic rocks of the Great Valley Sequence at its base (fig. 7.7); these include, in descending order, the Guinda, Funks, Sites, Yolo, Venado, and Fiske Creek Formations (Kirby, 1943; Almgren, 1986). These units were not explicitly incorporated into the three-dimensional model, both because of a lack of well data and because they were not relevant for the assessment of undiscovered petroleum resources.

The Forbes formation itself is a mud-rich basin-plain, deep-sea-fan, and slope turbidite (Imperato and others, 1990) probably derived from the Cordilleran arc system to the north and northeast and perhaps from the Idaho Batholith region (Mertz, 1990). Its deposition in the northern San Joaquin Basin (and in outcrop in the Diablo Range to the west) marks the southernmost extent of this southward-prograding deposit.

The Forbes CS is about 78 m.y. old (Hosford Scheirer and Magoon, this volume, chapter 5) and is comprised of well picks labeled Forbes formation as well as those called "F-zone" (referring to the benthic foraminiferal zone of Goudkoff, 1945). Well picks are limited to the northern part of the San Joaquin Basin (fig. 7.7*B*); thus, the layer is smoothly continued along the west side of the basin (fig. 7.7*A*, *C*) to serve as a base for better-determined, overlying layers. We know that this simple projection is incorrect on the westernmost part of the model because units of this age crop out on the valley's west side (green shading, fig. 7.1). However, as mentioned above, Cretaceous-aged outcrops on the western margin are variously labeled in surface geologic maps as Moreno or Panoche Formations (for example, Dibblee, 1981) or as "undivided Cretaceous sandstone, shale, and conglomerate," (for example, Jennings and others, 1977), making correlation with subsurface Cretaceous units difficult.

Where determined by well picks, the Forbes CS ranges between about 5,750 and 13,125 feet deep, with median and average values of about 8,500 and 9,200 feet deep, respectively (well values within blue polygon, fig. 7.7*C*). Approaching the eastern margin of the northern San Joaquin Basin, where the unit pinches out against Sierran basement rock, the Forbes Unit is less than 1,000 feet thick; approaching its outcrop in the Diablo Range on the western margin, the unit thickens substantially to perhaps as much as 15,000 feet thick (fig. 7.7*D*). This large value is reasonable: Imperato (1990) documents a maximum thickness for the Forbes formation of about 8,000 feet, and, as mentioned above, our model of the Forbes Unit incorporates not only Forbes formation but also undifferentiated, older Cretaceous and Jurassic units between the Forbes CS and the basement surface, which easily can sum to many thousands of feet of section (Moxon, 1990). Neither elevation nor thickness trends illustrate a well-developed basin axis at this level in the geologic model, perhaps because a coeval unit, the Marsh Creek Formation, prograded to the west and southwest, blanketing the basin axis as it propagated in a transverse direction (Moore, 1991). Alternatively, the basin axis may have been situated farther west during deposition of the Forbes formation.

Sacramento Composite Surface/Sacramento Unit

The Sacramento Composite Surface defines the top of the Sacramento Unit (layer) and is comprised mainly of the Sacramento shale of Callaway (1964; hereafter referred to as Sacramento shale) and overlies the Forbes Unit (fig. 7.8). Deposited basinwide during a relative sealevel highstand about 77 Ma (Hosford Scheirer and Magoon, this volume, chapter 5), the Sacramento shale is mainly comprised of siltstone with some shelf facies on the east side of the basin (fig. 7.6; Nilsen and Moore, 1997).

The Sacramento CS was modeled on the basis of well picks labeled Sacramento shale and base Lathrop sand of Callaway (1964; hereafter referred to as Lathrop sand). Subsurface elevations in the well-defined region (blue polygon, fig. 7.8*C*) range between about 5,500 and 13,000 feet deep, and average about 9,000 feet deep. As with the overlying Cretaceous layers, the Sacramento shale shallows and thins from west to east approaching Sierran basement (figs. 7.8*C*, *D*). The extreme thickening in the northwest corner in figure 7.8*D* is probably the expression of the Tracy Anticline near the Vernalis Fault (Sterling, 1992; Imperato, 1995). Model features within the area of unresolved complexity are unreliable.

Lathrop Composite Surface/Lathrop Unit

Overlying the Sacramento CS is the Lathrop Unit (layer) and Lathrop Composite Surface (top). The Lathrop sand is a sand-rich submarine fan deposit comprised of slope, channel, and basin-plain facies (Nilsen and Moore, 1997) deposited about 73.5 Ma (Hosford Scheirer and Magoon, this volume, chapter 5).

Nilsen and Moore (1997; fig. 7.6) define the top of the Lathrop sand as the base of the overlying Sawtooth shale of Hoffman (1964), except in the east, where marker "S50" marks the top of the unit (fig. 7.6; S50 lies within the Starkey sands of Hoffman, 1964; hereafter referred to as Starkey sands). In the model, the Lathrop CS was formed by combining well picks for Lathrop sand, a marker for the upper Lathrop sand, the base of the Sawtooth shale of Hoffman (1964), and the S50 marker (fig. 7.6).

Figure 7.9*B* shows that much of the northern part of the San Joaquin Basin is densely covered by well penetrations of the Lathrop CS. As with the underlying Sacramento Unit, the Lathrop Unit shallows sharply in the extreme northwest

corner of the basin as it approaches the outcrop belt; this model feature is supported by data in that region and may be related to a structure surrounding the Vernalis Fault known as the Tracy Anticline (Sterling, 1992; Imperato, 1995). The closed contour labeled −10,000 feet in figure 7.9*C* records a depression in the geosyncline at the time of Lathrop sand deposition that either marks the paleoaxis of deposition or indicates the locus of a later episode of deformation. The average depth of the Lathrop CS is 6,200 feet. The Lathrop Unit thins approaching the Sierran basement on the east, where it pinches out into correlative shelf and deltaic deposits. The unit also thins within the depression that presumably marks the paleobasin axis, perhaps due to a partially restricted subbasin, channelized thinning, or simply becoming more shale-rich at the distal edge of the submarine fan deposition (Applied Earth Technology, 1990). The unit thickens to as much as 4,000 feet near Modesto and on the southwest side of the well-constrained region approaching the area of unresolved complexity (fig. 7.9*D*). Thickness values within the region of good data coverage are in agreement with an isopach map of the Lathrop sand by Hoffman (1964).

Sawtooth Composite Surface/Sawtooth Unit

Overlying the Lathrop CS is the Sawtooth Unit, which is a basinwide condensed section that probably marks a period of relative sealevel rise (Nilsen and Moore, 1997) at about 73 Ma (Hosford Scheirer and Magoon, this volume, chapter 5). In this model of the San Joaquin Basin, the Sawtooth Composite Surface is mapped entirely with well picks of the Sawtooth shale of Hoffman (1964; hereafter referred to as Sawtooth shale). In the scheme of Cretaceous stratigraphy outlined by Nilsen and Moore (1997), the Sawtooth shale merges eastward into the deltaic complex formed by the Starkey sands and divides the S50 and S30 log markers (fig. 7.6), but we lacked information to extend the Sawtooth Unit into the Starkey sands. Thus, the eastern limit of the Sawtooth CS is defined by the limit of well penetrations approaching the Sierran shelf.

Well data indicate that the subsurface pattern of the Sawtooth Unit mimics that of the underlying units in the northern part of the basin, with a defined synform and shoaling margins both to the east and west (fig. 7.10). The Sawtooth Unit is everywhere less than 1,000 feet thick (fig. 7.10*D*). Depths in the well-determined northern San Joaquin Basin (blue polygon, fig. 7.10*C*) range between about 700 and 10,000 feet, with an average depth of about 5,700 feet (fig. 7.10*C*). In the central and southern part of the basin, where no data exists, we defined the Sawtooth Unit to be of constant thickness and to conform to underlying layers.

Tracy Composite Surface/Tracy Unit

Between the underlying Sawtooth shale and the overlying Ragged Valley silt of Hoffman (1964; hereafter referred to as Ragged Valley silt) lies the Tracy Unit, a submarine fan system composed mainly of the Tracy sands of Hoffman (1964; hereafter referred to as Tracy sands). Deposited about 72 Ma (Hosford Scheirer and Magoon, this volume, chapter 5), the Tracy sands prograded from northeast to southwest as they were fed by the middle part of the Starkey sands delta. Accordingly, we used well top picks for the Tracy sands, as well as for the S30 marker of Nilsen and Moore (1997; fig. 7.6), to construct the Tracy Composite Surface (fig. 7.11).

The Tracy Unit displays a number of interesting features. Structural depth contours within the area of well data (blue polygon, fig. 7.11*C*) match closely with those determined by Hoffman (1964). Depth values within the region of well penetrations range between 1,200 and 9,100 feet, with an average depth of about 4,700 feet. Like older underlying units, the Tracy CS illustrates a well-developed synform just south of the city of Modesto (fig. 7.11*C*). Because the trend of this synform is oblique to the trend of the San Joaquin Basin, we suggest that the depositional axis of the Tracy sands system farther south now lies in the outcrop belt of the Diablo Range (not shown). Additional structure is evident in the Tracy CS between the cities of Merced and Fresno in the vicinity of the northern gas fields; this is the oldest Cretaceous-aged surface in the three-dimensional model that we can map sufficiently to observe variation from simple homoclinal structure (fig. 7.11*A*, −6,000 foot contour in fig. 7.11*C*).

Where determined by well penetrations, the Tracy Unit ranges in thickness from a few hundred feet on the eastern margin of the northern San Joaquin Basin to as much as 2,000 feet in the central and western parts (fig. 7.11*D*), again in good agreement with earlier determinations (Hoffman, 1964). In the central and southern parts of the basin, where no data exists, we defined the Tracy Unit to be of constant thickness and to conform to underlying layers.

Ragged Valley Composite Surface/Ragged Valley Unit

Another highstand shale, the Ragged Valley silt, divides the underlying Tracy sands submarine fan system from the sands and shale of the overlying Moreno Formation (figs. 7.2 and 7.6). This condensed section is particularly useful to workers in the northern San Joaquin Basin because it contains distinctive e-log markers that facilitate identification (Hoffman, 1964; Nilsen and Moore, 1997). The Ragged Valley Composite Surface is modeled on the basis of more than 250 well picks, all located north of the city of Fresno except for two picks at the latitude of Coalinga field (fig. 7.12). Although the Ragged Valley Unit merges into the Starkey sands to the east (fig. 7.6), well control was sufficient to characterize the surface without introducing uncertainty by incorporating picks for Starkey sands.

The Ragged Valley silt is time transgressive, averaging about 1.5 m.y. older at its top in the central San Joaquin Basin (73 Ma) than in the northern part of the basin (71.5 Ma; Hosford Scheirer and Magoon, this volume, chapter 5). However, nearly all of our well picks of the unit are located in the northern basin and are part of the database acquired from Applied Earth Technology (1990), giving us confidence that the surface was consistently picked and can be considered a

true time-stratigraphic surface in this model of the San Joaquin Basin.

Everywhere less than 1,000 feet thick (where defined by well penetrations, fig. 7.12*D*), the Ragged Valley CS nonetheless exhibits significant structure. The synform marking the presumed paleobasin axis is defined by the −8,000 foot closed contour (fig. 7.12*C*). An intervening high at about 37°N latitude separates this northern depression from a less well developed southern one, also marked by the −8,000 foot contour (fig. 7.12*C*). As with underlying Cretaceous units, the surface rises to 1,000 feet depth or less where it onlaps Sierran basement to the east and similarly shoals on the western corner of the basin approaching outcrop.

Moreno Composite Surface/Moreno Unit

Capping the Cretaceous section in the 2003-vintage three-dimensional model of the San Joaquin Basin Province is the Moreno Unit, a model component that incorporates all strata between the Ragged Valley CS and the Garzas Sandstone Member of the Moreno Formation (figs. 7.2, 7.6) and ranges in age from about 71.5 Ma to 61 Ma from base to top (Hosford Scheirer and Magoon, this volume, chapter 5). This unit thus represents significant volume and time in the model and is the oldest unit with widespread data in this regional-scale model.

The Moreno Unit incorporates the Blewett and Starkey sands of Hoffman (1964), which together represent the final submarine fan-slope system and its feeder delta complex as discussed by Nilsen and Moore (1997), who observed a series of transgressive and regressive depositional cycles across the basin in the Late Cretaceous. The shallow-water Garzas Sandstone Member of the Moreno Formation blanketed the Late Cretaceous sandstone-shale succession and set the stage for a different depositional setting in the Cenozoic (Applied Earth Technology, 1990).

The Moreno Composite Surface is mapped in the three-dimensional model by combining well picks for the Cima Sandstone Lentil (5 picks), top "Cretaceous" (83 picks; a generic term used by well loggers to indicate the youngest observed Cretaceous unit), Dos Palos Shale Member (17 picks), Garzas Sandstone Member (249 picks), top Moreno Formation (259 picks), and Wheatville sand (34 picks) of Callaway (1964). The unit as defined here is a generalization of the Moreno Formation as defined by McGuire (1988b).

Geologic features at the model level of the Moreno CS are resolved with confidence in the area of correspondence (fig. 7.13). The Moreno CS forms a simple homocline in the central and eastern San Joaquin Basin; depths increase smoothly from about −1,000 feet on the eastern margin of the basin to about −12,000 feet at Trico gas field ("T," fig. 7.4). South of the Bakersfield Arch, the Moreno Unit and all older Cretaceous rocks are absent due to erosion, or less likely, nondeposition. The Moreno CS exhibits significant structural complexity in the vicinity of Coalinga and Vallecitos ("V," fig. 7.4) oil fields in the form of two local highs and an intervening saddle (fig. 7.13*C*). Structural depth contours in the southwest edge of the Moreno CS hint at the development of the northwest trending Buttonwillow depocenter, a feature that becomes prominent in overlying units. This feature is pinned at this level in the three-dimensional model by a well pick labeled "Cretaceous" at a depth of 23,000 feet in Elk Hills field (Nicholson, 1990; Alimi and Kaplan, 1997).

Sedimentary thicknesses in the Moreno Unit (fig. 7.13*D*) are highly variable, primarily because of the combination of varying facies into one stratigraphic unit. Within the stable eastern corridor, thicknesses range from about 1,000 feet or less to 3,500 feet where the Moreno Unit onlaps Sierran basement, in agreement with prior determinations (Reid, 1988). Approaching the northern province boundary and the central part of the basin, extreme thicknesses are evident, particularly in the vicinity of the two local highs noted above. In the northern San Joaquin Basin, thicknesses in the 4,000 to 8,000 feet range are reasonable given that Garzas Sandstone Member alone is more than 1,500 feet thick and the Blewett sands of Hoffman (1964) can be more than 3,500 feet thick (Applied Earth Technology, 1990; Suchsland and Peters, 1997). Thickness values and distributions within the area of unresolved complexity are unreliable at any particular point, but the value of about 12,000 feet in the vicinity of Coalinga oil field may be reasonable given that the Moreno Formation began to generate petroleum only a few million years following the end of its deposition (Peters, Magoon, Lampe, and others, this volume, chapter 12), a condition that generally requires 13,000 feet of sedimentary overburden (Zieglar and Spotts, 1978).

Summary of Cretaceous Rocks

Figure 7.14 summarizes the Cretaceous section of the 2003-era three-dimensional model of the San Joaquin Basin Province. Viewed from 40 degrees west of north, the alternating series of thin shale beds and much thicker sandstone beds is clearly evident. Approaching the eastern basin margin, all units thin and pinch out against Sierran basement, thereby marking basin-margin unconformities through time. An analysis of this Cretaceous section, including the position of the basin axis with time and how that relates to traps for natural gas, is discussed by Hosford Scheirer and Magoon (this volume, chapter 21). Incidentally, the uplifted basement block south of the White Wolf Fault is visible in this figure.

Paleocene-Eocene Rocks

Domengine Composite Surface/Domengine Unit

Deposition of the Domengine Formation marks a period of reorganization in the San Joaquin Basin about 48.5 Ma: subsidence enlarged the basin and opened it to the deep sea on its southwestern margin (Callaway, 1971) and western terranes began to contribute detritus into the basin

for the first time (Morelan, 1985). The Domengine Formation and equivalents blanket much of the San Joaquin Basin (fig. 7.15). In the three-dimensional model of the basin, the Domengine Composite Surface is comprised of well picks labeled "Domengine," Avenal Sandstone, Yokut Sandstone, Famoso sand of Edwards (1943), and Tejon Formation (just 2 well penetrations). This latter unit rests unconformably on the basement surface and is significant because it is the oldest noneroded unit south of the White Wolf Fault. However, there are few penetrations of the Tejon Formation in our well database (appendix 7.2), so it is not sufficiently determined in the three-dimensional model.

The Domengine Unit as constructed for the 2003 three-dimensional model implicitly includes all rock units between the Domengine CS and the Moreno CS; in the central San Joaquin Basin this means that the unit includes the Paleocene Lodo Formation (fig. 7.2). The Domengine Formation and equivalents crop out extensively in the Coast Ranges bordering the San Joaquin Basin, but these outcrops do not appear in this model.

Figure 7.15 shows structural depth contours of the Domengine CS and thickness for the Domengine Unit. Towards the east, the Domengine Unit thins and pinches out against basement rock. The Domengine CS ranges in depth from about 2,000 feet on the eastern margin to about 28,000 feet in the developing Buttonwillow depocenter on the west side (fig. 7.15*C*); this latter depth exceeds the deepest observed well penetration by about 8,000 feet, but the depth of the overlying Kreyenhagen Composite Surface, which is mapped on the basis of a regional seismic grid, requires these deep values.

The Domengine Unit is mostly eroded on and south of the Bakersfield Arch (Reid, 1988), and only a sliver of equivalent lower to middle Eocene rocks are preserved south of the White Wolf Fault (DeCelles, 1988; fig. 7.15*A*). The Domengine Unit where best determined averages 1,000 to perhaps 2,000 feet thick (fig. 7.15*D*); these values are an amalgamation of individual unit thicknesses for the Domengine Formation and for sandstone and shale units of the underlying Lodo Formation. Extreme thickness values within the area of unresolved complexity are likely in error, but folds in the Domengine CS in figure 7.15*A* are well resolved in that region (for example, seismic interpretation of Bloch and others, 1993) because they conform with better determined underlying (Moreno CS) and overlying units (Kreyenhagen CS).

Kreyenhagen Composite Surface/Kreyenhagen Unit

The Eocene Kreyenhagen Formation is one of the most important units in the San Joaquin Basin because of its role as a petroleum source rock (see Lillis and Magoon, this volume, chapter 9, and Peters, Magoon, Lampe, and others, this volume, chapter 12) and reservoir rock (in particular, the Point of Rocks Sandstone Member; Magoon and others, this volume, chapter 8). Composed chiefly of fine-grained biogenic shale and laminated sandstone, the Kreyenhagen Formation represents more than 10 m.y. of slope and basinal deposition during a sea-level highstand (Isaacson and Blueford, 1984; Milam, 1985).

The Kreyenhagen CS was constructed in the model by combining well picks for Kreyenhagen Formation, Walker Formation, and top "Eocene" (fig. 7.16). However, most of the control on the depth of the unit derives from a regional seismic grid from industry (dense stippling, fig. 7.16*B*). The Kreyenhagen CS represents a 37 m.y. old timeline (Hosford Scheirer and Magoon, this volume, chapter 5), although the top of the Kreyenhagen Formation is older than that in the northern part of the basin (fig. 7.2).

Figure 7.16 shows that like the underlying Domengine Formation, the Kreyenhagen Formation blankets much of the San Joaquin Basin. It crops out just north of Coalinga field, forms tight folds on the southwest margin, and covers the Bakersfield Arch. The Kreyenhagen Formation is the oldest layer in the model for which sufficient well and seismic data exist to characterize the giant anticline at Elk Hills field (fig. 7.16*A*; "EH," fig. 7.4). It is also the oldest layer in the model that hints at a pattern of two discrete centers of sediment deposition (fig. 7.16 *A*, *C)*, known in the petroleum literature as the Maricopa (sometimes called Tejon) and Buttonwillow depocenters (MacPherson, 1978; Zieglar and Spotts, 1978). Within the Buttonwillow depocenter, the Kreyenhagen Formation and equivalent units are about 5,000 feet thick (fig. 7.16*D*), probably reflecting the thick Point of Rocks Sandstone Member. The Kreyenhagen Formation thins eastward, but still attains as much as 2,000 feet thickness in the Maricopa depocenter (large thicknesses west of there in the area of unresolved complexity are in error). Finally, more of the White Wolf Fault block is covered with Kreyenhagen Formation-equivalent rocks than evident at any previous model level. The Kreyenhagen CS in that region forms a simple homocline deepening from west to east (fig. 7.16).

Eocene-Oligocene-Miocene Rocks

Temblor Composite Surface/Temblor Unit

The Temblor Formation is a significant unit in the San Joaquin Basin because its deposition coincided with a major change in regional deformation from convergence associated with subduction to transform margin tectonics associated with migration of the Mendocino Triple Junction (Bent, 1985). The Temblor Formation is stratigraphically complex, encompassing three major unconformities and four depositional sequences (Bent, 1985; Johnson and Graham, this volume, chapter 6). Facies vary dramatically from north to south as paleoenvironments fluctuated along the western margin of the basin. Generally, though, the Temblor Formation in the southwestern area of the basin consists of an alternating series of sandstone and shale units deposited over as much as 15 m.y. (for example., Carter, 1985), whereas the formation in

the northwestern area consists of marine sandstone deposited over just a few million years (fig. 7.2; Cooley, 1982; Hosford Scheirer and Magoon, this volume, chapter 5).

The Temblor Composite Surface in the three-dimensional geologic model of the San Joaquin Basin consists of well picks for Temblor Formation, its top-most Buttonbed Sandstone Member, Olcese Sand, and a 16.5 Ma sequence boundary (Johnson and Graham, this volume, chapter 6). A regional seismic grid provided the densest control on its areal distribution and depth (dense stippling in fig. 7.17*B*). As defined, the Temblor Unit implicitly incorporates the Tumey formation of Atwill (1935), thus extending the base of the unit into the late Eocene or early Oligocene.

The geographic distribution of the Temblor CS is more restricted than the underlying Kreyenhagen and Domengine Formations (fig. 7.17). This pattern reflects the uplift of the Diablo Range on the basin's western margin, which cut off part of the basin's connection with the deep sea (Bent, 1985). The Temblor CS is tightly folded on the basin's west side (fig. 7.17*A*, *C*). The Temblor Unit is the oldest layer in the three-dimensional model to completely cover both the basement surface on the Bakersfield Arch and the block south of the White Wolf Fault, indicating that the erosional event that removed early Eocene age and older rocks in those locations probably occurred during the late Eocene or early Oligocene. As with the underlying Kreyenhagen CS, the Buttonwillow and Maricopa depocenters appear well developed in the Temblor CS (fig. 7.17*A*, *C*).

The Temblor Unit is thickest near the basin's southwest margin and thins towards the east in a pattern of quasi-concentric ovals (fig. 7.17*D*). The unit is thickest in the west side fold belt, adjacent to its provenance region in the Temblor Range (Bent, 1985). Temblor Formation equivalent rocks south of the White Wolf Fault also attain great thickness, perhaps in excess of 8,000 feet (fig. 7.17*D*).

Monterey Composite Surface/Monterey Unit

The Monterey Formation is the most important unit in the three-dimensional model of the San Joaquin Basin in terms of both producing and containing petroleum (Magoon and others, this volume, chapter 8). It consists mainly of biogenic siliceous rocks (diatomite, porcelanite, and chert), but also contains significant siliciclastic sediment in the form of thick Stevens sand of Eckis (1940), a turbidite sandstone in the Maricopa depocenter (Graham and Williams, 1985), and the correlative Santa Margarita Sandstone (Ryder and Thomson, 1989). Both the base and the top of the Monterey Formation are time transgressive (Graham and Williams, 1985; fig. 7.2), although a regional electric-log and seismic horizon named the "N-Point" or "N-Chert" near the top of the Monterey Formation is nearly time synchronous and aids identification of the top of the unit (Imperato, 1995; Clark and others, 1996). For these purposes, the top of the Monterey Formation in the San Joaquin Basin is defined to be 5.5 m.y. old (for a detailed discussion on the age of the Monterey Formation, see Hosford Scheirer and Magoon, this volume, chapter 5).

The Monterey Composite Surface in the three-dimensional model of the San Joaquin Basin consists of well picks of Monterey Formation, "top Miocene," Antelope shale of Graham and Williams (1985), Fruitvale shale of Miller and Bloom (1939), the "N-Marker" chert horizon, and Reef Ridge Shale Member. A regional seismic depth grid, however, provides detailed imaging of the surface, capturing particularly well the tight folds on the basin's west side better than well picks alone (fig. 7.18).

The areal extent of the Monterey CS is equivalent to the underlying Temblor Formation (fig. 7.18), reflecting the continuation of the San Joaquin Basin as a deep-marine depocenter in late Miocene time (Graham and Williams, 1985). Present-day depths of the Monterey CS exceed 10,000 feet within the two Tertiary depocenters, where the Monterey Unit averages about 5,000 feet thick (fig. 7.18*C*). The Monterey Unit both shallows and thins radially from both depocenters—towards the east approaching the Sierran shelf, and towards the northwest at the northern edge of its range. Northwestward of Coalinga field, the Monterey Unit is completely absent in the subsurface of the San Joaquin Basin.

The Monterey Unit is the oldest layer in the model that illustrates a large influx of sediment that began in the late Miocene (Bartow, 1991). In the vicinity of South Belridge field ("SB," fig. 7.4), for example, the Monterey Unit is about 8,000 feet thick; this is immediately adjacent to its outcrop in Chico Martinez Creek, where the Monterey Formation is nearly 10,000 feet thick (Graham and Williams, 1985). Webb (1981) explains large sandstone thicknesses within the Monterey Formation as a result of channelization, tectonic thickening, or downwarping that allowed a gap to fill with sediment. Regardless of explanation, deposition of the Monterey Unit set the stage for incipient petroleum generation in the organic-rich part of the Kreyenhagen Formation in the northern Buttonwillow depocenter (Peters, Magoon, Lampe, and others, this volume, chapter 12).

Pliocene and Younger Rocks

Etchegoin Composite Surface/Etchegoin Unit

The Etchegoin Formation marks a significant change in depositional styles in the San Joaquin Basin (Reid, 1995). The basin's connection to the deep sea was nearly cut off by the uplift of both the Diablo and Temblor Ranges, and facies of the Etchegoin Formation are shelfal and tidal in character (Loomis, 1990; Reid, 1995). Hosford Scheirer and Magoon (this volume, chapter 5) document the time-transgressive nature of the base of the Etchegoin Formation, but the top of the unit, which is what is modeled here, was deposited about 4.5 Ma. The Etchegoin Composite Surface consists mainly of a regional seismic grid supplemented with well picks (dense stippling, fig. 7.19*B*).

The Etchegoin Unit is the youngest interval in the basin in which the two Tertiary-age, sedimentary depocenters remain evident (fig. 7.19). The Bakersfield Arch maintains a broad high between the two depocenters, where the Etchegoin CS is 6,000 to 8,000 feet deep. On the eastern edge of the basin, the elevation of the Etchegoin CS shoals to a depth of 1,000 feet or less. The unit is largely absent south of the White Wolf Fault, probably due both to erosion and deposition of nonmarine rock (Goodman and Malin, 1992).

The thickness pattern of the Etchegoin Unit is the most uniform in the entire model, with concentric, northwest-southeast trending ovals evident in the thickness map (fig. 7.19*D*). This uniformity may be due to the blanketing effect of the shallow Etchegoin Formation sandstone (Graham and Williams, 1985) or to adequate data coverage of this relatively shallow, important oil- and gas-bearing unit. Unit thicknesses are still quite large at this model level, with about 5,000 feet of section in the Maricopa depocenter and more than 8,000 feet of section in the Buttonwillow depocenter. The Etchegoin Unit thins dramatically in the vicinity of Midway Sunset ("MS," fig. 7.4) and Coalinga fields.

Deposition of thick Etchegoin Unit sediments created for the first time sufficient overburden rock in the Maricopa and Buttonwillow depocenters to generate petroleum in the organic-rich facies of the Monterey Formation and of the southern part of the Kreyenhagen Formation.

San Joaquin Composite Surface/San Joaquin Unit

The San Joaquin Formation is a marine to brackish unit that records the final presence of the sea within the San Joaquin Basin (Loomis, 1990). In the three-dimensional model, the San Joaquin Composite Surface is mapped chiefly on the basis of well picks. The geographic distribution of the formation shown in figure 7.20*A* is misleading. In the subsurface the unit is restricted to the southern part of the basin; outcrop extends farther north on the west side, causing the gridding routine in the modeling software to extend the layer farther to the northeast than it should. The top of the unit was deposited about 2.5 Ma (Hosford Scheirer and Magoon, this volume, chapter 5).

The most obvious feature in the map of the San Joaquin CS is its regression relative to older units, marking the shrinking of the San Joaquin sea (Loomis, 1990; Reid, 1995; fig. 7.20). The Tertiary depocenters lose their well-developed character at this level in the three-dimensional model of the San Joaquin Basin, with depths averaging 3,000 feet and less, but thicknesses remain considerable (fig. 20*D*), especially just north of the White Wolf Fault and just southeast of Kettleman North Dome field ("KND," fig. 7.4).

Tulare Composite Surface/Tulare Unit

The Tulare Composite Surface (fig. 7.21) is the youngest layer in the three-dimensional model of the San Joaquin Basin and is defined by surface topography (stippling, fig. 7.21*B*). The Tulare Unit implicitly includes the nonmarine Pliocene to Pleistocene Tulare Formation and overlying Quaternary alluvial, fluvial, and lacustrine deposits. The Tulare Unit generally averages less than about 2,000 feet thick but may be as much as 9,000 feet thick in the Maricopa depocenter (fig. 7.21).

Summary of Cenozoic Rocks

Cenozoic rocks attain great thickness in the San Joaquin Basin. With this regional scale model of the basin, the enormous sediment load and burial depths of petroleum source rocks can be more rigorously quantified for the first time. Figure 7.22 shows that post-Cretaceous rocks may be as much as 25,000 feet thick in the Maricopa depocenter, consistent with the estimate of Zieglar and Spotts (1978), and at least that thick in the Buttonwillow depocenter.

Figure 7.23 illustrates two additional views of the 2003-vintage three-dimensional model of the San Joaquin Basin Province. The top panel (fig. 7.23*A*) cuts into the model along a transect through the eastern edge of Paloma oil field ("P," fig. 7.4) and along the western edge of Trico Northwest and Harvester gas fields ("TNW" and "H," fig. 7.4). This view illustrates uplifted strata south of the White Wolf Fault, the large accumulation of sediment in the Maricopa depocenter at the south end of the basin, and the Bakersfield Arch just to the north of the depocenter. It also shows Cretaceous strata (pink color, fig. 7.23*A*) pinching out against the northern edge of the arch. The second panel (fig. 7.23*B*) cuts the model just east of Lost Hills field ("LH," fig. 7.4) and through Elk Hills field. It emphasizes the thick sedimentary section within the Buttonwillow depocenter and the west side fold belt.

Applications of Three-Dimensional Model

The modeling effort in the San Joaquin Basin Province for the 2003 National Oil and Gas Assessment Project originally focused on organizing the many thousands of well picks and seismic lines into a three-dimensional database that would, in turn, allow the development of an integrated stratigraphic framework for the assessment of undiscovered petroleum. Indeed, this endeavor proved effective for integrating diverse datasets and determining general sedimentary architecture through time. The resulting three-dimensional model unexpectedly became a valuable tool for realizing other goals of the assessment process, including the definition of assessment unit volumes, the evaluation of resource potential at depth, and the development of a petroleum system model. It also served as a real-time, interactive product during the assessment meeting itself.

Definition and Visualization of Assessment Units

The fundamental entity for the USGS's estimation of undiscovered oil and gas resources is the assessment unit (AU; Magoon and Schmoker, 2000). Defined as a volume of rock within a total petroleum system that contains a relatively homogeneous collection of discovered and undiscovered petroleum pools (Magoon and Schmoker, 2000), the AU is traditionally examined in map view rather than in three dimensions (for example, Garrity and others, 2005). That is, for each AU a series of structure-contour, thickness, petroleum-system, and other maps are constructed and used as the basis of assessment.

In contrast, the three-dimensional geologic model of the San Joaquin Basin Province allowed the assessment team to construct and examine the AU in its true form—as a volume. Confirmed petroleum plays in the San Joaquin Basin were iteratively constructed in three dimensions using information from previous assessments, geochemical data, distribution of known accumulations, well penetrations, and many other relevant types of data—all of which were plotted in three dimensions in the model of the San Joaquin Basin. The volume of rock assigned to each AU was then isolated from the three-dimensional model and analyzed. This process was especially useful in locations where assessment units are vertically stacked; most AUs extend from basement to topography in the depth dimension, but several in the central basin overlap in map view, so defining the AUs volumetrically was essential for avoiding double assessment. See Gautier and others (this volume, chapter 2) for the definitions of the 10 assessment units.

The assessment unit volumes were rigorously analyzed during the assessment process. The southern part of the Lower Bakersfield Arch Assessment Unit, for example, lacks known accumulations and contains only a few prospect wells (see fig. 14.3 in Gautier and Hosford Scheirer, this volume, chapter 14). The three-dimensional model allowed the assessment team to examine the relative positions of petroleum source and reservoir rocks, wells, among other factors, and to use that information to assess undiscovered petroleum accumulations.

Resource Potential at Depth

A topic of prime importance in the 2003 assessment of the San Joaquin Basin was the Deep Fractured Pre-Monterey AU. Restricted to the basin's structurally complex west side below 14,000 feet depth in rocks predating the Monterey Formation, the AU has been the location of several gas blowouts and was hypothesized to contain a significant undiscovered gas resource. The area proved difficult to assess for undiscovered accumulations, however, due to a near-total absence of exploration data—only about 30 wells, as of 2004, penetrated rocks older than the Monterey Formation at depths greater than 14,000 feet within the AU. In the absence of a discovery history, which typically serves as an analog for assessment, we were faced with an unsatisfying degree of uncertainty regarding this AU.

To initiate our assessment of the AU, we quantitatively estimated potential resources by identifying possible traps on industry-supplied structure contour maps of the top of the Temblor Formation and the Point of Rocks Sandstone Member of the Kreyenhagen Formation. We then assumed a success rate for discovery, applied it to the estimated 200 prospects, and then calculated the volumes of gas in each prospect using standard engineering equations (Tennyson and Hosford Scheirer, this volume, chapter 20). Although the 2003-vintage three-dimensional model of the San Joaquin Basin is known to be in error in the area of unresolved complexity, the model is sufficiently well determined in the vicinity of the large oil fields that are relevant to this deep gas assessment unit (for example, Lost Hills field). Further, reliance on individual structure-contour maps of formations relevant to the problem minimized error in the assessment of undiscovered resource.

Petroleum System Modeling

A major application of the 2003-era three-dimensional model of the San Joaquin Basin was its use in the project's petroleum system modeling effort (Peters, Magoon, Lampe, and others, this volume, chapter 12). The three-dimensional model forms the backbone of the petroleum system model because it incorporates key petroleum source and reservoir rocks—essential elements for predicting the timing and location of petroleum generation-migration-accumulation. Important petroleum reservoirs rocks that were omitted from the model presented here, such as the Stevens sand of Eckis (1940) and the Point of Rocks Sandstone Member of the Kreyenhagen Formation, were added to the petroleum system model by splitting the Monterey Formation and the Kreyenhagen Formation, respectively (Peters, Magoon, Lampe, and others, this volume, chapter 12).

Data Archive

The three-dimensional model of the San Joaquin Basin incorporates myriad and varied data. These data are of different scales, densities, certainties, resolutions, and even generations. By tying these data together into a digital model, it becomes an archive that can be continually updated as more data become available. Future workers can evaluate the model, included as appendix 7.1.

Conclusions

This three-dimensional model of the San Joaquin Basin represents digitally the geology from the top of the basement unconformity to the ground surface. Based primarily on thousands of well picks and five regional seismic surfaces, the model illustrates the present-day geology of 15 chronostratigraphic horizons, called composite surfaces. Because the model incorporates key petroleum source and reservoir rocks, it constitutes a valuable tool for play analysis and resource assessment. It is also documents the development of

the important Maricopa and Buttonwillow depocenters and forms the backbone of a four-dimensional petroleum system model. Finally, the model archives myriad data into a consistent framework that can be updated as additional data become available.

The model iteration presented in this chapter was completed for a USGS assessment meeting held in November 2003. During development, decisions were required to reconcile inconsistent data and to simplify structurally and stratigraphically complex areas, while ensuring that the model remained robust enough to serve an important role in the assessment process. This model served this requirement well. Other reports in this volume (Peters, Magoon, Lampe, and others, this volume, chapter 12; Gautier and Hosford Scheirer, this volume, chapter 14; Hosford Scheirer and Magoon, this volume, chapter 21) clearly illustrate the importance of having a digital representation of subsurface geology in this petroleum-rich province, especially in the central and eastern parts of the model that are the best determined.

This three-dimensional model could benefit from additional work, such as to include important sandstone bodies like the Stevens sand of Eckis (1940) within the Monterey Formation and the Point of Rocks Sandstone Member of the Kreyenhagen Formation; the Tumey formation of Atwill (1935), a suspected petroleum source rock (Lillis and Magoon, this volume chapter 9); various members of the Temblor Formation; and the unique stratigraphy south of the White Wolf Fault. Inclusion of more faults, particularly on the structurally complex west side of the basin, would provide valuable geologic framework and enhance petroleum trapping in the petroleum system model of Peters, Magoon, Lampe, and others (this volume, chapter 12). For the sake of completeness, it would also improve the model to include detailed surface geology, specifically in the western part of the map area where the model is much less accurate.

There are many possible applications of this three-dimensional model. Indeed, a groundwater availability study of California's entire Great Valley (San Joaquin Valley and Sacramento Valley combined) uses the San Joaquin Formation from the model as one of just three rock units specified in the hydrologic model (other units in the model are included on the basis of their physical properties; Faunt and others, 2009). The model could be used as input to seismic-shaking software to assess earthquake hazards within the San Joaquin Valley, although more detailed surface geology should be incorporated in this case. It could also be used for numerical calculations of carbon sequestration in existing oil and gas fields. The fundamental strength of this model is that it is fully digital and thus can be employed in a vast array of numerical manipulations.

Acknowledgments

The author thanks Don Gautier and Bob Jachens, both of the USGS in Menlo Park, Calif., for enthusiastically suggesting this effort in the fall of 2002, and Chris Schenk (USGS, Denver) for funding the work through the National Oil and Gas Assessment Project. Les Magoon, Lynn Tennyson, Steve Graham, Ken Peters, Tor Nilsen, and many others provided comments, data, and advice along the way. Zenon Valin provided valuable GIS support. Skip Pack, Graham Brew, Paul White, and Robert McFaul at Dynamic Graphics, Inc., provided advice and technical support. Dan Scheirer provided valuable assistance throughout the project. This product was supported in part by the National Cooperative Geologic Mapping Program of the USGS. This paper was improved by the comments of Russ Graymer and Geoff Phelps of the U.S. Geological Survey in Menlo Park, Calif., and by Graham Brew of Dynamic Graphics, Inc.

References Cited

Alimi, H., and Kaplan, I.R., 1997, Petroleum geochemistry of the deep well NPR-934-29R drilled in Elk Hills Field, San Joaquin Basin, California [abs.]: American Association of Petroleum Geologists Bulletin, v. 81, no. 4, p. 695.

Almgren, A.A., 1986, Benthic foraminiferal zonation and correlations of Upper Cretaceous strata of the Great Valley of California—A modification, *in* Abbott, P.L., ed., Cretaceous stratigraphy, Western North America: Los Angeles, Pacific Section, Society of Economic Paleontologists and Mineralogists, p. 137–152.

Applied Earth Technology, Inc., 1990, Campanian, Maestrichtian, and Danian strata, northern San Joaquin Basin: Redwood City, Calif., 474 p.

Atwill, E.R., 1935, Oligocene Tumey Formation of California: Bulletin of the American Association of Petroleum Geologists, v. 19, no. 8, p. 1192–1204.

Bartow, J.A., 1983, Map showing configuration of the basement surface, northern San Joaquin Valley, California: U.S. Geological Survey Miscellaneous Field Studies Map 1430, scale 1:250,000.

Bartow, J.A., 1991, The Cenozoic evolution of the San Joaquin Valley, California: Washington, D. C., U.S. Geological Survey Professional Paper 1501, 40 p.

Bartow, J.A., and Nilsen, T.H., 1990, Review of the Great Valley Sequence, eastern Diablo Range and northern San Joaquin Valley, central California: U.S. Geological Survey Open-File Report 90–226, 25 p.

Bawden, G.W., 2001, Source parameters for the 1952 Kern County earthquake, California—A joint inversion of leveling and triangulation observations: Journal of Geophysical Research, v. 106, no. 1, p. 771–785.

Bent, J.V., 1985, Provenance of upper Oligocene-middle Miocene sandstones of the San Joaquin Basin, California, *in* Graham, S.A., ed., Geology of the Temblor Formation, western San Joaquin Basin, California: Los Angeles, Pacific Section, Society of Economic Paleontologists and Mineralogists, v. 44, p. 97–120.

Beyer, L.A., 1996, San Joaquin Basin Province, *in* Gautier, D.L., Dolton, G.L., Takahashi, K.I., and Varnes, K.L., eds., 1995 National assessment of United States oil and gas resources—Results, methodology, and supporting data: U.S. Geological Survey Digital Data Series 30, release 2.

Beyer, L.A., and Bartow, J.A., 1987, Summary of geology and petroleum plays used to assess undiscovered recoverable petroleum resources, San Joaquin Basin Province, California: United States Geological Survey Open-File Report 87–450Z, 80 p.

Bishop, C.C., 1970, Upper Cretaceous stratigraphy on the west side of the Northern San Joaquin Valley, Stanislaus and San Joaquin counties, California: Sacramento, Calif., California Division of Mines and Geology Special Report 104, 29 p.

Bloch, R.B., 1991a, San Andreas Fault to Sierra Nevada Range, Sheet 3 of 3, *in* Bloch, R.B., and Graham, S.A., eds., West coast regional cross section: Tulsa, Okla., American Associations of Petroleum Geologists, p. 1 sheet.

Bloch, R.B., 1991b, Studies of the stratigraphy and structure of the San Joaquin Basin, California: Stanford, Calif., Stanford University, Ph.D. dissertation, 319 p.

Bloch, R.B., Huene, R.V., Hart, P.E., and Wentworth, C.M., 1993, Style and magnitude of tectonic shortening normal to the San Andreas Fault across Pyramid Hills and Kettleman Hills South Dome, California: Geological Society of America Bulletin, v. 105, no. 4, p. 464–478.

California Department of Conservation, Division of Oil, Gas, and Geothermal Resources, 2003, 2002 Annual Report of the State Oil and Gas Supervisor: Sacramento, Calif., California Department of Conservation, Division of Oil, Gas, and Geothermal Resources, Publication No. PR06, 263 p. (Also available at ftp://ftp.consrv.ca.gov/pub/oil/annual_reports/2002/.)

California Department of Conservation, Division of Oil, Gas, and Geothermal Resources, [2007], Oil, Gas & Geothermal—Geothermal—Annual Reports: California Department of Conservation database, accessed June 15, 2012, at http://www.consrv.ca.gov/DOG/pubs_stats/annual_reports/Pages/annual_reports.aspx.

California Department of Conservation, Division of Oil, Gas, and Geothermal Resources, [2012]: California Department of Conservation database, accessed August 26, 2012, at http://www.conservation.ca.gov/dog/maps/Pages/GISMapping2.aspx.

California Division of Oil and Gas, 1982, Oil and gas prospect wells drilled in California through 1980: Sacramento, Calif., California Division of Oil and Gas Publication No. TR01, 258 p.

Callaway, D.C., 1964, Distribution of uppermost Cretaceous sands in the Sacramento-Northern San Joaquin Basin of California: Selected Papers Presented to San Joaquin Geological Society, v. 2, p. 5–18.

Callaway, D.C., 1971, Petroleum potential of San Joaquin Basin, California, *in* Cram, I.H., ed., Future petroleum provinces of the United States—Their geology and potential: Tulsa, Okla., American Association of Petroleum Geologists Memoir 15, p. 239–253.

Callaway, D.C., 1990, Organization of stratigraphic nomenclature for the San Joaquin Basin, California, *in* Kuespert, J.G., and Reid, S.A., eds., Structure, stratigraphy, and hydrocarbon occurrences of the San Joaquin Basin, California: Bakersfield, Calif., Pacific Sections, Society of Economic Paleontologists and Mineralogists and American Association of Petroleum Geologists, v. 64, p. 5–21.

Carter, J.B., 1985, Depositional environments of the type Temblor Formation, Chico Martinez Creek, Kern County, California, *in* Graham, S.A., ed., Geology of the Temblor Formation, western San Joaquin Basin, California: Los Angeles, Pacific Section, Society of Economic Paleontologists and Mineralogists, v. 44, p. 5–18.

Chen, J.H., and Moore, J.G., 1982, Uranium-lead isotopic ages from the Sierra Nevada Batholith, California: Journal of Geophysical Research, v. 87, no. 6, p. 4761–4784.

Cherven, V.B., 1981, A delta-slope-submarine fan model for the Maastrichtian part of the Great Valley Sequence, southern Sacramento and northern San Joaquin Basin, California: Stanford, Calif., Stanford University, Ph.D. dissertation, 141 p.

Cherven, V.B., 1983, A delta-slope-submarine fan model for Maestrichtian part of Great Valley Sequence, Sacramento and San Joaquin Basins, California: American Association of Petroleum Geologists Bulletin, v. 67, p. 772–816.

Clark, M.S., Beckley, L.M., Crebs, T.J., and Singleton, M.T., 1996, Tectono-eustatic controls on reservoir compartmentalisation and quality—An example from the Upper Miocene of the San Joaquin basin, California: Marine and Petroleum Geology, v. 13, p. 475–491.

Cooley, S.A., 1982, Depositional environments of the lower and middle Miocene Temblor Formation of Reef Ridge, Fresno and Kings counties, California, *in* Williams, L.A., and Graham, S.A., eds., Monterey Formation and associated coarse clastic rocks, central San Joaquin Basin, California: Los Angeles, Pacific Section, Society of Economic Paleontologists and Mineralogists, p. 55–71.

Davis, T.L., and Lagoe, M.B., 1988, A structural interpretation of major tectonic events affecting the western and southern margins of the San Joaquin Valley, California, *in* Graham, S.A., and Olson, H.C., eds., Studies of the geology of the San Joaquin Basin: Los Angeles, Pacific Section, Society of Economic Paleontologists and Mineralogists, book 60, p. 65–87.

DeCelles, P.G., 1988, Middle Cenozoic depositional, tectonic, and sea level history of southern San Joaquin Basin, California: American Association of Petroleum Geologists Bulletin, v. 72, p. 1297–1322.

Dibblee, T.W., Jr., 1968, Geologic map of Temblor Range, San Luis Obispo and Kern counties, California, *in* Karp, S.E., ed., Guidebook, Geology and oil fields, West side southern San Joaquin Valley, 43rd Annual Meeting: Pacific Sections, American Association of Petroleum Geologists, Society of Exploration Geophysicists, Society of Economic Paleontologists and Mineralogists.

Dibblee, T.W., Jr., 1981, Upper Mesozoic rock units in the central Diablo Range between Hollister and New Idria and their depositional environments, *in* Frizzell, V., ed., Geology of the central and northern Diablo Range, California: Los Angeles, Pacific Section, Society of Economic Paleontologists and Mineralogists, p. 13–20.

Dickinson, W.R., 2002, Reappraisal of hypothetical Franciscan thrust wedging at Coalinga—Implications for tectonic relations along the Great Valley flank of the California Coastal Ranges: Tectonics, v. 21, no. 5, p. 14.

Eckis, R., 1940, The Stevens sand, southern San Joaquin Valley, California [abs.]: Bulletin of the American Association of Petroleum Geologists, v. 24, no. 12, p. 2195–2196.

Edwards, E.C., 1943, Kern Front area of the Kern River oil field, *in* Jenkins, O.P., ed., Geologic formations and economic development of the oil and gas fields of California: San Francisco, Calif., State of California, Department of Natural Resources, Division of Mines Bulletin No. 118, p. 571–574.

Faith, J.R., Blome, C.D., Pantea, M.P., Puckette, J.O., Halihan, T., Osborn, N., Christenson, S., and Pack, S., 2010, Three-dimensional geologic model of the Arbuckle-Simpson Aquifer, South-Central Oklahoma: U.S. Geological Survey Open-File Report 2010–1123, 29 p.

Faunt, C.C., Hanson, R.T., Belitz, K., Schmid, W., Predmore, S.P., Rewis, D.L., and McPherson, K., 2009, Numerical model of the hydrologic landscape and groundwater flow in California's Central Valley, *in* Faunt, C.C., ed., Groundwater availability of the Central Valley Aquifer, California: U.S. Geological Survey Professional Paper 1766, chapter C, p. 121–212. (Also available at http://pubs.usgs.gov/pp/pp1766/.)

Garrity, C.P., Houseknecht, D.W., Bird, K.J., Potter, C.J., Moore, T.E., Nelson, P.H., and Schenk, C.J., 2005, U.S.

Geological Survey 2005 oil and gas resource assessment of the central North Slope, Alaska—Play maps and results: U.S. Geological Survey Open-File Report 2005–1182, 29 p.

Gautier, D.L., Dolton, G.L., Takahashi, K.I., and Varnes, K.L., 1996, 1995 National assessment of United States oil and gas resources—Results, methodology, and supporting data: U.S. Geological Survey Digital Data Series 30, Release 2.

Gautier, D.L., Hosford Scheirer, A., Tennyson, M.E., Peters, K.E., Magoon, L.B., Lillis, P.G., Charpentier, R.R., Cook, T.A., French, C.D., Klett, T.R., Pollastro, R.M., and Schenk, C.J., 2004, Assessment of Undiscovered Oil and Gas Resources of the San Joaquin Basin Province of California, 2003: U.S. Geological Survey Fact Sheet 2004–0343. (Also available at http://pubs.usgs.gov/fs/2004/3043/.)

Goodman, E.D., and Malin, P.E., 1992, Evolution of the southern San Joaquin Basin and mid-Tertiary "transitional" tectonics, central California: Tectonics, v. 11, p. 478–498.

Goudkoff, P.P., 1943, Correlation of oil field formations on west side of San Joaquin Valley, *in* Jenkins, O.P., ed., Geologic formations and economic development of the oil and gas fields of California: San Francisco, Calif., State of California, Department of Natural Resources, Division of Mines Bulletin No. 118, p. 247–252.

Goudkoff, P.P., 1945, Stratigraphic relations of Upper Cretaceous in Great Valley, California: Bulletin of the American Association of Petroleum Geologists, v. 29, no. 7, p. 956–1007.

Graham, S.A., 1985, Introduction, *in* Graham, S.A., ed., Geology of the Temblor Formation, western San Joaquin Basin, California: Los Angeles, Pacific Section, Society of Economic Paleontologists and Mineralogists, v. 44, p. 1–3.

Graham, S.A., McCloy, C., Hitzman, M., Ward, R., and Turner, R., 1984, Basin evolution during change from convergent to transform continental margin in central California: American Association of Petroleum Geologists Bulletin, v. 68, no. 3, p. 233–249.

Graham, S.A., and Williams, L.A., 1985, Tectonic, depositional, and diagenetic history of Monterey Formation (Miocene), central San Joaquin Basin, California: American Association of Petroleum Geologists Bulletin, v. 69, no. 3, p. 385–411.

Graham, S.E., Mahony, T.M., Blissenbach, J.L., Mariant, J.J., and Wentworth, C.M., 1999, Regional geologic map of San Andreas and related faults in Carrizo Plain, Temblor, Caliente and La Panza Ranges and vicinity, California—A digital database: U.S. Geological Survey Open-File Report 99–14.

Graymer, R.W., Ponce, D.A., Jachens, R.C., Simpson, R.W., Phelps, G.A., and Wentworth, C.M., 2005, Three-dimensional geologic map of the Hayward fault, northern California—Correlation of rock units with variations in seismicity, creep rate, and fault dip: Geology, v. 33, no. 6, p. 521–524.

Grender, G.C., Rapoport, L.A., and Segers, R.G., 1974, Experiment in quantitative geologic modeling: American Association of Petroleum Geologists Bulletin, v. 58, p. 488–498.

Harness, P.E., and Tran, T., 2004, 3-D modeling of sinusoidal fluvial channels in the Kern River field: American Association of Petroleum Geologists Bulletin, v. 88, no. 13 (supplement).

Hoffman, R.D., 1964, Geology of the northern San Joaquin Valley: Selected Papers Presented to San Joaquin Geological Society, v. 2, p. 30–45.

Imperato, D.P., 1995, Studies of the stratigraphy and structure of the Great Valley of California and implications for plate tectonics: Santa Barbara, Calif., University of California Santa Barbara, Ph.D. dissertation, 271 p.

Imperato, D.P., Nilsen, T.H., and Moore, D.W., 1990, Regional stratigraphy of the mud-rich turbidite system of the Forbes formation, Sacramento Basin, California, *in* Ingersoll, R.V., and Nilsen, T.H., eds., Sacramento Valley Symposium and Guidebook: Los Angeles, Pacific Section, Society of Economic Paleontologists and Mineralogists, bk. 65, p. 69–79.

Ingersoll, R.V., 1978, Paleogeography and paleotectonics of the late Mesozoic forearc basin of northern and central California, *in* Howell, D.G., and McDougall, K.A., eds., Mesozoic paleogeography of the Western United States: Los Angeles, Pacific Section, Society of Economic Paleontologists and Mineralogists, p. 471–482.

Isaacson, K.A., and Blueford, J.R., 1984, Kreyenhagen Formation and related rocks—A history, *in* Blueford, J.R., ed., Kreyenhagen Formation and related rocks: Los Angeles, Pacific Section, Society of Economic Paleontologists and Mineralogists, v. 37, p. 1–7.

Jachens, R.C., Griscom, A., and Roberts, C.W., 1995, Regional extent of Great Valley basement west of the Great Valley, California—Implications for extensive tectonic wedging in the California Coast Ranges: Journal of Geophysical Research, v. 100, p. 12769–12790.

Jachens, R.C., Wentworth, C.M., Simpson, R.W., Graymer, R.W., Graham, S., Williams, R.A., McLaughlin, R.J., and Langenheim, V.E., 2005, Three-dimensional geologic map of the Santa Clara Valley and adjacent uplands, California: Geological Society of America Abstracts with Programs, v. 37, no. 4, p. 89.

Jennings, C.W., Strand, R.G., and Rogers, T.H., 1977, Geologic map of California: California Department of Conservation, Division of Mines and Geology Geologic Data Map No. 2, scale 1:750,000.

Johnson, C.L., Bloch, R.B., and Graham, S.A., 2005, Tertiary sequences of the central San Joaquin Basin, California—Age control and eustatic versus tectonic forcing factors: Pacific Section, American Association of Petroleum Geologists MP49, 1 sheet.

Kasline, F.E., 1942, Edison oil field, *in* Summary of operations, California oil fields: San Francisco, Calif., Annual Report of the State Oil and Gas Supervisor, v. 26, p. 12–18 [also available *in* California Division of Oil and Gas, Summary of Operations, 1915-1999: California Division of Conservation, Division of Oil, Gas, and Geothermal Resources, Publication No. CD-3, and at ftp://ftp.consrv.ca.gov/pub/oil/Summary_of_Operations/1940/].

Kirby, J.M., 1943, Upper Cretaceous stratigraphy of the west side of Sacramento Valley south of Willows, Glenn County, California: Bulletin of the American Association of Petroleum Geologists, v. 27, no. 3, p. 279–305.

Liu, Y., Harding, A., Abriel, W., and Strebelle, S., 2004, Multiple-point simulation integrating wells, three-dimensional seismic data, and geology: American Association of Petroleum Geologists Bulletin, v. 88, no. 7, p. 905–921.

Loken, K.P., 1959, Gill Ranch gas field, *in* Summary of operations, California oil fields: San Francisco, Calif., Annual Report of the State Oil and Gas Supervisor, v. 45, no. 1, p. 27–32 [also available *in* California Division of Oil and Gas, Summary of Operations, 1915-1999: California Division of Conservation, Division of Oil, Gas, and Geothermal Resources, Publication No. CD-3, and at ftp://ftp.consrv.ca.gov/pub/oil/Summary_of_Operations/1959/].

Loomis, K.B., 1990, Depositional environments and sedimentary history of the Etchegoin Group, West-central San Joaquin Valley, California, *in* Kuespert, J.G., and Reid, S.A., eds., Structure, stratigraphy, and hydrocarbon occurrences of the San Joaquin Basin, California: Bakersfield, Calif., Pacific Sections, Society of Economic Paleontologists and Mineralogists and American Association of Petroleum Geologists, v. 64, p. 231–246.

MacPherson, B.A., 1978, Sedimentation and trapping mechanism in upper Miocene Stevens and older turbidite fans of southeastern San Joaquin Valley, California: American Association of Petroleum Geologists Bulletin, v. 62, p. 2243–2274.

Magoon, L.B., and Dow, W.G., 1994, The petroleum system, *in* Magoon, L.B., and Dow, W.G., eds., The petroleum system—From source to trap: Tulsa, Okla., American Association of Petroleum Geologists Memoir 60, p. 3–24.

Magoon, L.B., and Schmoker, J.W., 2000, The total petroleum system—The natural fluid network that constrains the assessment unit, *in* U.S. Geological Survey World Energy Assessment Team, ed., U.S. Geological Survey world petroleum assessment 2000—Description and results: U.S. Geological Survey Digital Data Series 60.

McCabe, C.A., K., M.D., Valin, Z.C., McLaughlin, R.J., Jachens, R.C., Langenheim, V.E., and Wentworth, C.M., 2004, Preliminary 3-dimensional geologic map of the Santa Rosa Plain, northern California: Eos Transactions, American Geophysical Union, v. 85, no. 47, Fall Meeting Supplement, Abstract T11D-1289.

McGuire, D.J., 1988a, Depositional framework of the Upper Cretaceous-lower Tertiary Moreno Formation, central San Joaquin Basin, California, *in* Graham, S.A., and Olson, H.C., eds., Studies of the geology of the San Joaquin Basin: Los Angeles, Pacific Section, Society of Economic Paleontologists and Mineralogists, book 60, p. 173–188.

McGuire, D.J., 1988b, Stratigraphy, depositional history, and hydrocarbon source-rock potential of the Upper Cretaceous-Lower Tertiary Moreno Formation, central San Joaquin Basin, California: Stanford, Calif., Stanford University, Ph.D. dissertation, 309 p.

McMasters, J.H., 1948, Oceanic sand [abs.]: Bulletin of the American Association of Petroleum Geologists, v. 32, no. 12, p. 2320.

Mertz, K.A., Jr., 1990, Summary of the diagenetic history of the Upper Cretaceous Forbes, Starkey, and Winters formations, Sacramento Basin, California, *in* Ingersoll, R.V., and Nilsen, T.H., eds., Sacramento Valley Symposium and Guidebook: Los Angeles, Pacific Section, Society of Economic Paleontologists and Mineralogists, bk. 65, p. 53–67.

Milam, R.W., 1985, Biostratigraphy and sedimentation of the Eocene and Oligocene Kreyenhagen Formation, central California: Stanford, Calif., Stanford University, Ph.D. dissertation, 240 p.

Miller, R.H., and Bloom, C.V., 1939, Mountain View oil field, *in* Summary of operations, California oil fields: San Francisco, Calif., Annual Report of the State Oil and Gas Supervisor, v. 22, no. 4, p. 5–36 [also available *in* California Division of Oil and Gas, Summary of Operations, 1915-1999: California Division of Conservation, Division of Oil, Gas, and Geothermal Resources, Publication No. CD-3, and at ftp://ftp.consrv.ca.gov/pub/oil/Summary_of_Operations/1937/].

Moore, D.W., 1991, Stratigraphy, sedimentology, and provenance of the lower Campanian Forbes and Marsh Creek formations, southern Sacramento and northern San Joaquin basins, California: San Jose, Calif., San Jose State University, M.S. thesis, 168 p.

Morelan, A.E., 1985, The Avenal Formation (Eocene) of Reef Ridge, Central California—A transgressive shelf facies succession: Los Angeles, Calif., University of California, Los Angeles, M.S. thesis, 218 p.

Moxon, I.W., 1990, Stratigraphic and structural architecture of the San Joaquin-Sacramento Basin: Stanford, Calif., Stanford University, Ph.D. dissertation, 371 p.

Nicholson, G.E., 1990, Structural overview of Elk Hills, *in* Kuespert, J.G., and Reid, S.A., eds., Structure, stratigraphy, and hydrocarbon occurrences of the San Joaquin Basin, California: Bakersfield, Calif., Pacific Sections, Society of Economic Paleontologists and Mineralogists and American Association of Petroleum Geologists, v. 64, p. 133–140.

Nilsen, T.H., and Moore, D.W., 1997, Regional Upper Cretaceous stratigraphy and depositional systems of the northern San Joaquin Basin, California, *in* Cressy, F.B., Jr., and Simmons, M.L., eds., Geology of the northern San Joaquin Basin gas province: Bakersfield, Calif., Pacific Section, American Association of Petroleum Geologists, MP 43, p. 1–12.

Noble, E.B., 1940, Rio Bravo oil field, Kern County, California: Bulletin of the American Association of Petroleum Geologists, v. 24, no. 7, p. 1330–1333.

Pantea, M.P., Cole, J.C., Smith, B.D., Faith, J.R., Blome, C.D., and Smith, D.V., 2008, Three-dimensional geologic model of complex fault structures in the upper Seco Creek area, Medina and Uvalde Counties, south-central Texas: Reston, Va, U.S. Geological Survey Scientific Investigations Report 2008–5131, 9 p.

Park, W.H., 1966, Main area of Mountain View oil field, *in* Summary of operations, California oil fields: Sacramento, Calif., Annual Report of the State Oil and Gas Supervisor, v. 52, no. 1, p. 37–45 [also available *in* California Division of Oil and Gas, Summary of Operations, 1915-1999: California Division of Conservation, Division of Oil, Gas, and Geothermal Resources, Publication No. CD-3, and at ftp://ftp.consrv.ca.gov/pub/oil/Summary_of_Operations/1966/].

Phelps, G.A., Boucher, A., Jachens, R.C., and Simpson, R.W., 2009, Constructing a 3D geologic map [abs.]: Geological Society of America Abstracts with Programs, v. 41, no. 7, p. 37.

Phelps, G.A., Graymer, R.W., Jachens, R.C., Ponce, D.A., Simpson, R.W., and Wentworth, C.M., 2008, Three-dimensional geologic map of the Hayward Fault zone, San Francisco Bay region, California: U.S. Geological Survey Scientific Investigations Map 3045. (Also available at http://pubs.usgs.gov/sim/3045/.)

Ponek, M., Harris, J., Harness, P., Hatlen, J., Logan, M., and Shotts, K., 2000, "A Super Giant, Part 1", 3D Modeling to Enhance Field Development Strategies, Midway-Sunset Oil Field, California: American Association of Petroleum Geologists Bulletin, v. 84, no. 6.

Ponti, D.J., Ehman, K.D., Edwards, B.D., Tinsely, J.C., III, Hildenbrand, T., Hillhouse, J.W., Hanson, R.T., McDougall, K., Powell, C.L., II, Wan, E., Land, M., Mahan, S., and Sarna-Wojcicki, A.M., 2007, A 3-dimensional model of water-bearing sequences in the Dominguez Gap region, Long Beach, California: U.S. Geological Survey Open-File Report 2007–1013, 38 p.

PS-AAPG, 1957a, Cenozoic correlation section across south San Joaquin Valley from San Andreas Fault to Sierra Nevada foot hills: Pacific Section, American Association of Petroleum Geologists, prepared by the San Joaquin Valley Sub-committee on the Cenozoic of the Geologic Names and Correlation Committee of the American Association of Petroleum Geologists (Church, H.V., Jr. and Krammes, K., co-chairmen), Section 8, 1 sheet.

PS-AAPG, 1957b, Correlation section across central San Joaquin Valley from San Andreas Fault to Sierra Nevada foot hills, California: Pacific Section, American Association of Petroleum Geologists, prepared by the San Joaquin Valley Sub-committee on the Cenozoic of the Geologic Names and Correlation Committee of the American Association of Petroleum Geologists (Church, H.V., Jr. and Krammes, K., co-chairmen), Section 9, 1 sheet.

PS-AAPG, 1958a, Correlation section longitudinally north-south through central San Joaquin Valley from Rio Vista through Riverdale (10 north) and Riverdale through Tejon Ranch area (10 south), California: Pacific Section, American Association of Petroleum Geologists, prepared by the San Joaquin Valley Sub-committee on the Cenozoic of the Geologic Names and Correlation Committee of the American Association of Petroleum Geologists (Church, H.V., Jr. and Krammes, K., co-chairmen), Section 10N, 1 sheet.

PS-AAPG, 1958b, Correlation section longitudinally north-south through central San Joaquin Valley from Rio Vista through Riverdale (10 north) and Riverdale through Tejon Ranch area (10 south), California: Pacific Section, American Association of Petroleum Geologists, prepared by the San Joaquin Valley Sub-committee on the Cenozoic of the Geologic Names and Correlation Committee of the American Association of Petroleum Geologists (Church, H.V., Jr. and Krammes, K., co-chairmen), Section 10S, 1 sheet.

PS-AAPG, 1959, Correlation section longitudinally north-south through Coalinga to Midway Sunset and across San Andreas Fault into southeast Cuyama Valley, California: Pacific Section, American Association of Petroleum Geologists, prepared by the San Joaquin Valley Sub-committee on the Cenozoic of the Geologic Names and Correlation Committee of the American Association of Petroleum Geologists (Church, H.V., Jr. and Krammes, K., co-chairmen), Section 11, 1 sheet.

PS-AAPG, 1989, Correlation section no. 27 through central San Joaquin Valley from Turk Anticline (Cantua Creek) to the Transverse Range, Fresno, King and Kern counties, California: Pacific Section, American Association of Petroleum Geologists, prepared by the San Joaquin Valley Sub-committee on the Cenozoic of the Geologic Name Correlation Committee of the American Association of Petroleum Geologists (Villanueva, L. and Kappeler, J., chairmen), 1 sheet.

Raymond, L.A., 1973, Tesla-Ortigalita fault, Coast Range thrust fault, and Franciscan metamorphism, Northeastern Diablo Range, California: Geological Society of America Bulletin, v. 84, p. 3547–3562.

Reid, S.A., 1988, Late Cretaceous and Paleogene sedimentation along the east side of the San Joaquin Basin, *in* Graham, S.A., and Olson, H.C., eds., Studies of the geology of the San Joaquin Basin: Los Angeles, Pacific Section, Society of Economic Paleontologists and Mineralogists, book 60, p. 157–171.

Reid, S.A., 1995, Miocene and Pliocene depositional systems of the southern San Joaquin basin and formation of sandstone reservoirs in the Elk Hills area, California, *in* Fritsche, A.E., ed., Cenozoic paleogeography of the western United States—II: Pacific Section, Society of Economic Paleontologists and Mineralogists, p. 131–150.

Ryder, R.T., and Thomson, A., 1989, Tectonically controlled fan delta and submarine fan sedimentation of late Miocene age, southern Temblor Range, California: Washington, D.C., U.S. Geological Survey Professional Paper 1442, 59 p.

Saucedo, G.J., Bedford, J.W., Raines, G.L., Miller, R.J., and Wentworth, C.M., 2000, GIS data for the geologic map of California: Sacramento, Calif., California Department of Conservation, Division of Mines and Geology CD-ROM 2000-007.

Stein, R.S., and Thatcher, W., 1981, Seismic and aseismic deformation associated with the 1952 Kern County, California, earthquake and relationship to the Quaternary history of the White Wolf Fault: Journal of Geophysical Research, v. 86, no. B6, p. 4913–4928.

Sterling, R.H., Jr., 1992, Intersection of the Stockton and Vernalis faults, southern Sacramento Valley, California, *in* Cherven, V.B., and Edmondson, W.F., eds., Structural geology of the Sacramento Basin: Bakersfield, Calif., Pacific Section, American Association of Petroleum Geologists, p. 143–151.

Suchsland, R.J., and Peters, J.F., 1997, Exploration and development of the Blewett trend, Northern San Joaquin Basin, California, *in* Cressy, F.B., Jr., and Simmons, M.L., eds., Geology of the northern San Joaquin Basin gas province: Bakersfield, Calif., Pacific Section, American Association of Petroleum Geologists, MP43, p. 29–48.

Sullivan, J.C., 1963, Guijarral Hills oil field, *in* Summary of operations, California oil fields: San Francisco, Calif., Annual Report of the State Oil and Gas Supervisor, v. 48, no. 2, p. 37–51 [also available *in* California Division of Oil and Gas, Summary of Operations, 1915-1999: California Division of Conservation, Division of Oil, Gas, and Geothermal Resources, Publication No. CD-3, and at ftp://ftp.consrv.ca.gov/pub/oil/Summary_of_Operations/1962/].

U.S. Geological Survey, 2012, Land Processes Distributed Active Archive Center: U.S. Department of the Interior database, accessed June 15, 2012, at http://lpdaac.usgs.gov/get_data.

Wagner, D.L., Greene, H.G., Saucedo, G.J., and Pridmore, C.L., 2002, Geologic map of Monterey 30’ × 60’ Quadrangle and adjacent areas, California—A digital database: California Department of Conservation, California Geological Survey CD 2002-04.

Wagoner, J., 2009, 3D geologic modeling of the Southern San Joaquin Basin for the Westcarb Kimberlina demonstration project—A status report: Lawrence Livermore National Laboratory LLNL-TR-410813, 27 p.

Webb, G.W., 1981, Stevens and earlier Miocene turbidite sandstones, southern San Joaquin Valley, California: American Association of Petroleum Geologists Bulletin, v. 65, p. 438–465.

Wentworth, C.M., Blake, M.C., Jr., Jones, D.L., Walter, A.W., and Zoback, M.D., 1984, Tectonic wedging associated with emplacement of the Franciscan assemblage, California Coast Ranges, *in* Blake, M.C., Jr., ed., Franciscan Geology of Northern California: Bakersfield, Calif., Pacific Section, Society of Economic Paleontologists and Mineralogists, p. 163–173.

Wentworth, C.M., Blake, M.C., Jr., McLaughlin, R.J., and Graymer, R.W., 1999, Preliminary geologic map of the San Jose 30 × 60 minute quadrangle, California—A digital database: U.S. Geological Survey Open-File Report 98–795.

Wentworth, C.M., Fisher, G.R., Levine, P., and Jachens, R.C., 1995, The surface of crystalline basement, Great Valley and Sierra Nevada, California—A digital map database: U.S. Geological Survey Open-File Report 95–96, 16 p.

White, J.L., 1955, Edison oil Field, *in* Summary of operations, California oil fields: San Francisco, Calif., Annual Report of the State Oil and Gas Supervisor, v. 41, no. 2, p. 5–23. (Also available *in* California Division of Oil and Gas, Summary of Operations, 1915–1999: California Division of Conservation, Division of Oil, Gas, and Geothermal Resources, Publication No. CD-3, and at ftp://ftp.consrv.ca.gov/pub/oil/Summary_of_Operations/1955/.)

Wilkinson, E.R., 1960, Vallecitos field, *in* Summary of operations, California oil fields: San Francisco, Calif., Annual Report of the State Oil and Gas Supervisor, v. 45, no. 2, p. 17–33. (Also available *in* California Division of Oil and Gas, Summary of Operations, 1915–1999: California Division of Conservation, Division of Oil, Gas, and Geothermal Resources, Publication No. CD-3, and at ftp://ftp.consrv.ca.gov/pub/oil/Summary_of_Operations/1959/.)

Zieglar, D.L., and Spotts, J.H., 1978, Reservoir and source-bed history of Great Valley, California: American Association of Petroleum Geologists Bulletin, v. 62, p. 813–826.

Figures 7.1–7.23

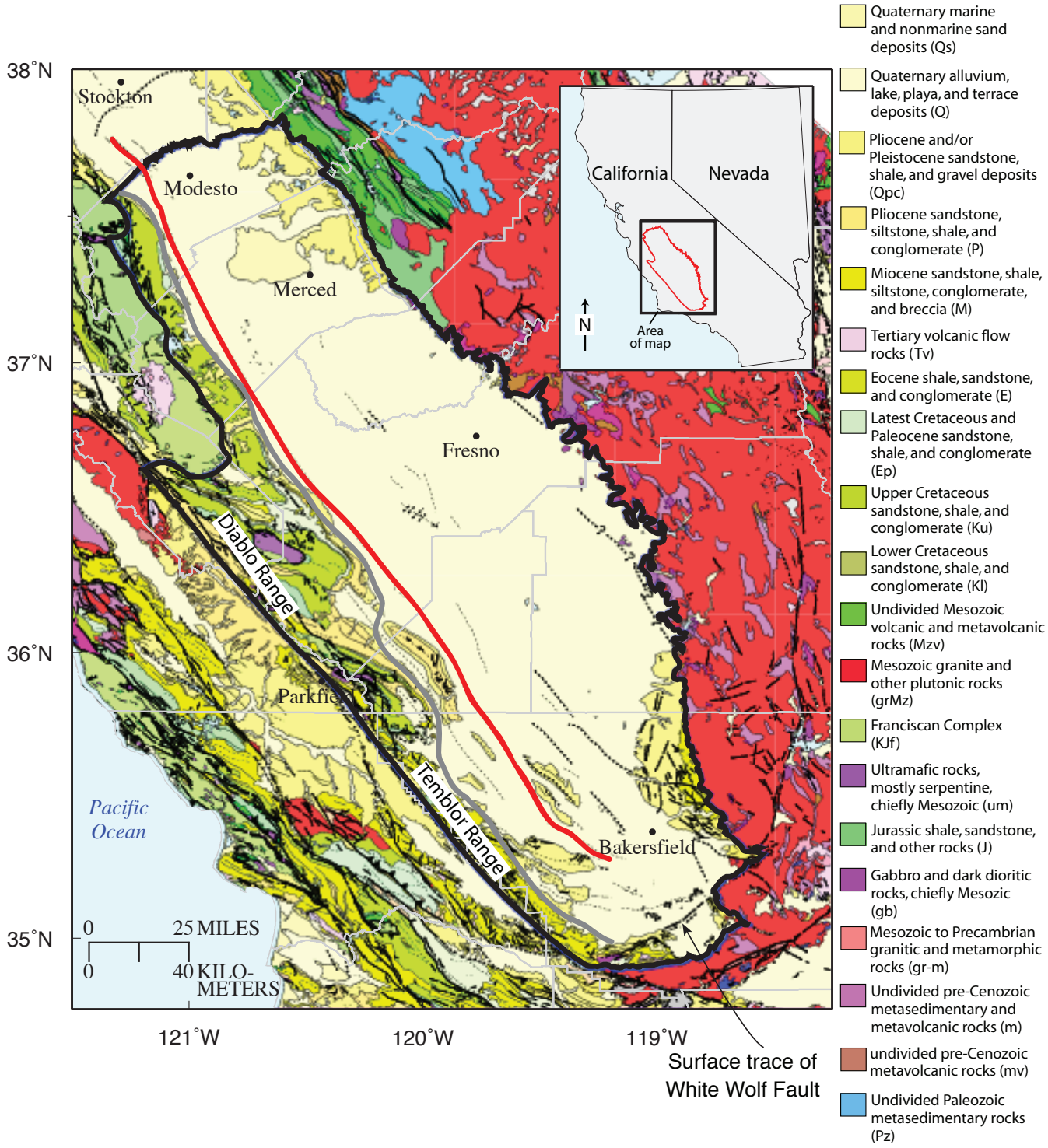

Figure 7.1. Geologic map of the San Joaquin Basin Province and adjacent area, displayed in Mercator projection, based on the work of Jennings (1977) as represented digitally by Saucedo and others (2000). Heavy dark line marks the province boundary of the basin; heavy red line marks location of present day basin axis; heavy gray line separates the area of correspondence (east) from the area of unresolved complexity (west; see text for explanation); thin gray lines mark county boundaries. Abbreviations in legend refer to rock units of Saucedo and others (2000). Inset: Map shows the location of the San Joaquin Basin Province (red line) relative to California and Nevada borders. Heavy rectangle marks region of main map.

Figure 7.2. *A*, San Joaquin Basin Province stratigraphy showing petroleum reservoir rocks and potential petroleum source rocks. See Hosford Scheirer and Magoon (this volume, chapter 5) for complete explanation of the figure. Note that ages of basement rock exceed the timescale shown in figure. Formation names in italics are informal and are defined as follows (in approximate age order): Forbes formation of Kirby (1943), Sacramento shale and Lathrop sand of Callaway (1964), Sawtooth shale and Tracy sands of Hoffman (1964), Brown Mountain sandstone of Bishop (1970), Ragged Valley silt, Starkey sands, and Blewett sands of Hoffman (1964), Wheatville sand of Callaway (1964), San Carlos sand of Wilkinson (1960), Gatchell sand of Goudkoff (1943), Oceanic sand of McMasters (1948), Leda sand of Sullivan (1963), Tumey formation of Atwill (1935), Famoso sand of Edwards (1943), Rio Bravo sand of Noble (1940), Nozu sand of Kasline (1942), Zilch formation of Loken (1959), Stevens sand of Eckis (1940), Fruitvale shale of Miller and Bloom (1939), and Antelope shale of Graham and Williams (1985). *B*, Stratigraphic columns shown in figure 7.2*A* except rock units are grouped chronostratigraphically, colored as in accompanying three-dimensional model, and numbered as in table 7.1. Heavy, red dashed lines indicate the composite surfaces. *C*, Explanation of additional features in San Joaquin Basin Province (black outline). The regional subdivisions—north, central, and south—are explained in Hosford Scheirer and Magoon (this volume, chapter 5). The subsurface trace (dashed line) of the White Wolf Fault (WWF) bounds the stratigraphic column on the south. Oil fields are outlined in green and gas fields are outlined in red. The basin axis (heavy red line) is mapped in the three-dimensional model on the Temblor Composite Surface in the central and southern regions and on the Ragged Valley Composite Surface in the northern region. Heavy gray line that is somewhat parallel to the basin axis divides the area of correspondence (east) from the area of unresolved complexity (hachured area to the west).

A

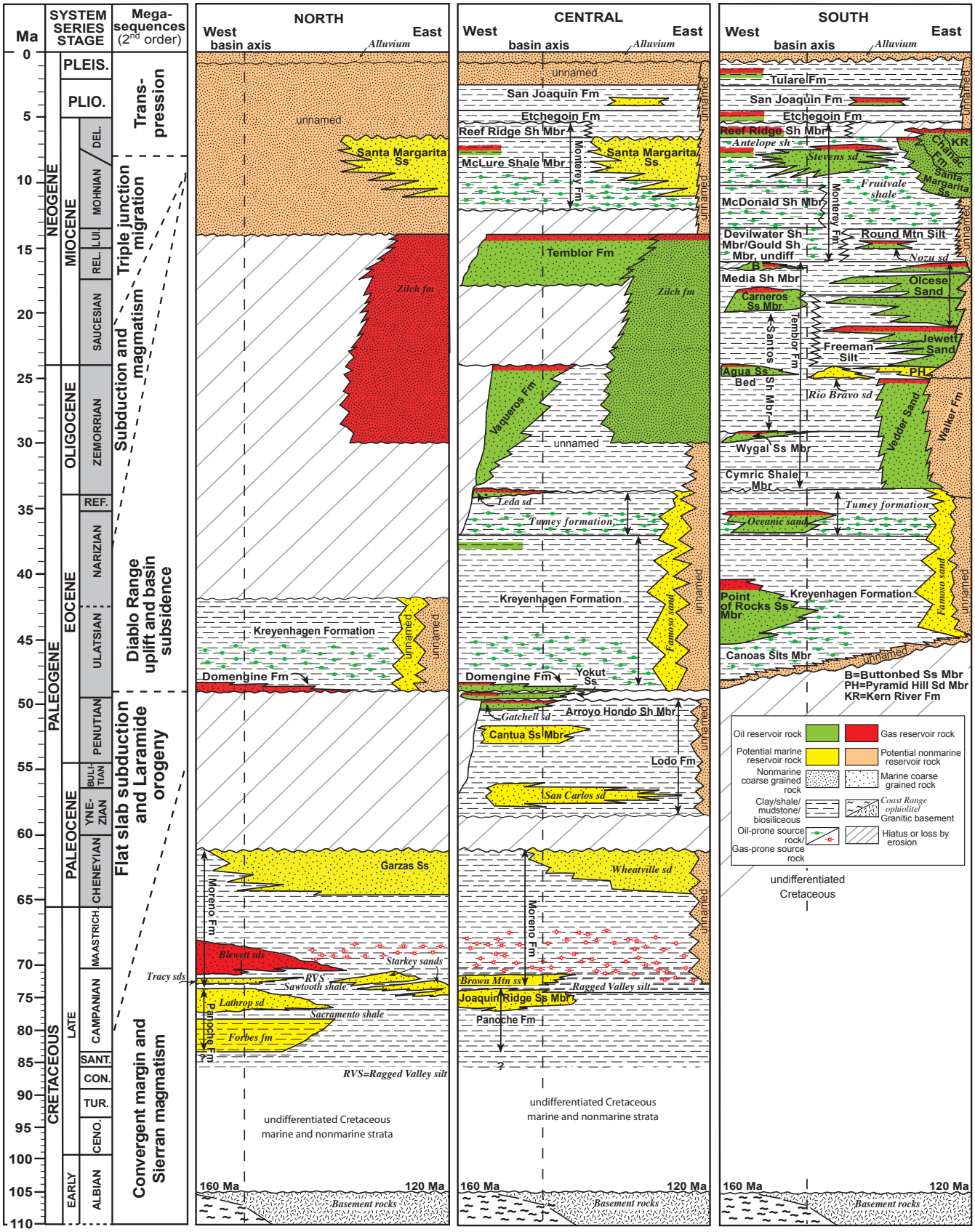
Ma
SYSTEM SERIES STAGE
Mega-sequences (2nd order)
Trans-pression
Triple junction migration
Subduction and magmatism
Diablo Range uplift and basin subsidence
Flat slab subduction and Laramide orogeny
Convergent margin and Sierran magmatism
NORTH
CENTRAL
SOUTH
West
East
basin axis
Alluvium
unnamed
Santa Margarita Ss
Zilch fm
Kreyenhagen Formation
Domengine Fm
Garzas Ss
Blewett sds
Tracy sds
RVS
Sawtooth shale
Starkey sands
Lathrop sd
Sacramento shale
Forbes fm
RVS=Ragged Valley silt
undifferentiated Cretaceous marine and nonmarine strata
Basement rocks
160 Ma
120 Ma
San Joaquin Fm
Etchegoin Fm
Reef Ridge Sh Mbr
McLure Shale Mbr
Monterey Fm
Temblor Fm
Vaqueros Fm
Leda sd
Tumey formation
Famoso sand
Yokut Ss
Gatchell sd
Arroyo Hondo Sh Mbr
Cantua Ss Mbr
Lodo Fm
San Carlos sd
Moreno Fm
Wheatville sd
Brown Mtn ss
Ragged Valley silt
Joaquin Ridge Ss Mbr
Panoche Fm
Tulare Fm
Antelope sh
Stevens sd
Fruitvale shale
McDonald Sh Mbr
Devilwater Sh Mbr/Gould Sh Mbr, undiff
Round Mtn Silt
Nozu sd
Media Sh Mbr
Olcese Sand
Carneros Ss Mbr
Santos Sh Mbr
Freeman Silt
Jewett Sand
PH
Agua Ss Bed
Rio Bravo sd
Vedder Sand
Walker Fm
Wygal Ss Mbr
Cymric Shale Mbr
Oceanic sand
Point of Rocks Ss Mbr
Canoas Slts Mbr
B=Buttonbed Ss Mbr
PH=Pyramid Hill Sd Mbr
KR=Kern River Fm
Oil reservoir rock
Gas reservoir rock
Potential marine reservoir rock
Potential nonmarine reservoir rock
Nonmarine coarse grained rock
Marine coarse grained rock
Clay/shale/mudstone/biosiliceous
Coast Range ophiolite
Granitic basement
Oil-prone source rock/Gas-prone source rock
Hiatus or loss by erosion
undifferentiated Cretaceous

B

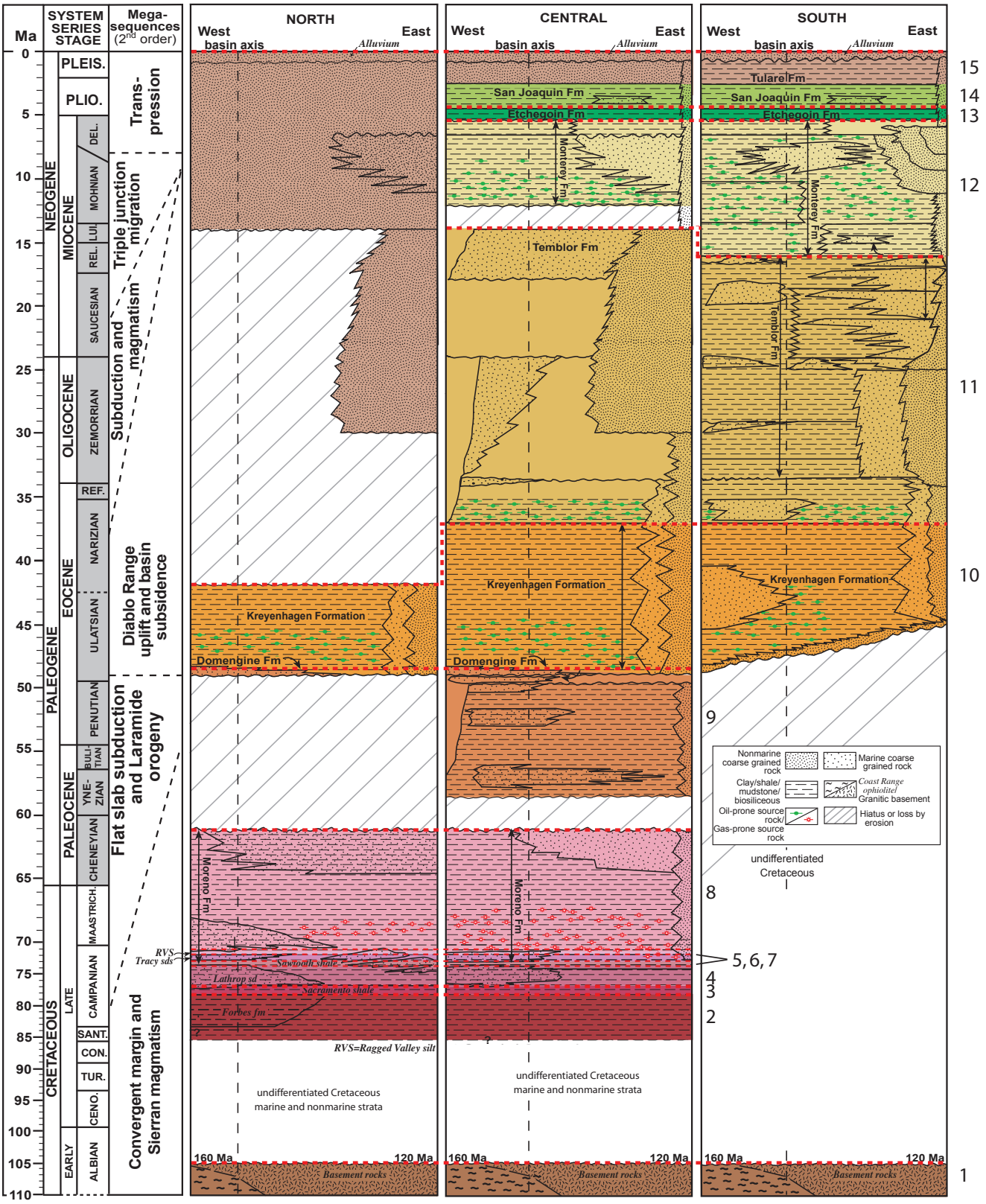

Figure 7.2.—Continued

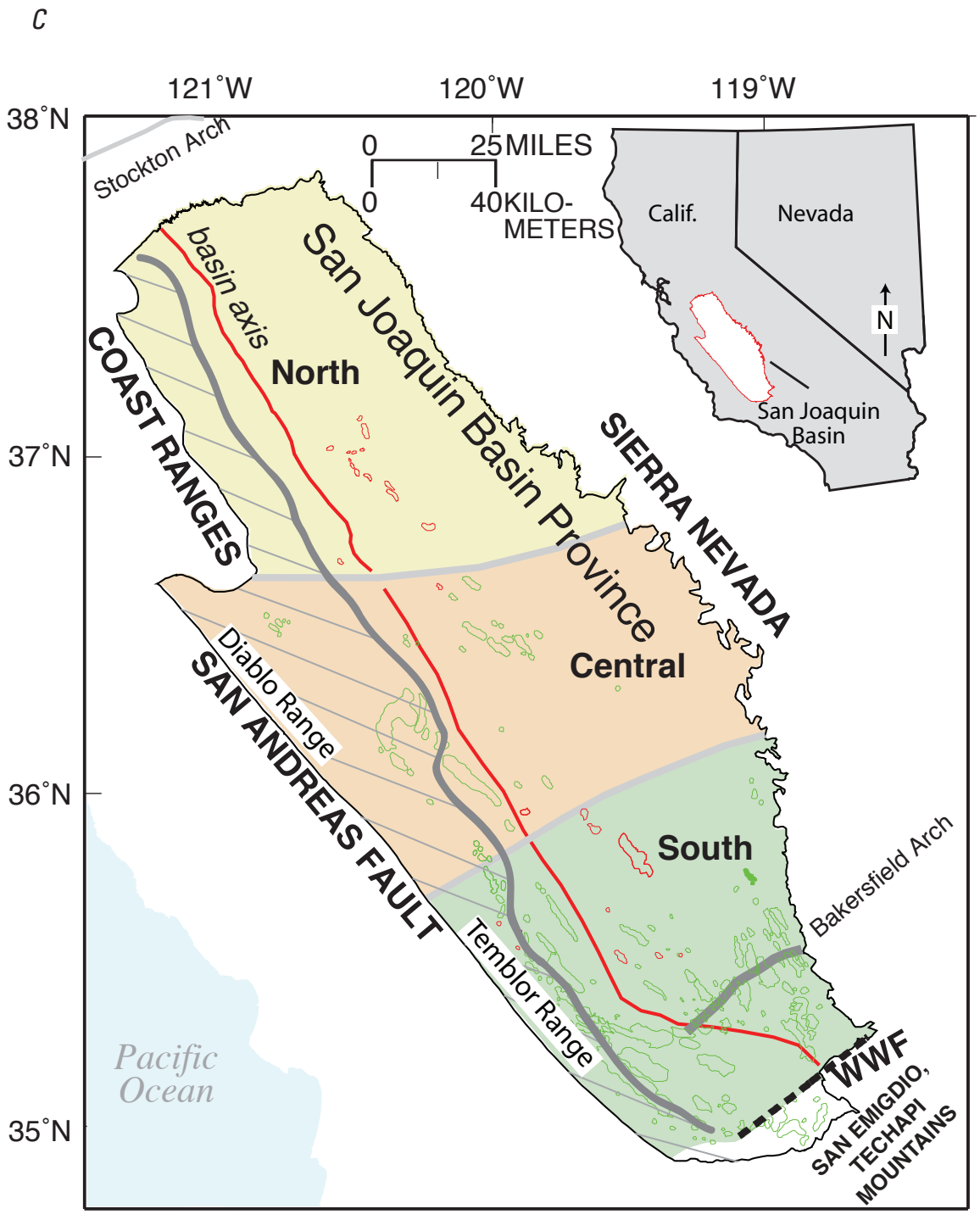

Figure 7.2.—Continued

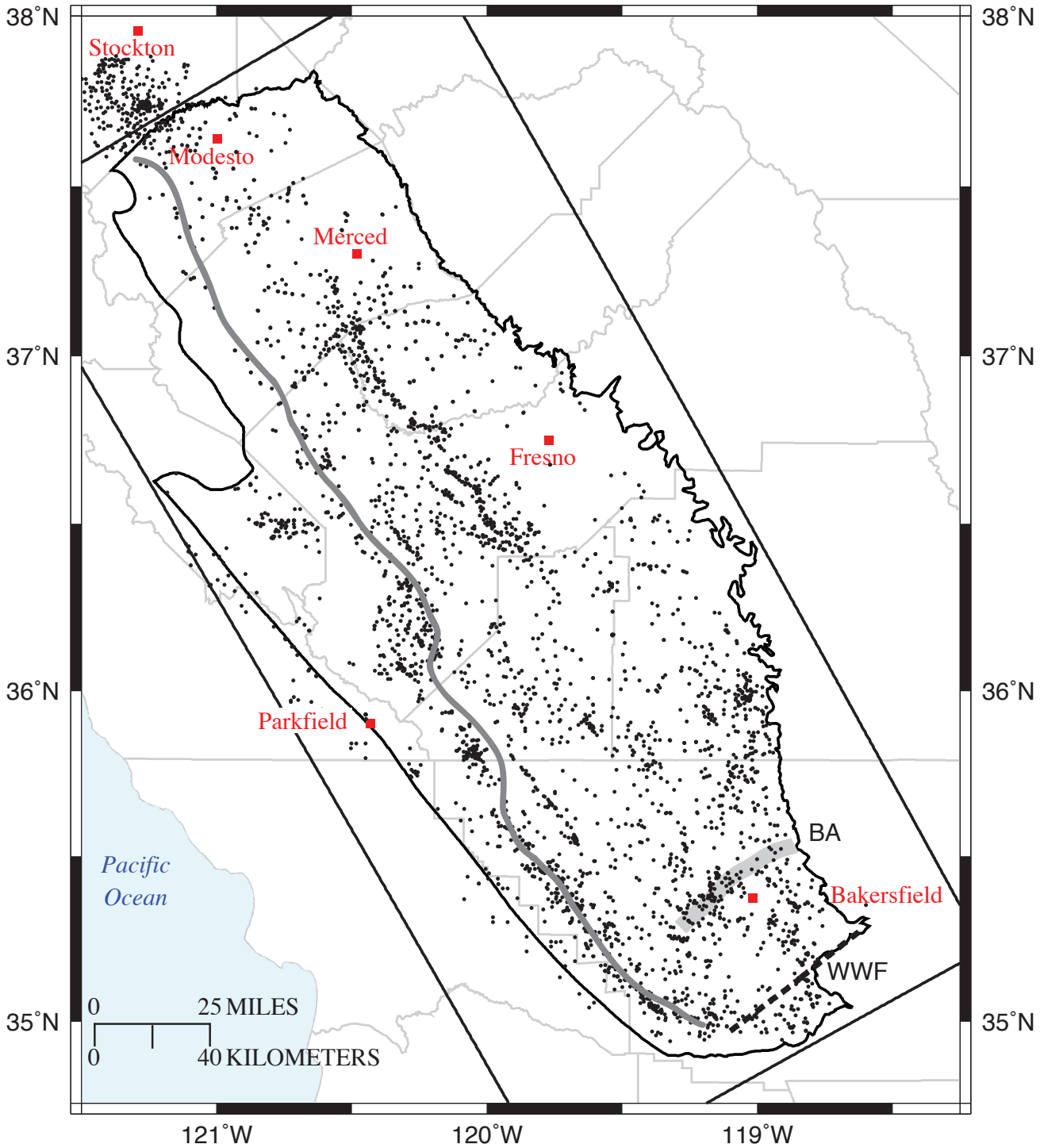

Figure 7.3. Geographic distribution of wells in the database (appendix 7.2) used to create the geologic model of the San Joaquin Basin. Heavy black line marks the province boundary, heavy gray line divides the area of correspondence (east) from the area of unresolved complexity (west), and surrounding bold rectangle defines the rectangular model space. Thin gray lines mark county boundaries. Broad gray shaded line location of the Bakersfield Arch (BA) and thin gray lines mark county boundaries. Dashed line indicates approximate location of White Wolf Fault (WWF). Well locations, shown as solid dots, are from the California Department of Conservation, Division of Oil, Gas, and Geothermal Resources (2012).

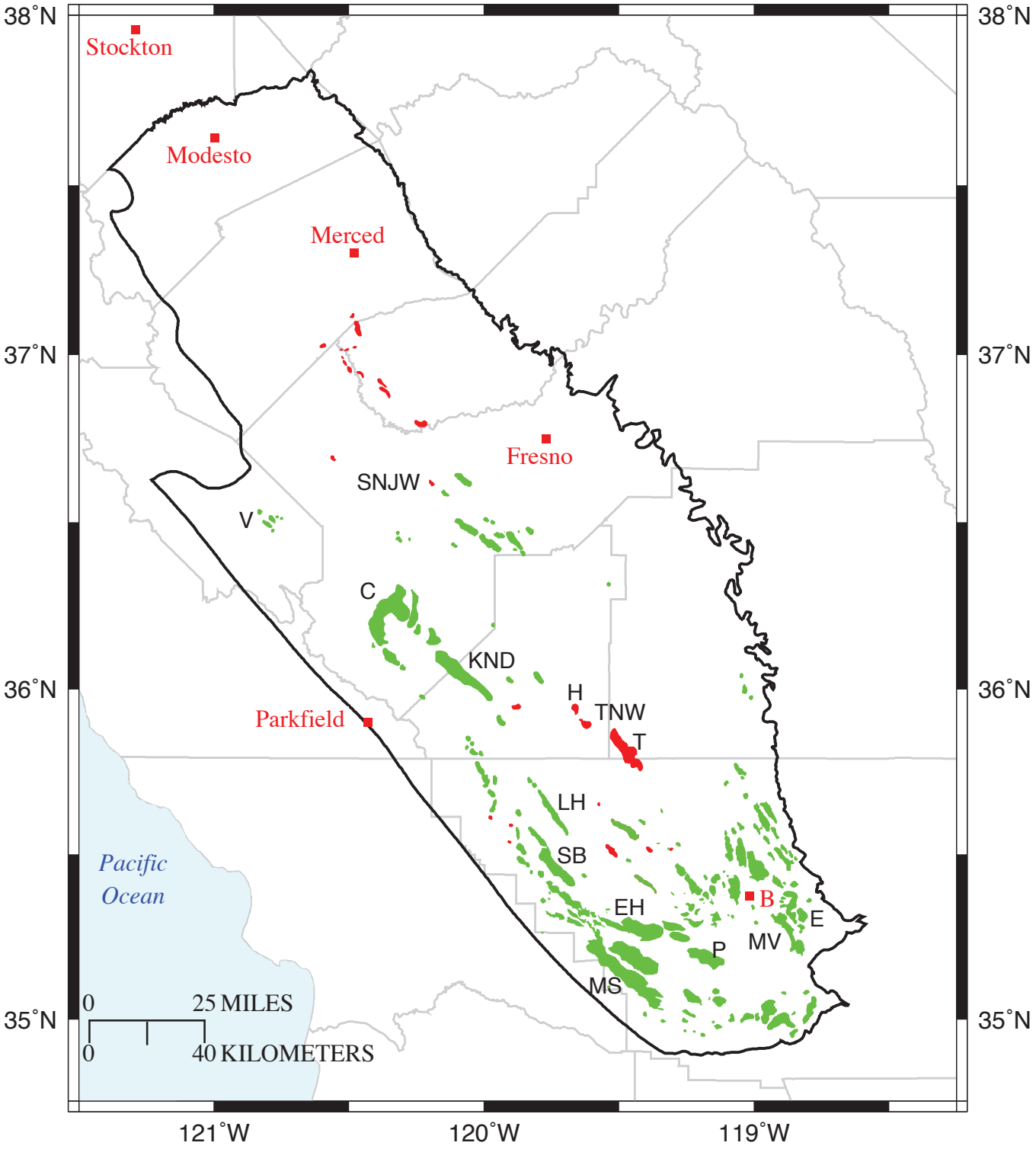

Figure 7.4. Index map of San Joaquin Basin Province oil (green) and gas (red) fields referred to in the text. Heavy black line marks the province boundary and thin gray lines mark county boundaries. The location of the city of Bakersfield is abbreviated (B) in red. Field abbreviations are: C, Coalinga; E, Edison; EH, Elk Hills; H, Harvester; KND, Kettleman North Dome; LH, Lost Hills; MS, Midway Sunset; MV, Mountain View; P, Paloma; SB, South Belridge; SJNW, San Joaquin Northwest; T, Trico; TNW, Trico Northwest; V, Vallecitos.

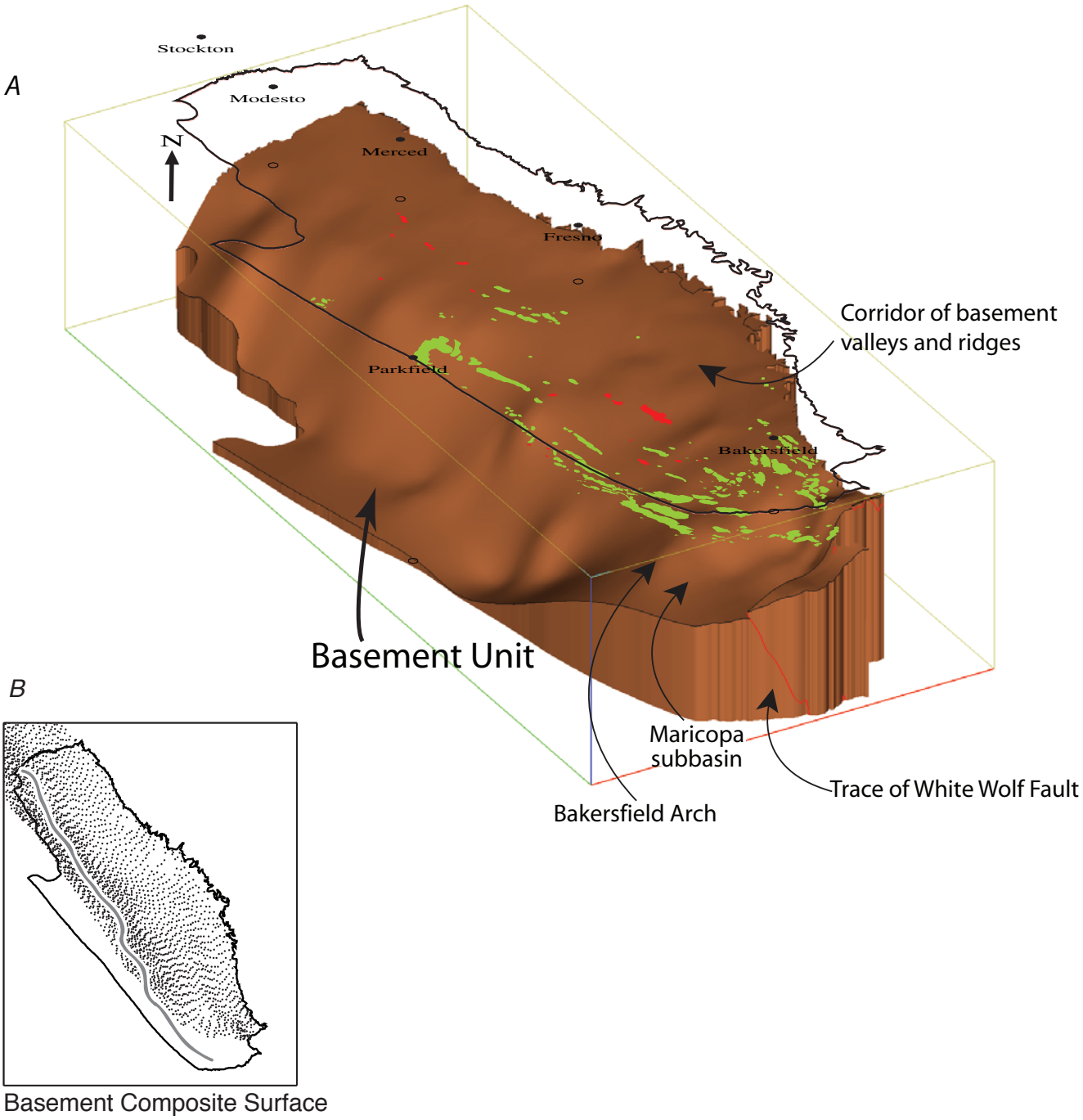

Figure 7.5. *A*, Oblique view of the Basement Composite Surface extracted from the three-dimensional model of the San Joaquin Basin Province. Oil and gas field outlines are draped on the surface with green and red fill, respectively. View is from due south at a 30° inclination angle. Grid resolution is 0.5 mile. In this and all other images of its type, the bounding polygon illustrates the model space within which the geologic map is assembled; the San Joaquin Basin Province boundary (bold stroke) and the city names and locations float above the model space, and the vertical exaggeration is 4×. *B*, Geographic distribution of basement rock observations. Dark stippling indicates dense seismic grid, reduced by a factor of 10 to avoid crowding in the figure. Black heavy line marks the province boundary and heavy grey line divides the area of correspondence (east) from the area of unresolved complexity (west). *C*, Structure contour map of the basement composite surface output from the three-dimensional geologic model. Contour interval is 2,000 feet. Broad gray band marks the location and trend of the Bakersfield Arch. White labels and dashed lines define basement corridors as discussed in text. In this map and subsequent maps of this type, dashed line marks the surface trace of the White Wolf Fault as modeled by Bawden (2001). Thin gray lines mark county boundaries.

C

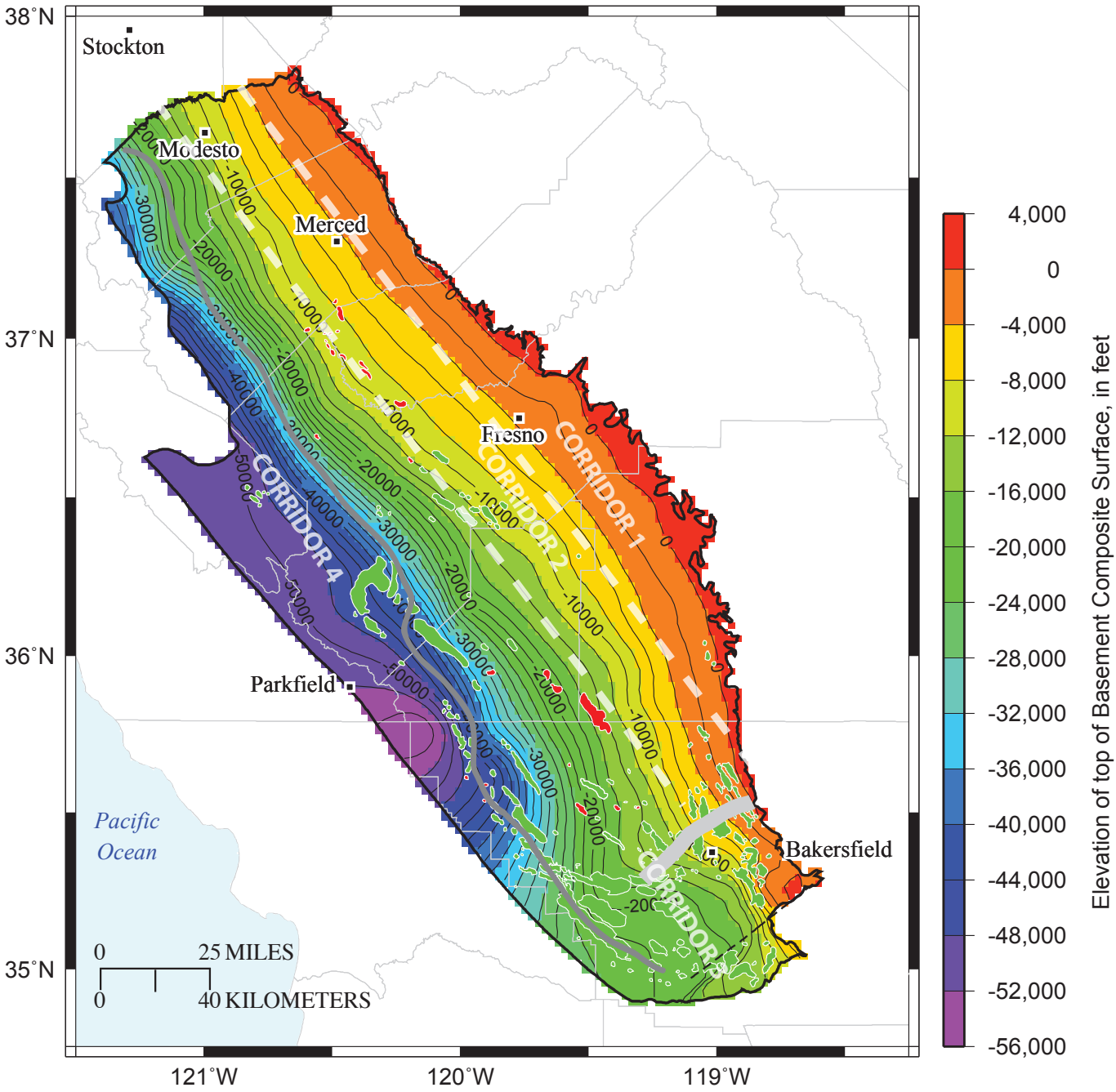

Figure 7.5.—Continued

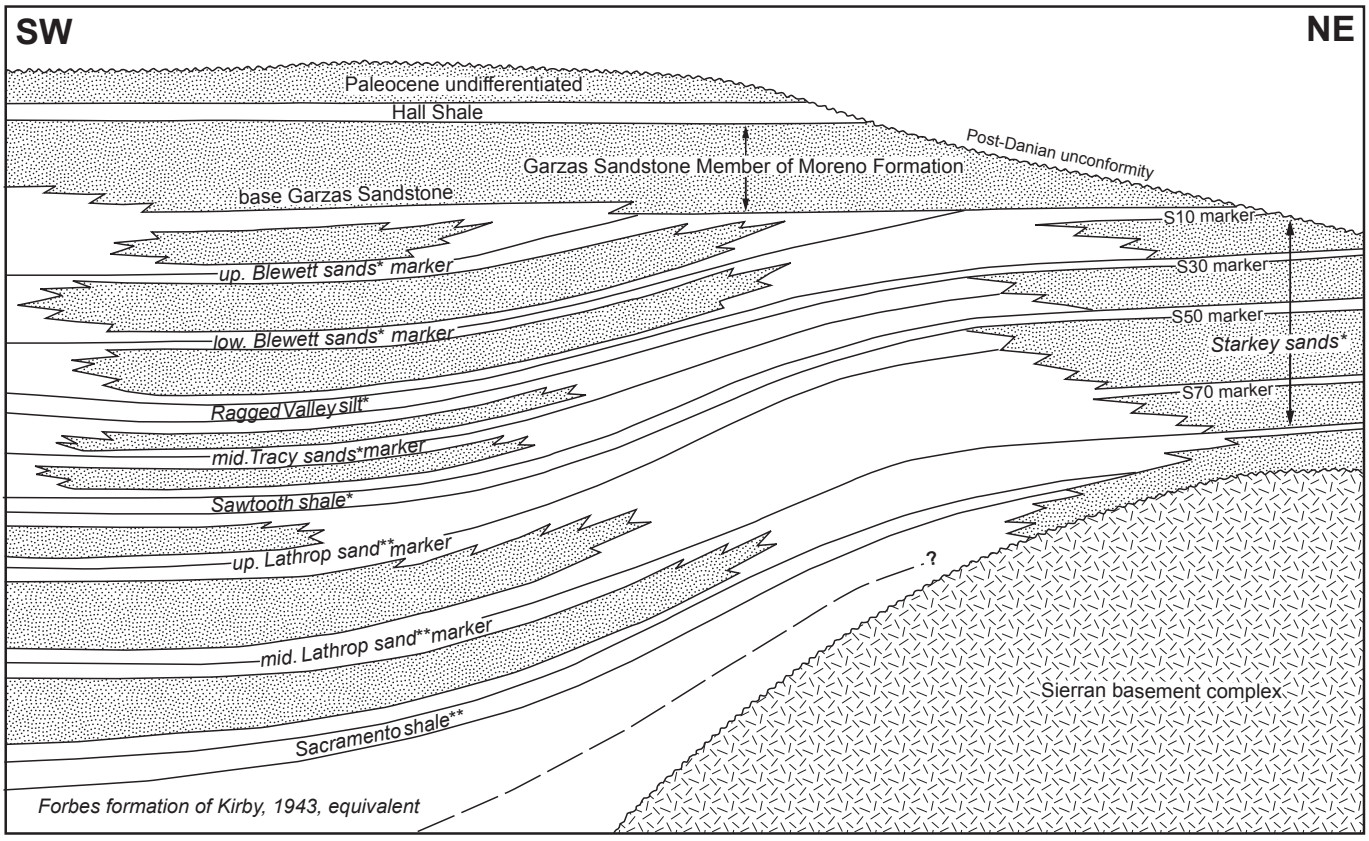

Figure 7.6. Schematic depositional framework and stratigraphic relationships for the Late Cretaceous sedimentary sequence in the northern San Joaquin Valley. Figure modified from Nilsen and Moore (1997) and reprinted with permission from the Pacific Section of the American Association of Petroleum Geologists. Formation names in figure are modified in accordance with standard U.S. Geological Survey geologic names usage; italics denote informal geologic names. "S10 marker," "S30 marker," "S50 marker," and "S70 marker" refer to intraformational markers identified on well logs by Applied Earth Technology (1990). low., lower; mid., middle; up., upper.

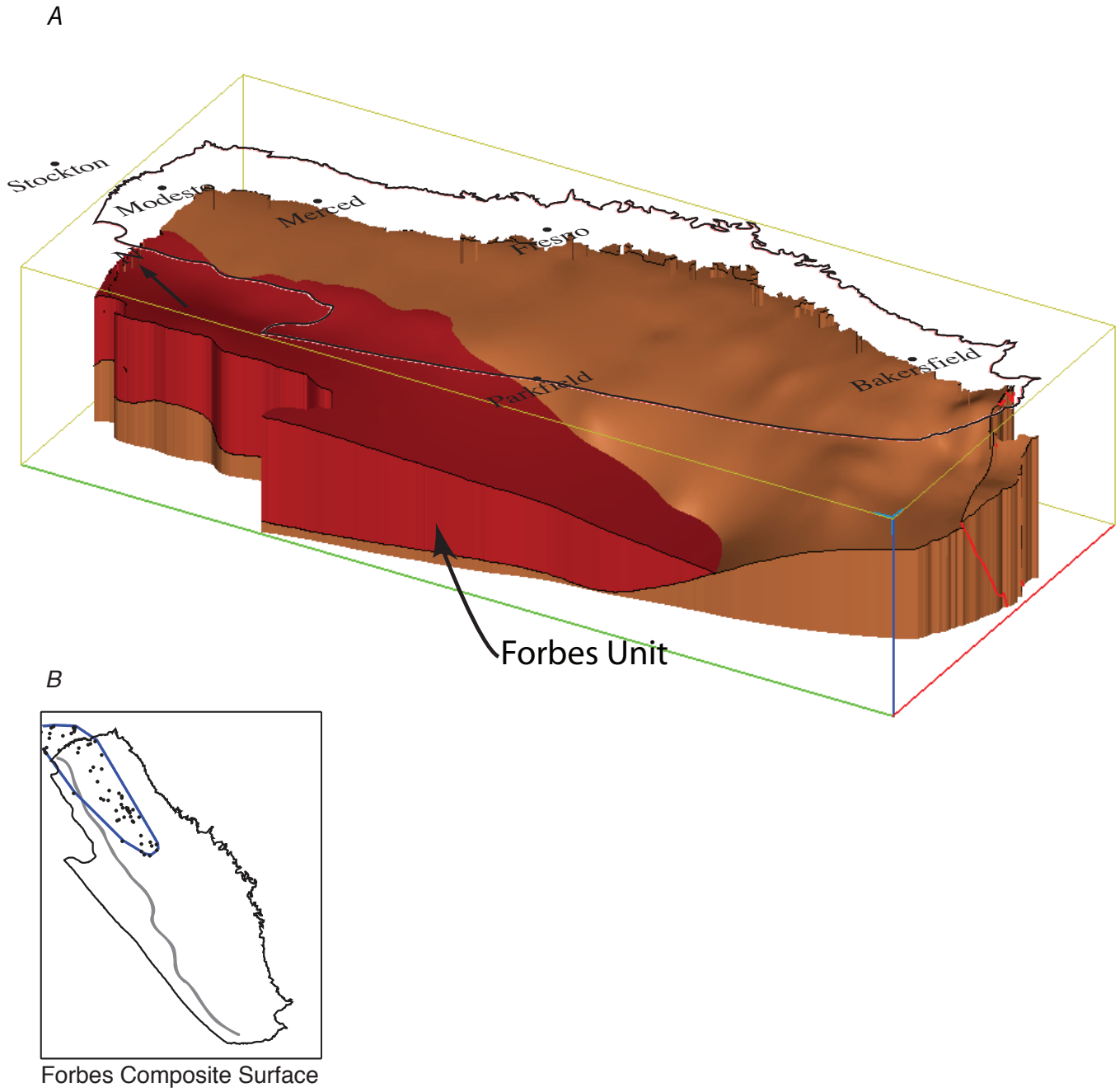

Figure 7.7. *A*, Oblique view of the Forbes Composite Surface. View is from 30° west of south at a 30° inclination angle. Grid resolution is 1 mile. *B*, Geographic distribution of observations; these can be viewed page-size in Hosford Scheirer and Magoon (this volume, chapter 5). *B*, In panels *B, C*, and *D*, heavy black line marks the province boundary, heavy grey line divides the area of correspondence (east) from the area of unresolved complexity (west), and blue polygon surrounds input well data and thus encloses best-determined part of the surface. *C* , Structure contour map of the elevation of the Forbes Composite Surface. Contour interval is 2,000 feet. In panels *C* and *D*, thin gray lines mark county boundaries. Note that age-equivalent units crop out on the basin's margin, as shown in figure 7.1, so the model is known to be inaccurate there. *D*, Thickness of the unit bounded by the Forbes Composite Surface (top) and the basement composite surface (base).

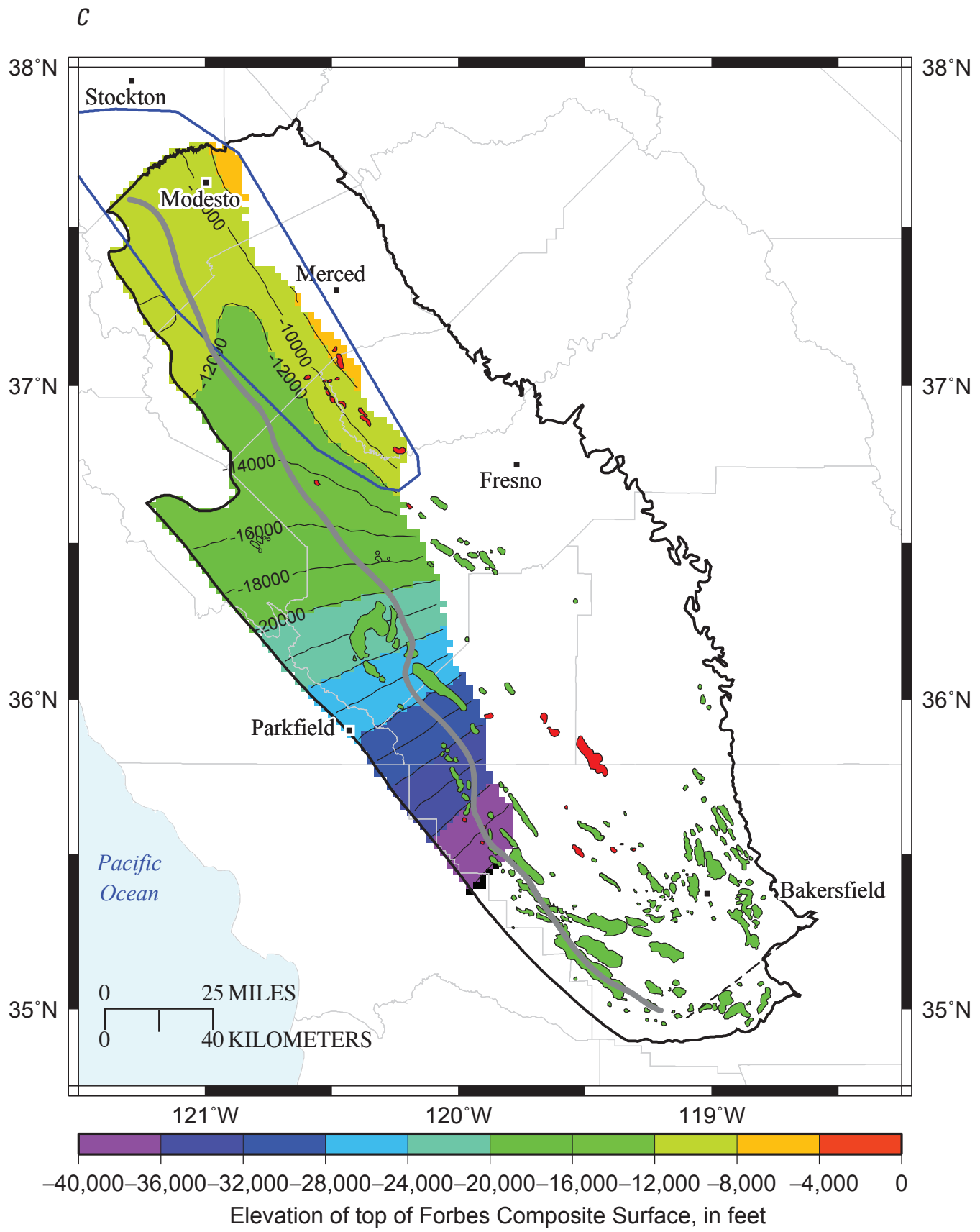

Figure 7.7.—Continued

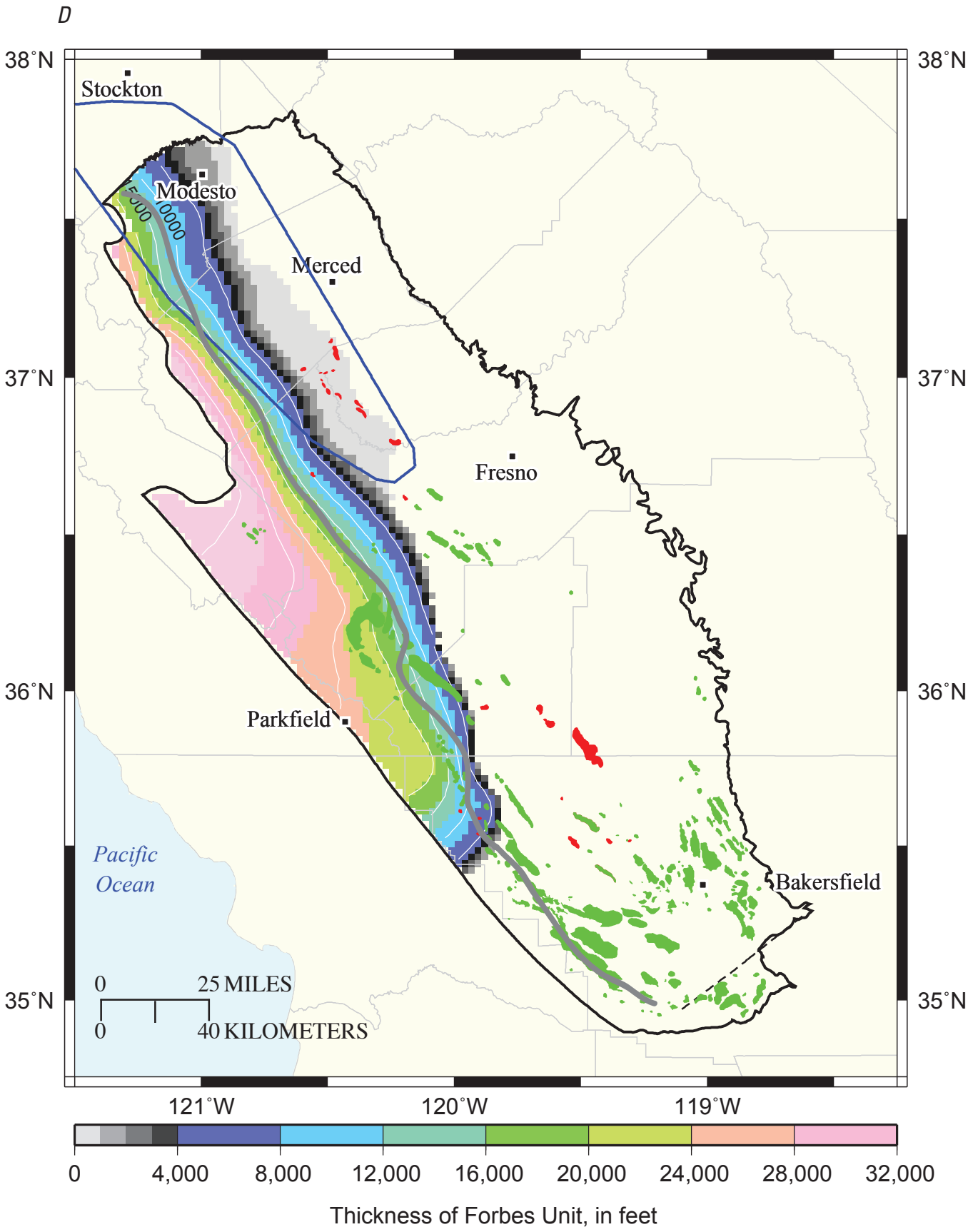

Figure 7.7.—Continued

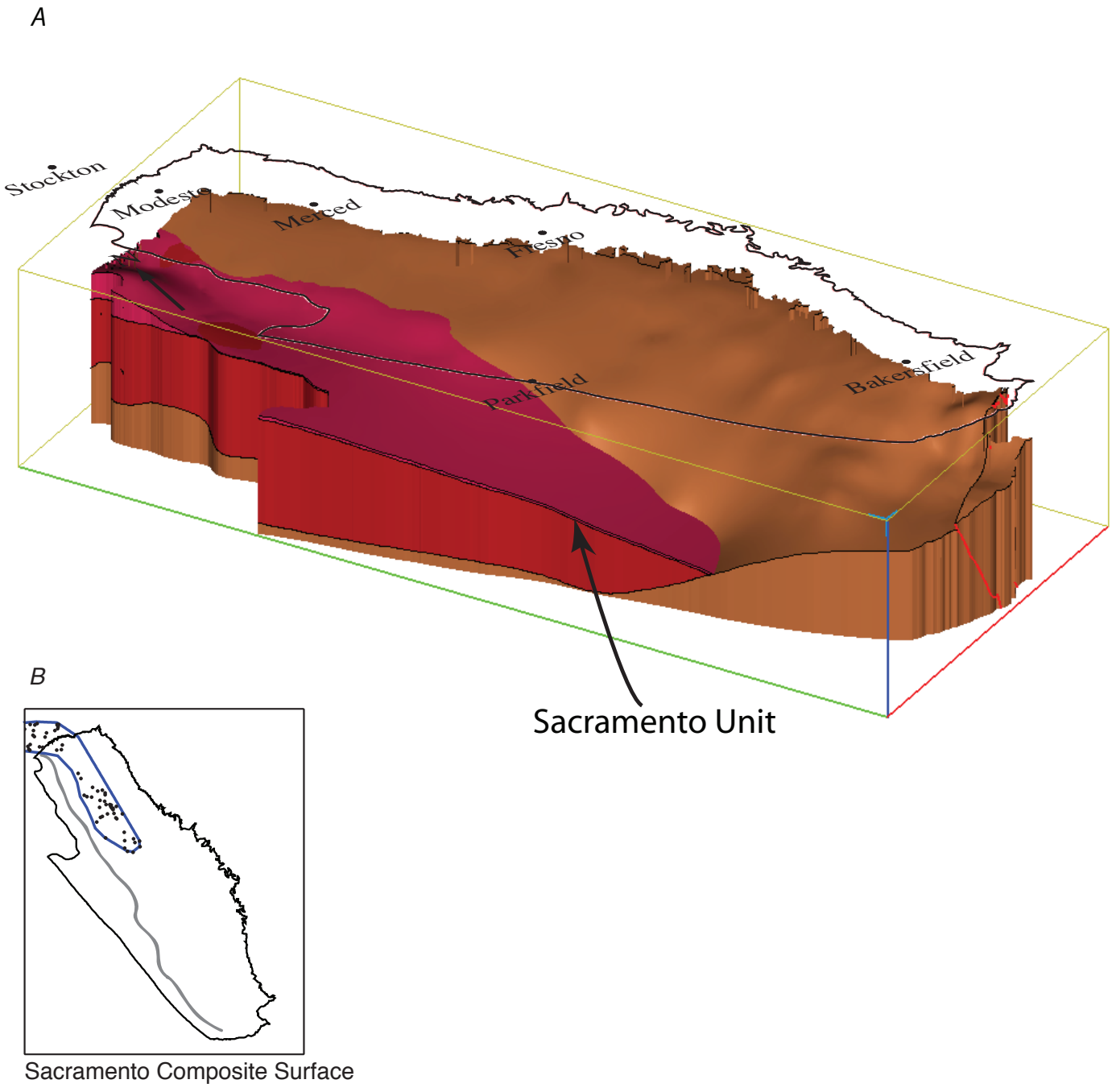

Figure 7.8. *A*, Oblique view of the Sacramento Composite Surface. View is from 30° west of south at a 30° inclination angle. Grid resolution is 1 mile. *B*, Geographic distribution of observations; these can be viewed page-size in Hosford Scheirer and Magoon (this volume, chapter 5). In panels *B, C*, and *D,* heavy black line marks the province boundary, heavy gray line divides the area of correspondence (east) from the area of unresolved complexity (west), and blue polygon surrounds input well data and thus encloses best-determined part of the surface. *C*, Structure contour map of the elevation of the Sacramento Composite Surface. Contour interval is 2,000 feet. In panels *C* and *D*, thin gray lines mark county boundaries. *D*, Thickness of the unit bounded by the Sacramento Composite Surface (top) and the Forbes Composite Surface (base).

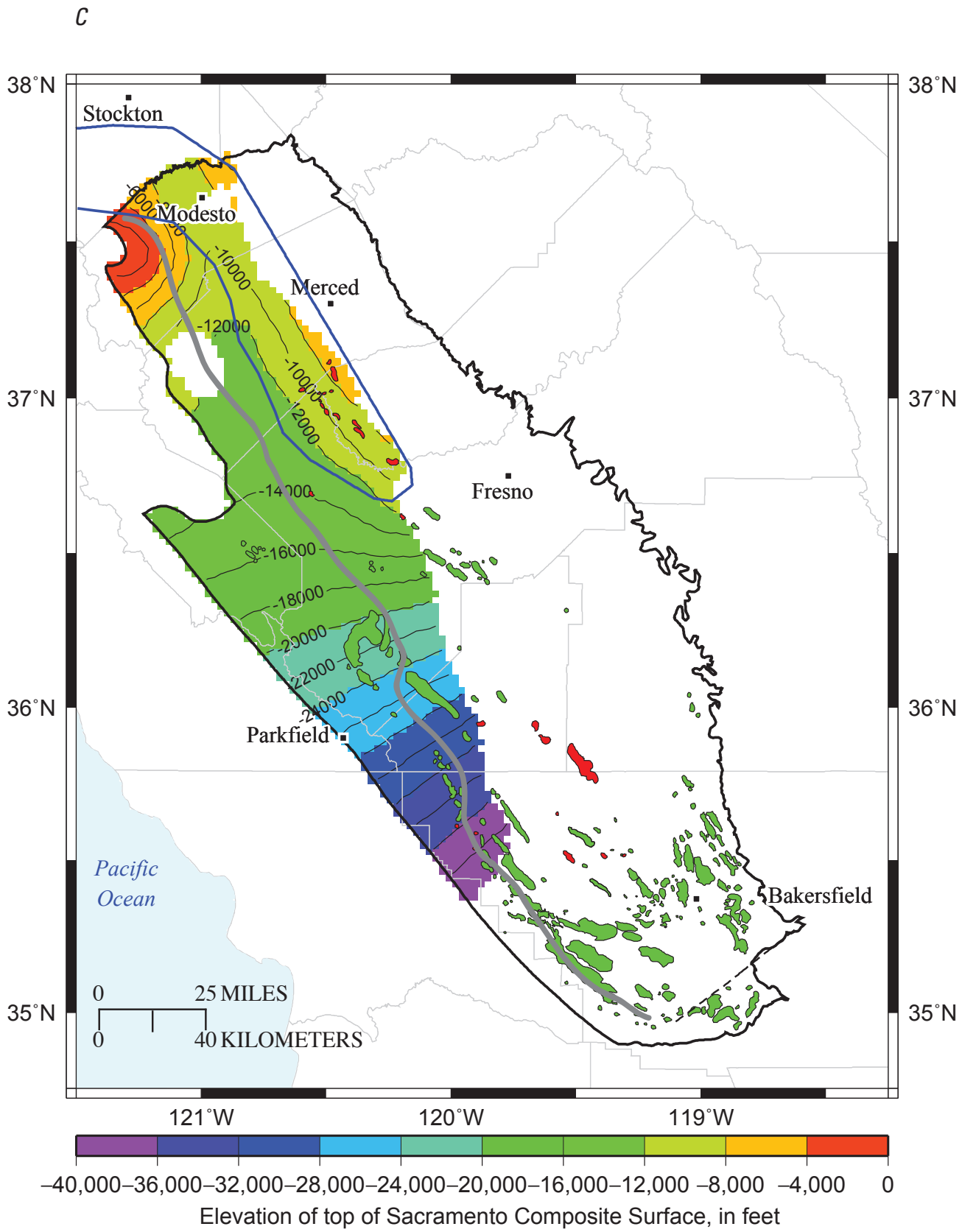

Figure 7.8.—Continued

D

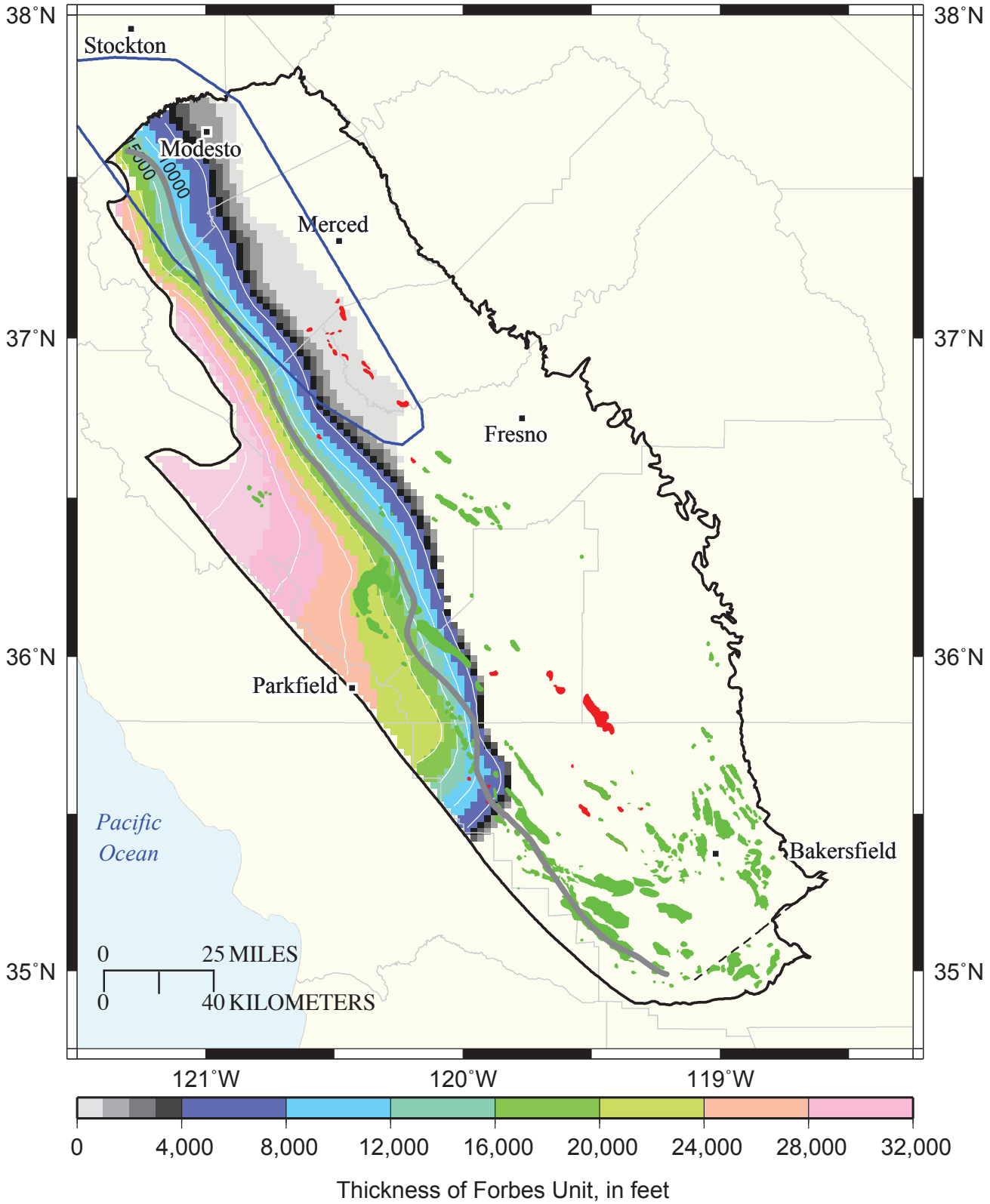

Figure 7.8.—Continued

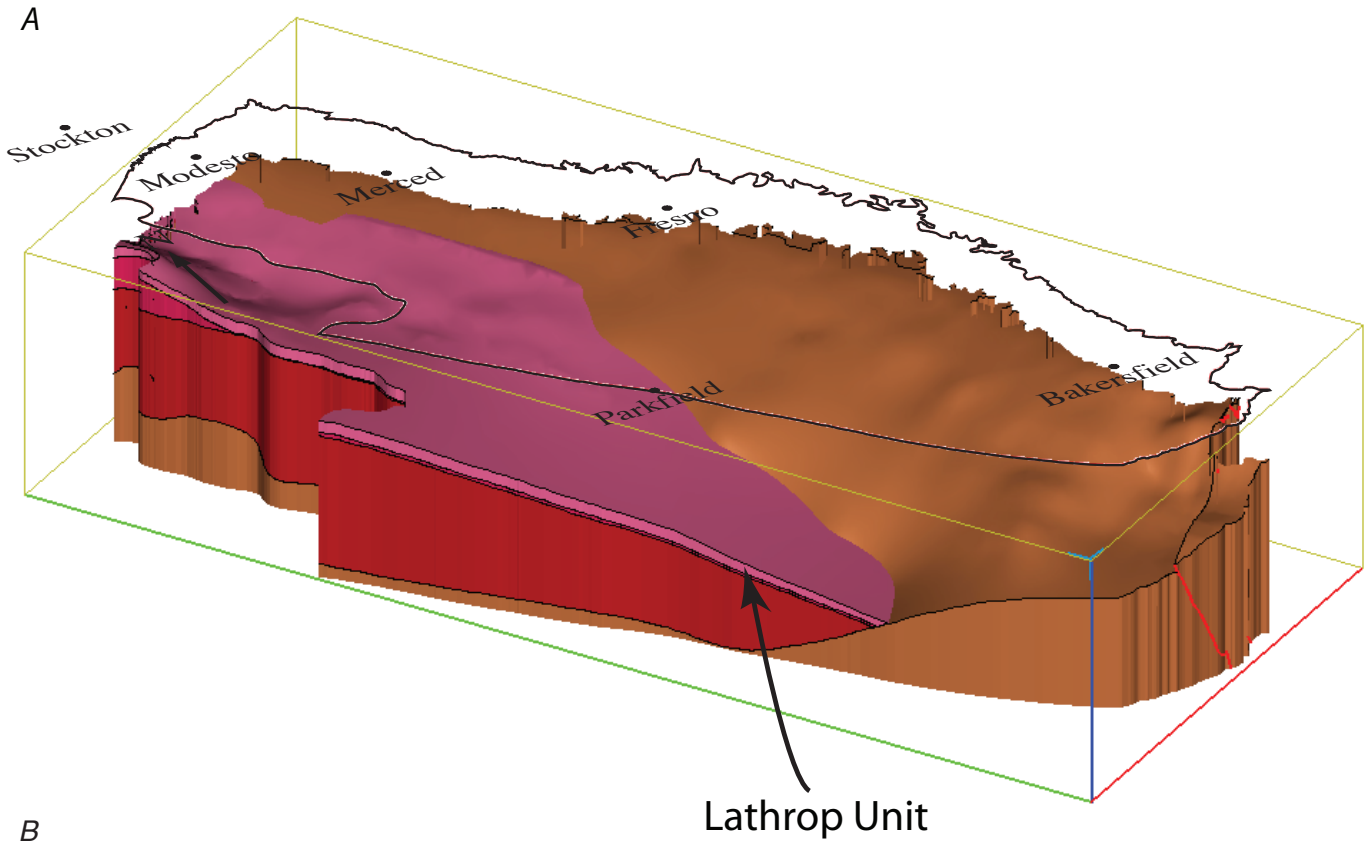

Figure 7.9. *A*, Oblique view of the Lathrop Composite Surface. View is from 30° west of south at a 30° inclination angle. Grid resolution is 1 mile. *B*, Geographic distribution of observations; these can be viewed page-size in Hosford Scheirer and Magoon (this volume, chapter 5). In panels *B, C,* and *D,* heavy black line marks the province boundary, heavy gray line divides the area of correspondence (east) from the area of unresolved complexity (west), and blue polygon surrounds input well data and thus encloses best-determined part of the surface. *C*, Structure contour map of the elevation of the Lathrop Composite Surface. Contour interval is 2,000 feet. In panels *C* and *D*, thin gray lines mark county boundaries. *D*, Thickness of the unit bounded by the Lathrop Composite Surface (top) and the Sacramento Composite Surface (base).

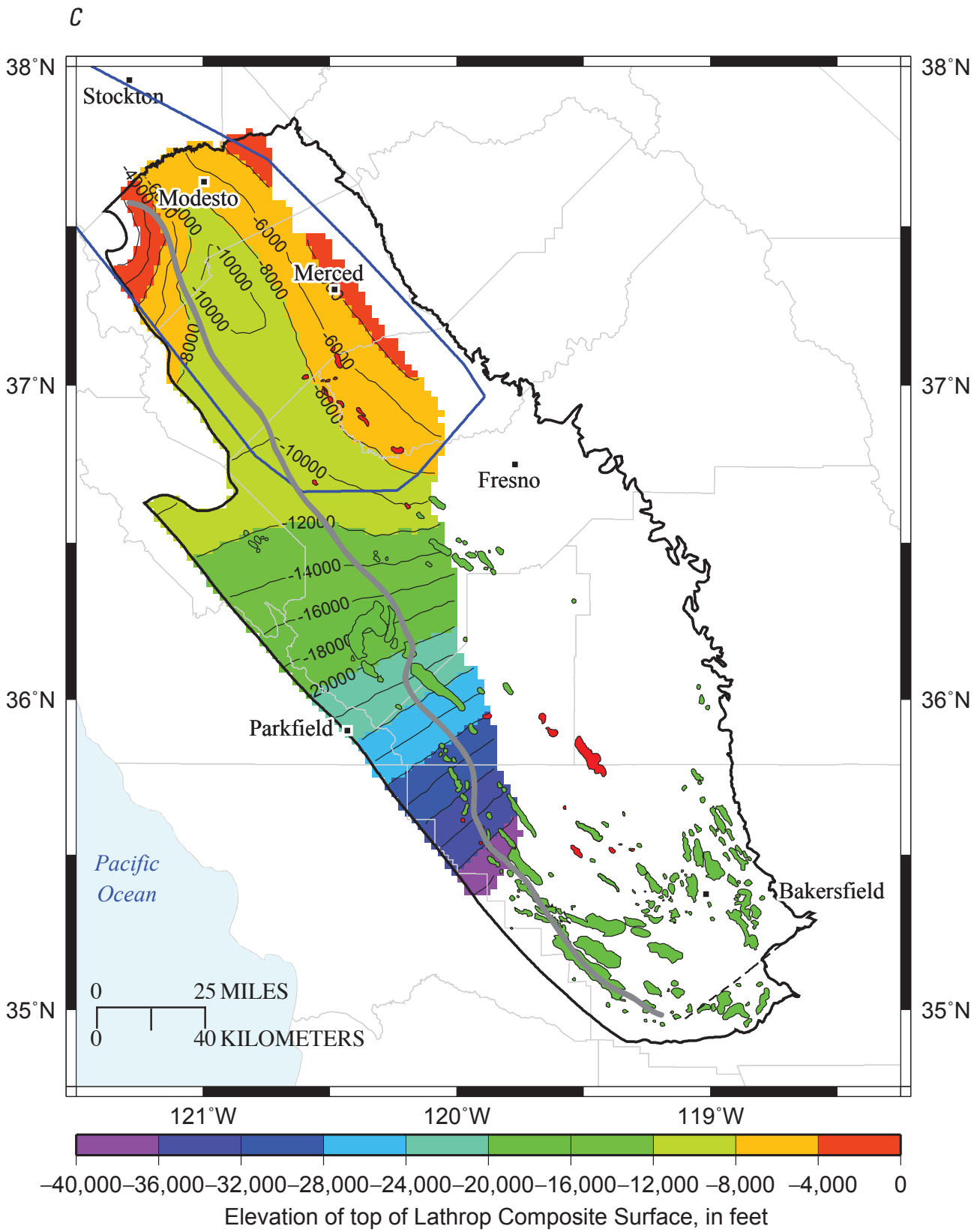

Figure 7.9.—Continued

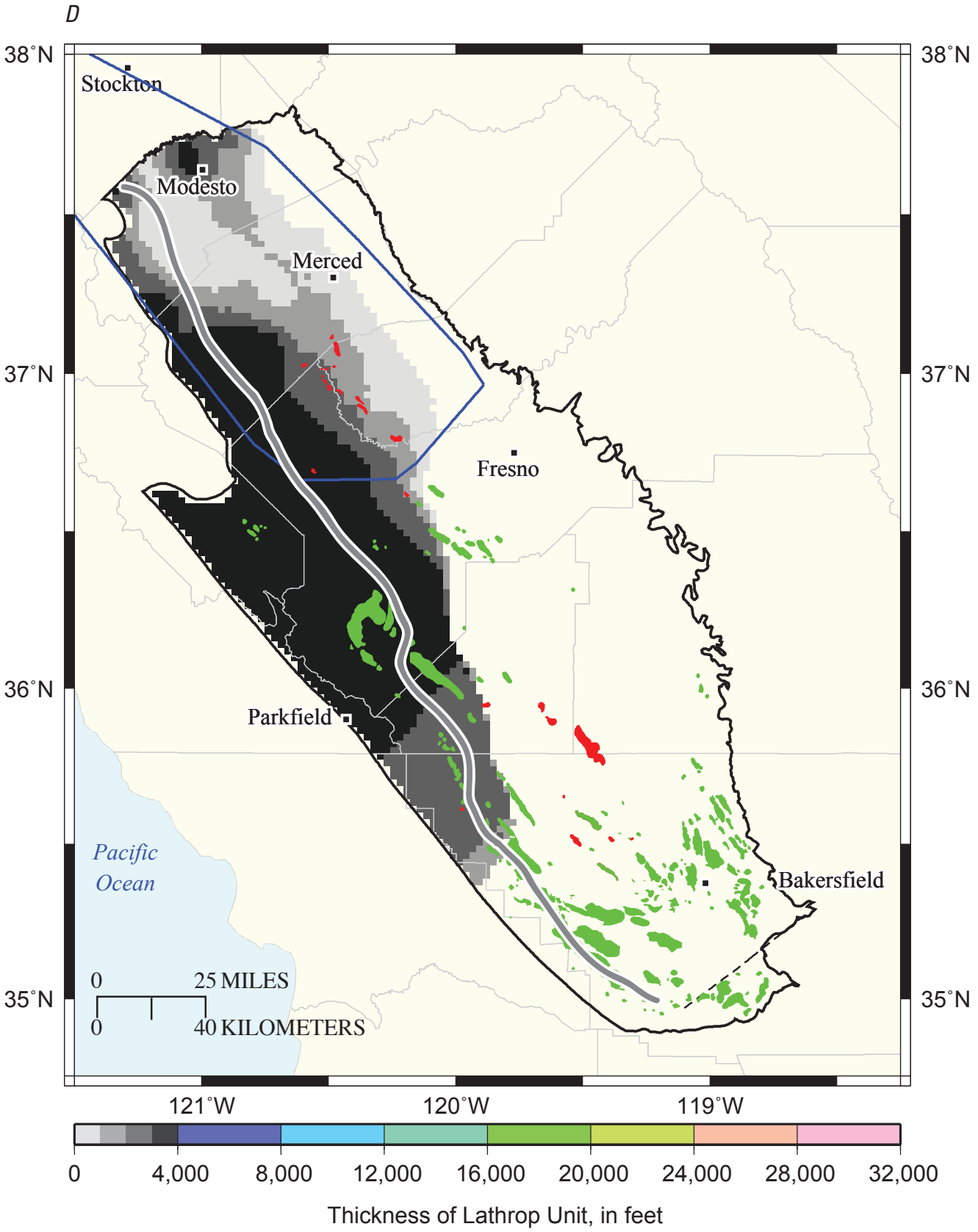

Figure 7.9.—Continued

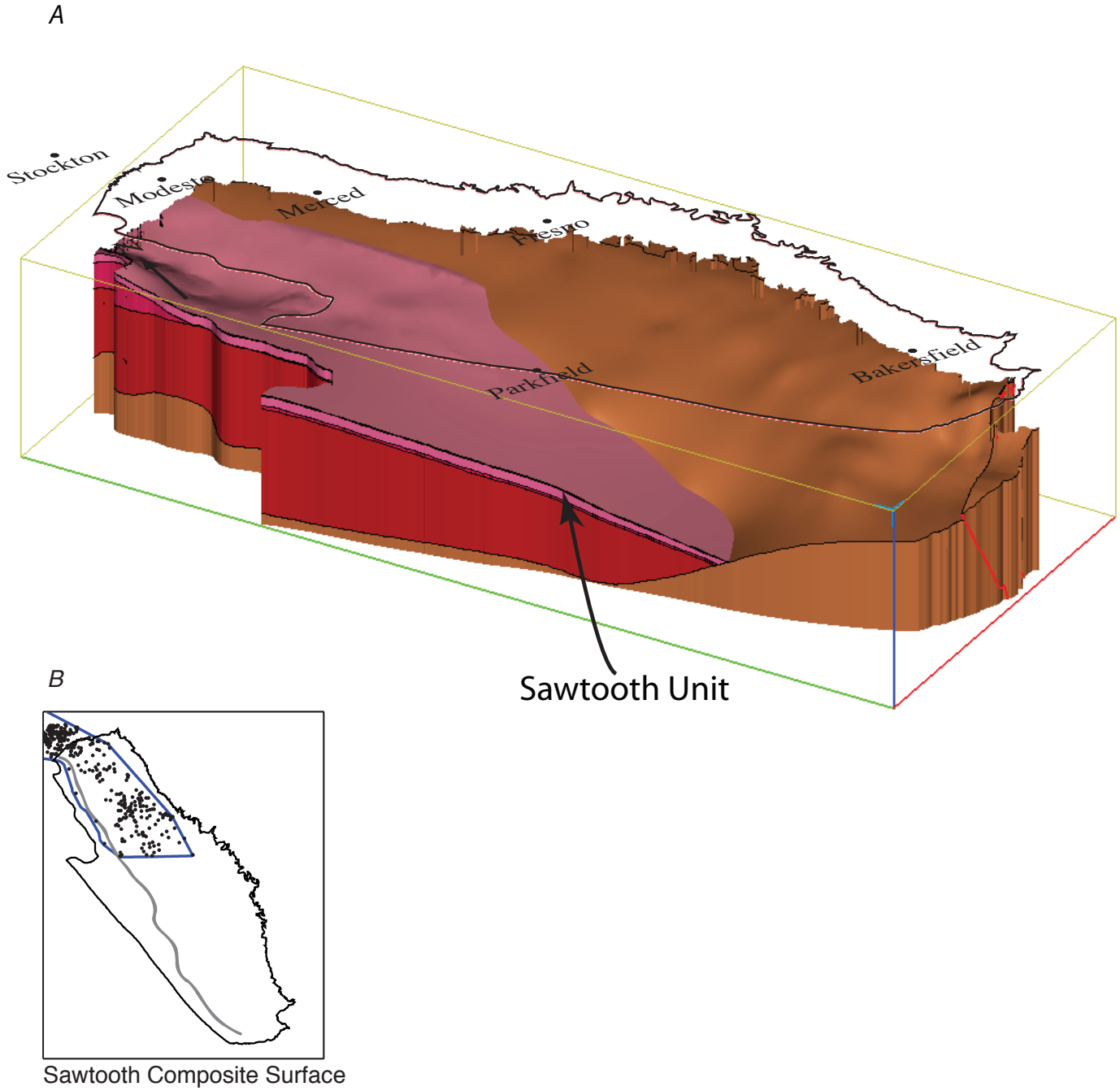

Figure 7.10. *A*, Oblique view of the Sawtooth Composite Surface. View is from 30° west of south at a 30° inclination angle. Grid resolution is 1 mile. *B*, Geographic distribution of observations; these can be viewed page-size in Hosford Scheirer and Magoon (this volume, chapter 5). In panels *B, C,* and *D,* heavy black line marks the province boundary, heavy gray line divides the area of correspondence (east) from the area of unresolved complexity (west), and blue polygon surrounds input well data and thus encloses best-determined part of the surface. *C,* Structure contour map of the elevation of the Sawtooth Composite Surface. Contour interval is 2,000 feet. In panels *C* and *D*, thin gray lines mark county boundaries. *D*, Thickness of the unit bounded by the Sawtooth Composite Surface (top) and the Lathrop Composite Surface (base). Dashed contours are 200-foot increments.

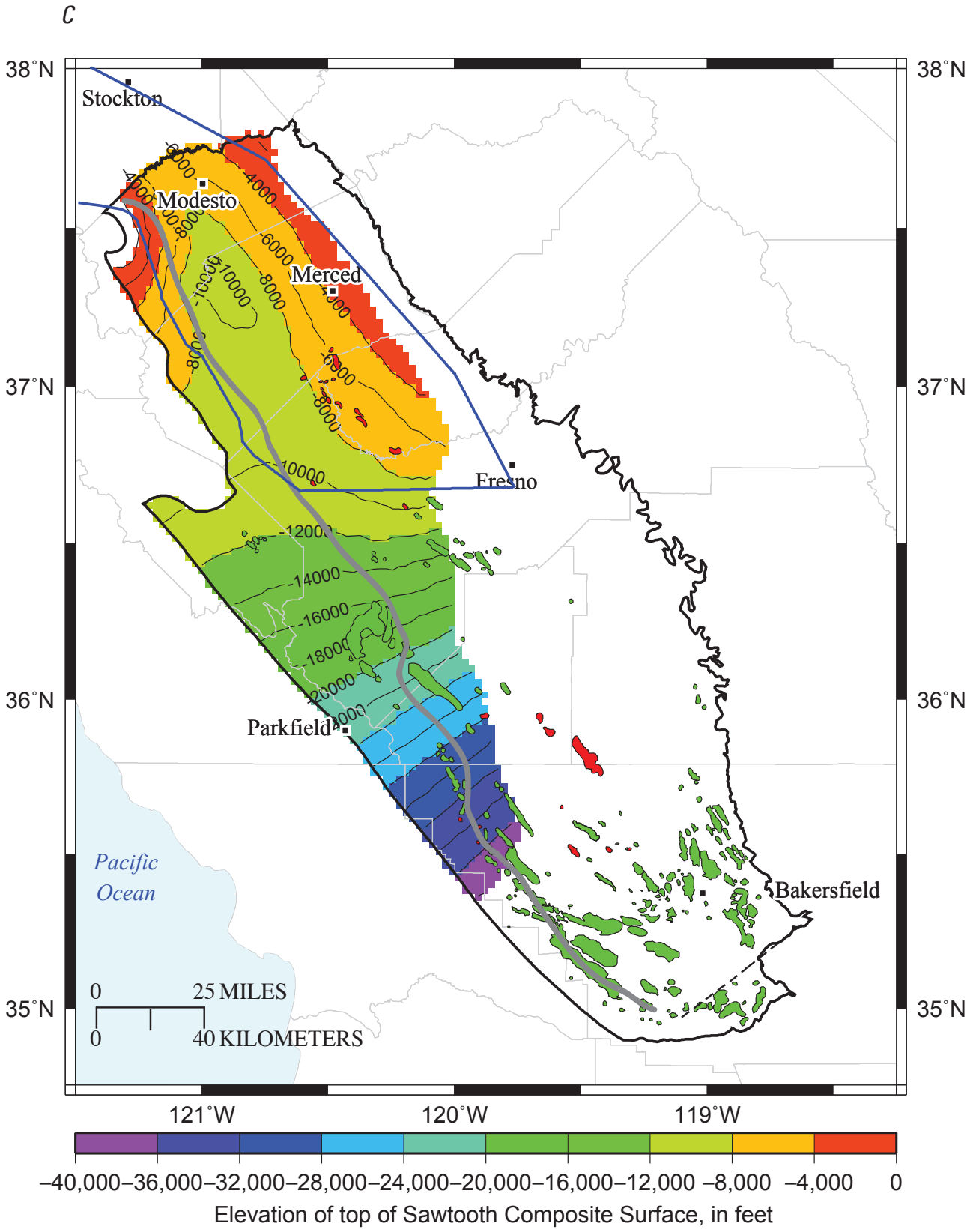

Figure 7.10.—Continued

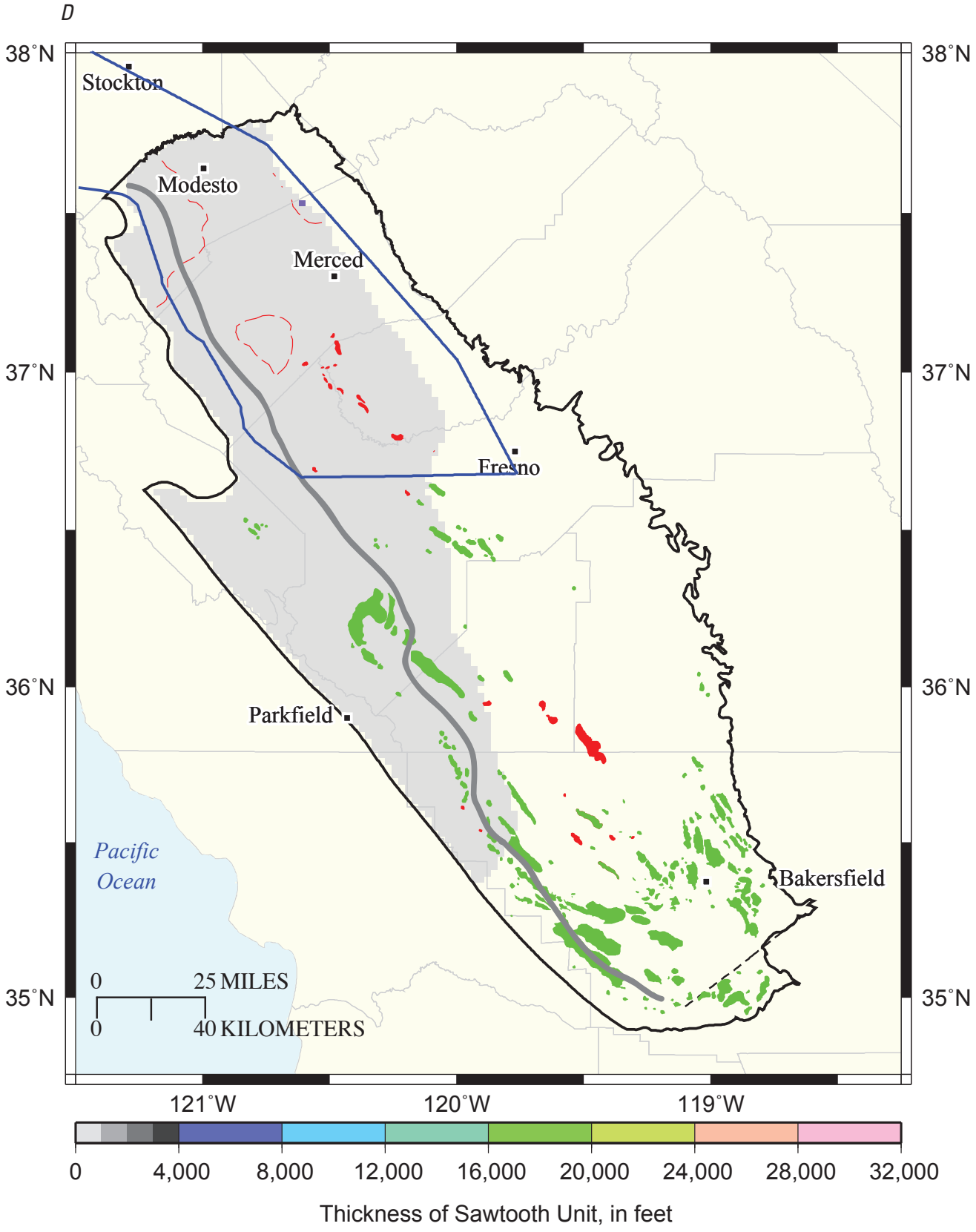

Figure 7.10.—Continued

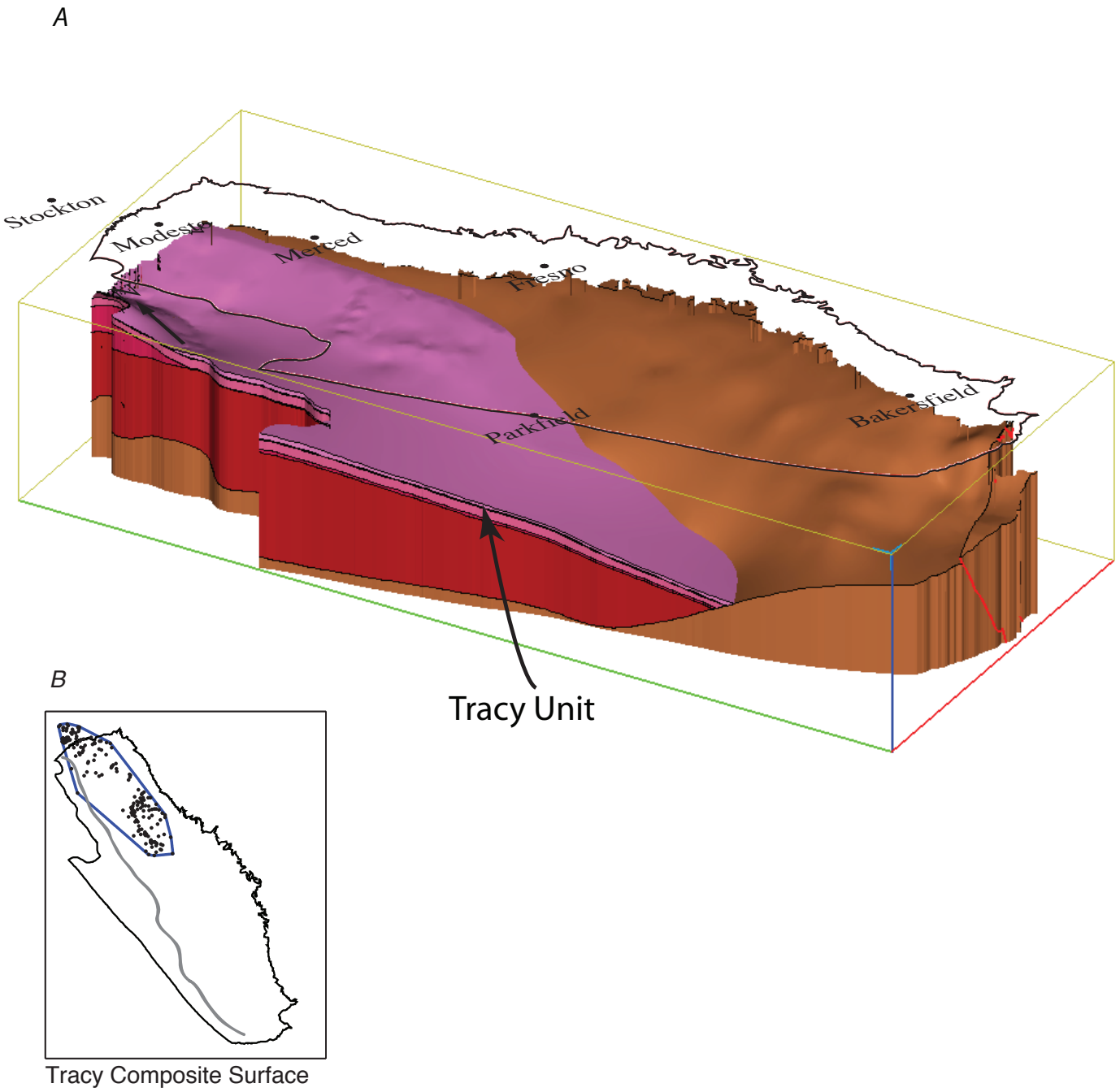

Figure 7.11. *A*, Oblique view of the Tracy Composite Surface. View is from 30° west of south at a 30° inclination angle. Grid resolution is 1 mile. *B*, Geographic distribution of observations; these can be viewed page-size in Hosford Scheirer and Magoon (this volume, chapter 5). In panels *B, C,* and *D*, heavy black line marks the province boundary, heavy gray line divides the area of correspondence (east) from the area of unresolved complexity (west), and blue polygon surrounds input well data and thus encloses best-determined part of the surface. *C*, Structure contour map of the elevation of the Tracy Composite Surface. Contour interval is 2,000 feet. In panels *C* and *D*, thin gray lines mark county boundaries. *D*, Thickness of the unit bounded by the Tracy Composite Surface (top) and the Sawtooth Composite Surface (base).

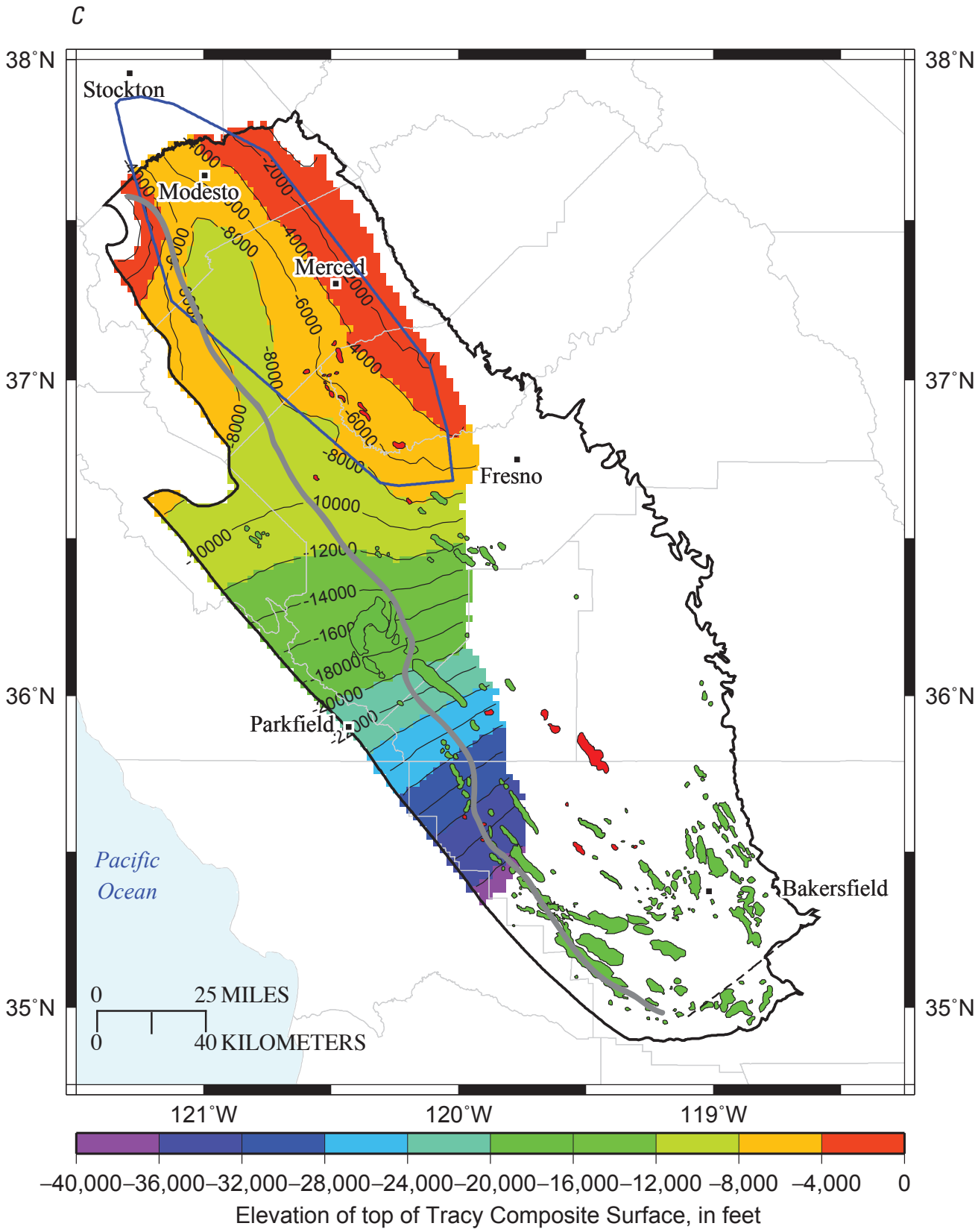

Figure 7.11.—Continued

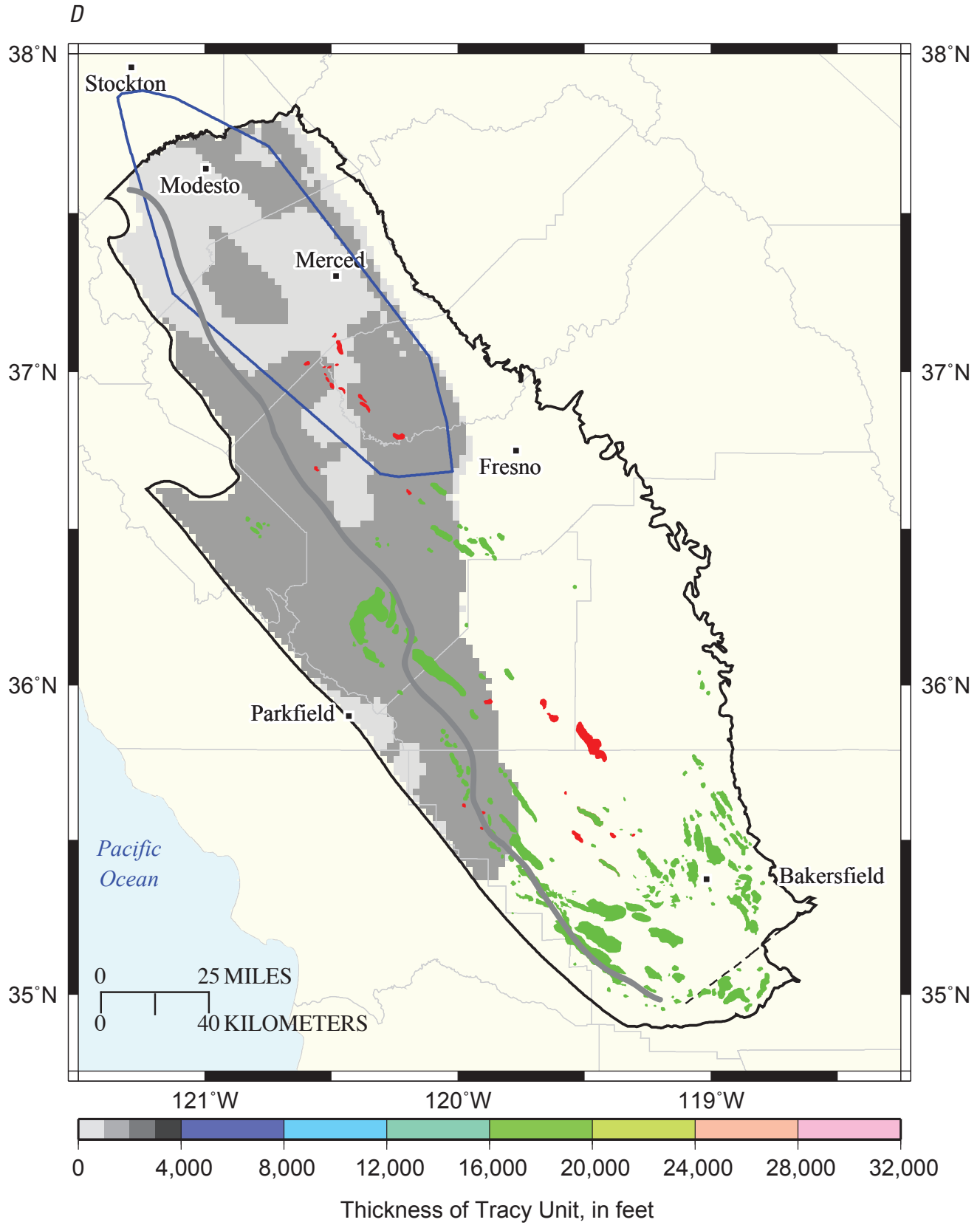

Figure 7.11.—Continued

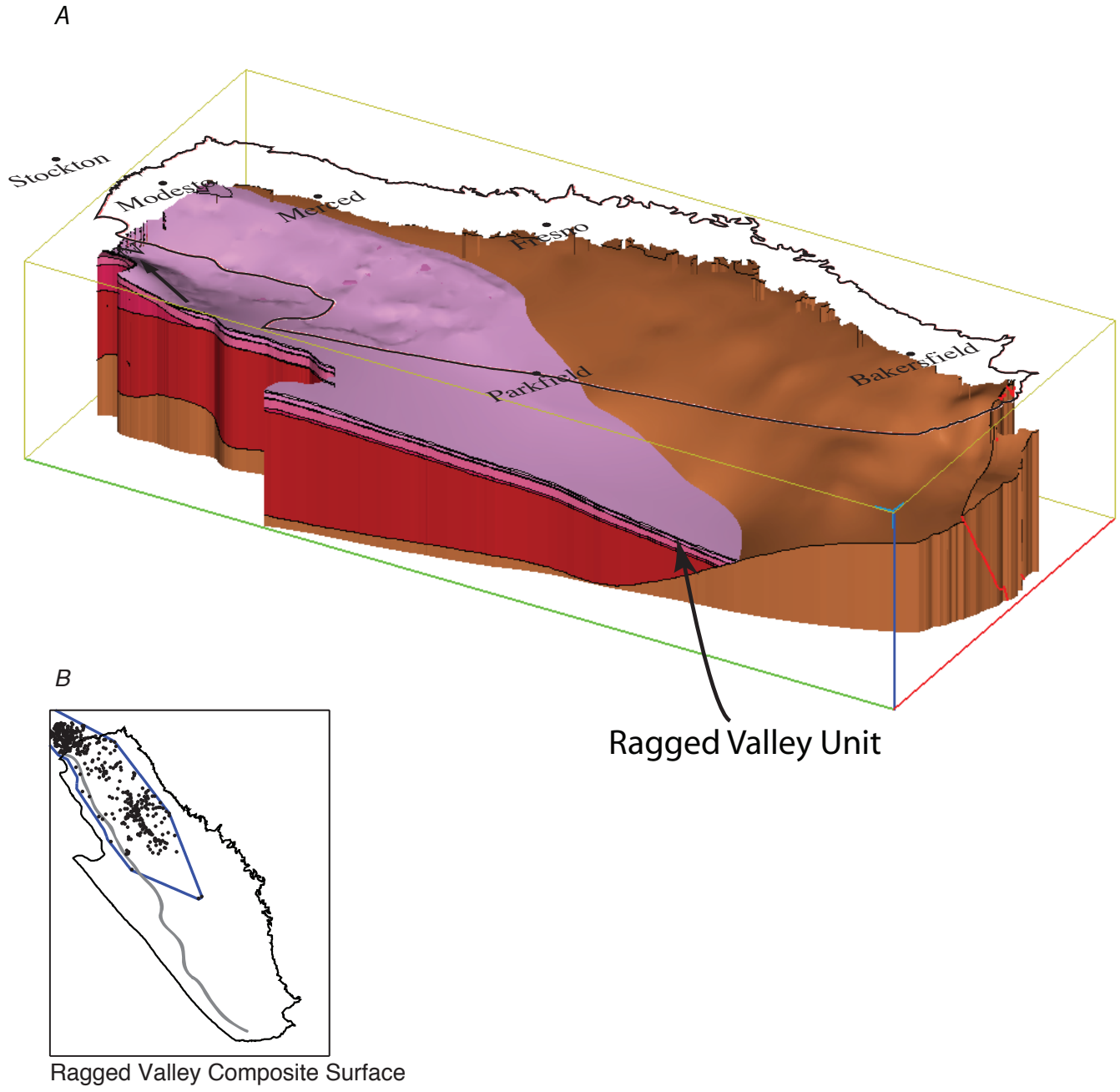

Figure 7.12. *A*, Oblique view of the Ragged Valley Composite Surface. View is from 30° west of south at a 30° inclination angle. Grid resolution is 1 mile. *B*, Geographic distribution of observations; these can be viewed page-size in Hosford Scheirer and Magoon (this volume, chapter 5). In panels *B, C*, and *D*, heavy black line marks the province boundary, heavy gray line divides the area of correspondence (east) from the area of unresolved complexity (west), and blue polygon surrounds input well data and thus encloses best-determined part of the surface. *D*, Thickness of the unit bounded by the Tracy Composite Surface (top) and the Sawtooth Composite Surface (base). *D,* Thickness of the unit bounded by the Tracy Composite Surface (top) and the Sawtooth Composite Surface (base). *D*, Thickness of the unit bounded by the Ragged Valley Composite Surface (top) and the Tracy Composite Surface (base). Dashed contours are 200-foot increments.

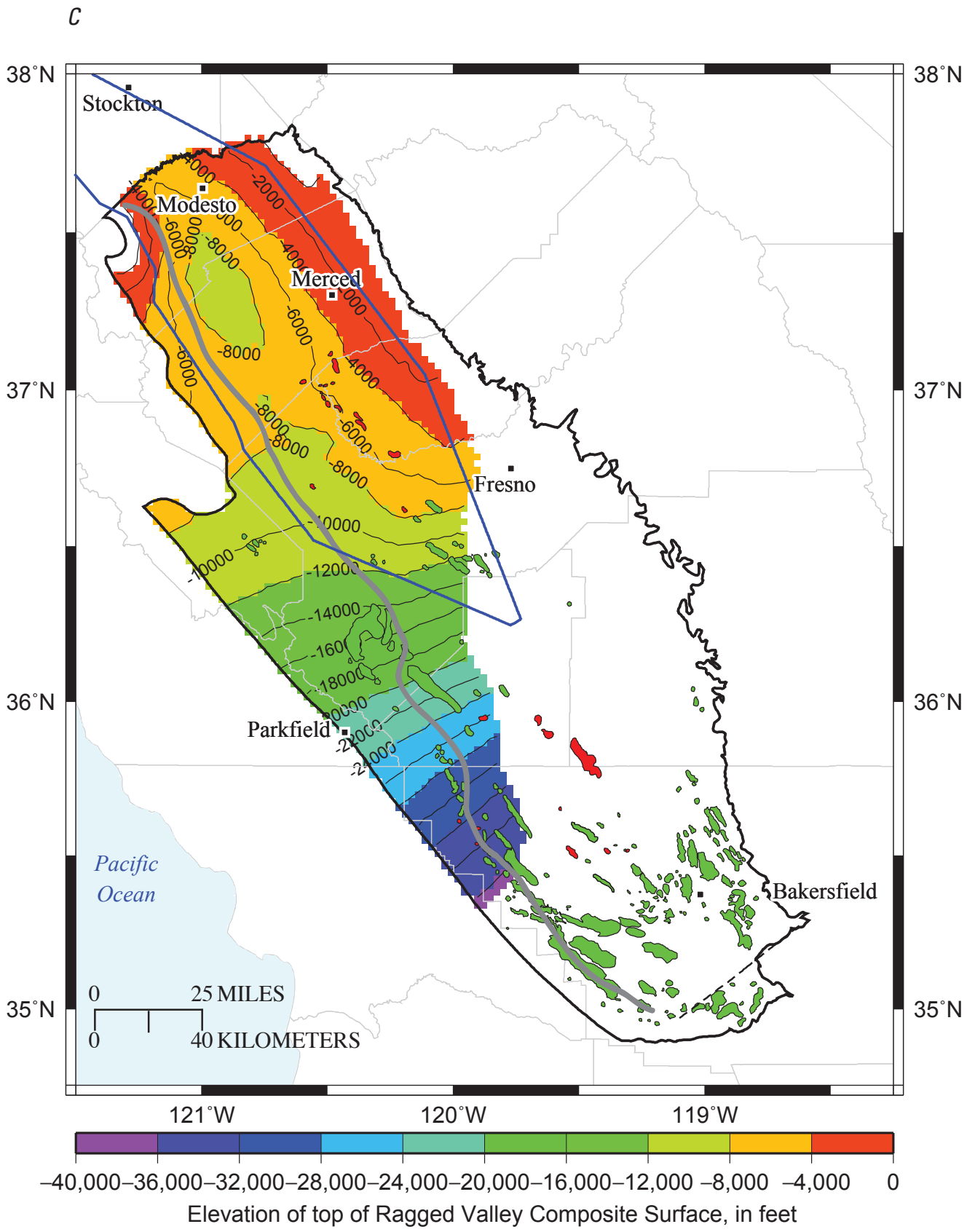

Figure 7.12.—Continued

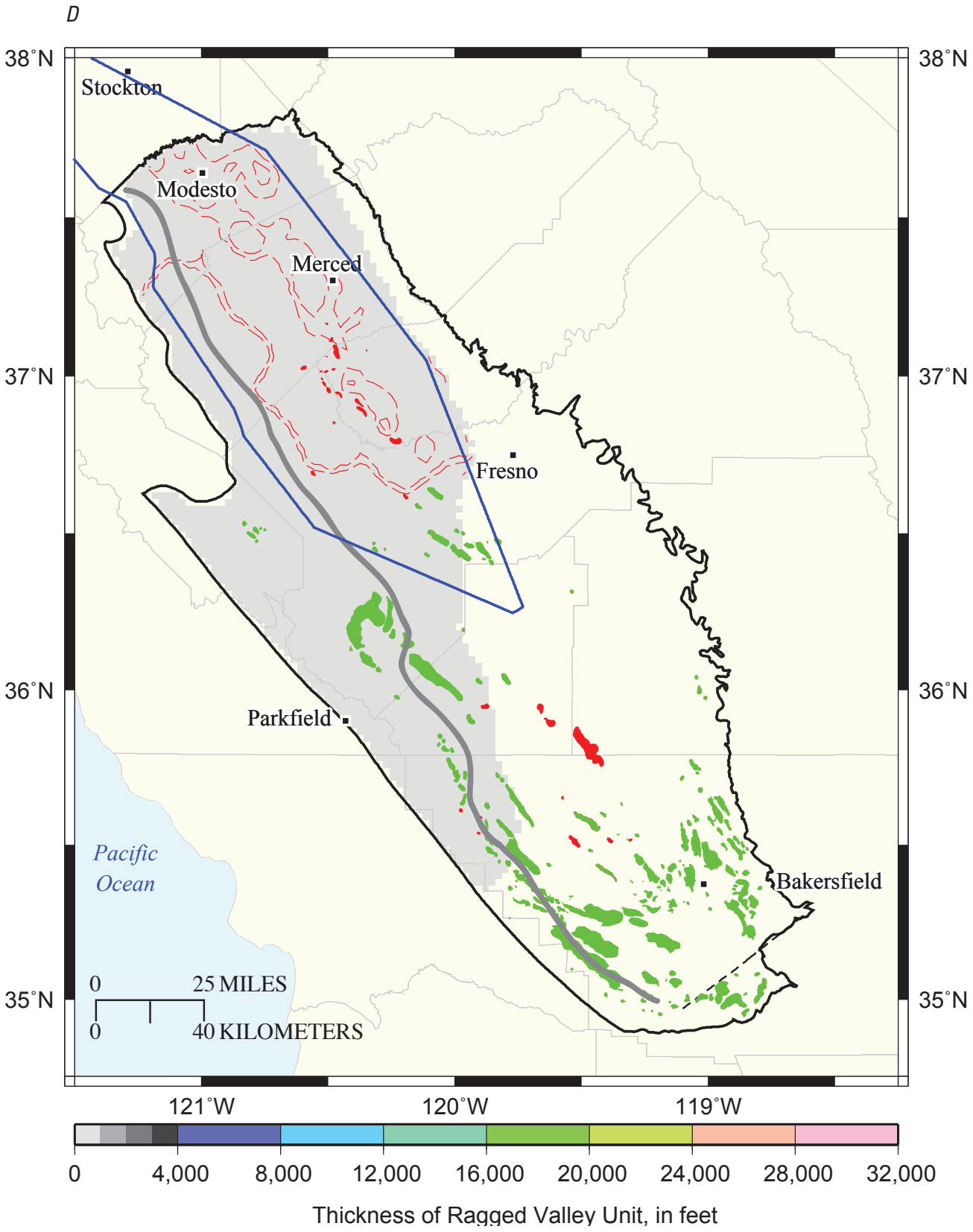

Figure 7.12.—Continued

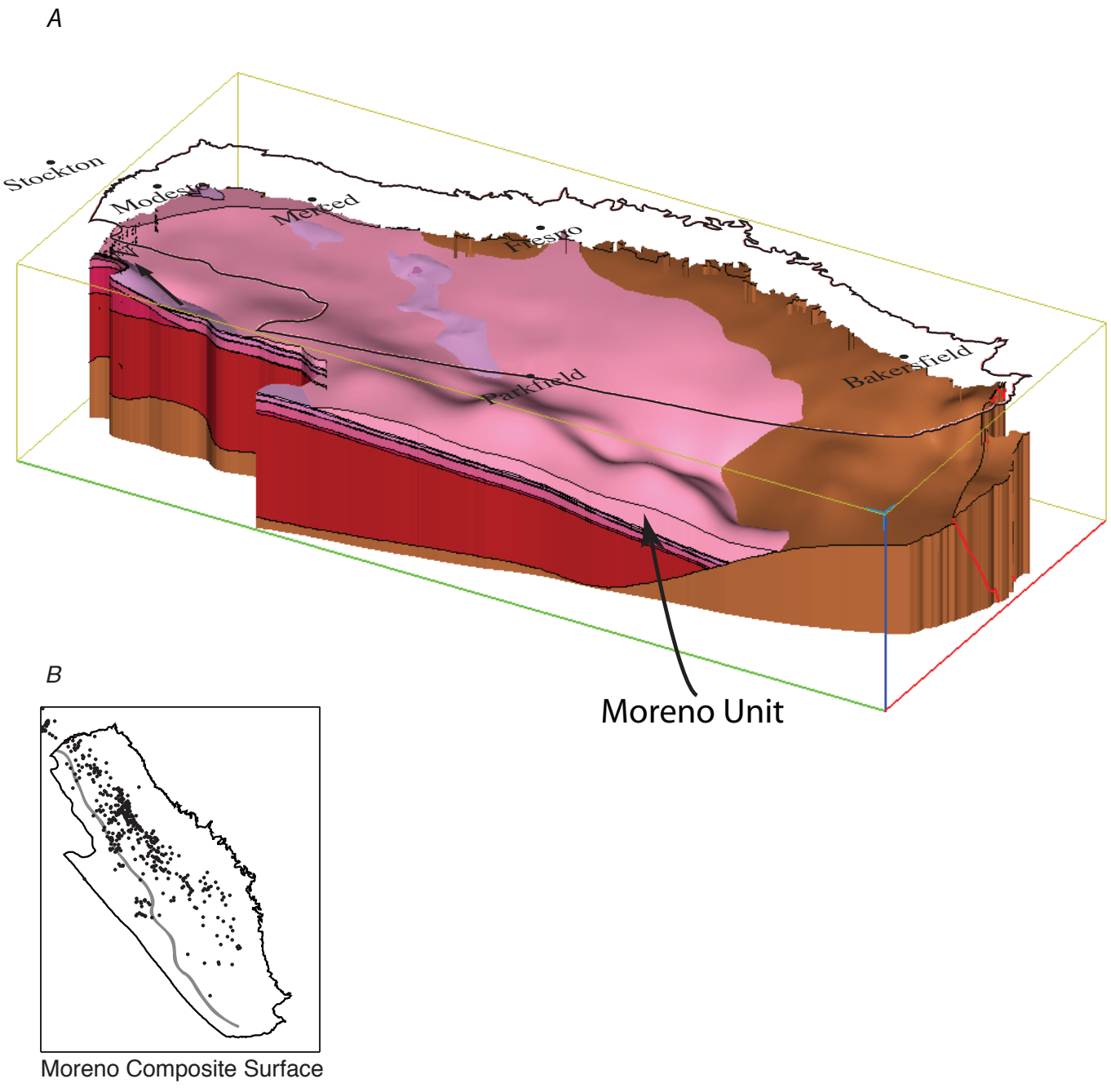

Figure 7.13. *A*, Oblique view of the Moreno Composite Surface. View is from 30° west of south at a 30° inclination angle. Grid resolution is 1 mile. *B*, Geographic distribution of observations; these can be viewed page-size in Hosford Scheirer and Magoon (this volume, chapter 5). In panels *B, C,* and *D*, heavy black line marks the province boundary and heavy gray line divides the area of correspondence (east) from the area of unresolved complexity (west). *C*, Structure contour map of the elevation of the Moreno Composite Surface. Contour interval is 2,000 feet. In panels *C* and *D*, thin gray lines mark county boundaries. *D*, Thickness of the unit bounded by the Moreno Composite Surface (top) and the Ragged Valley Composite Surface (base).

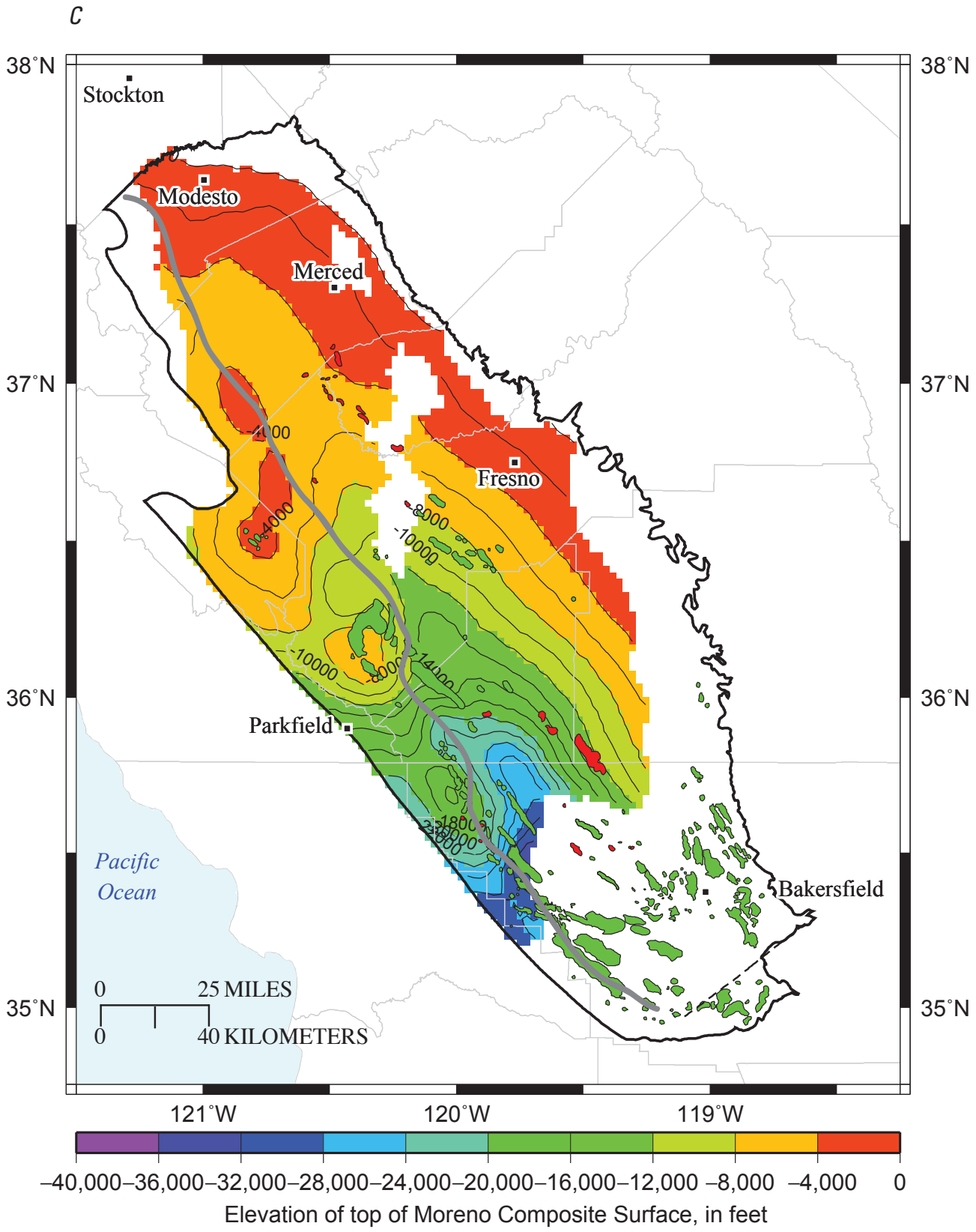

Figure 7.13.—Continued

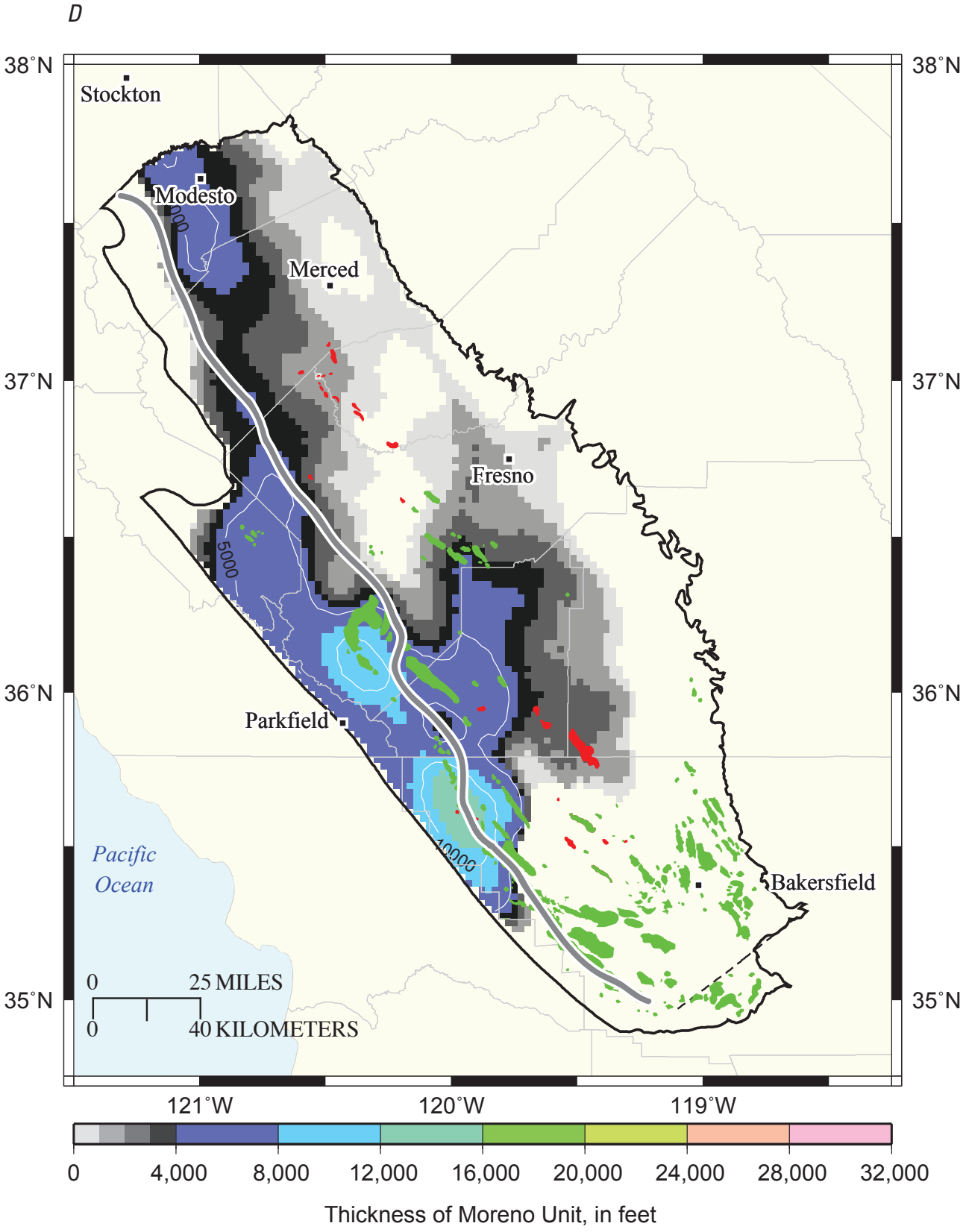

Figure 7.13.—Continued

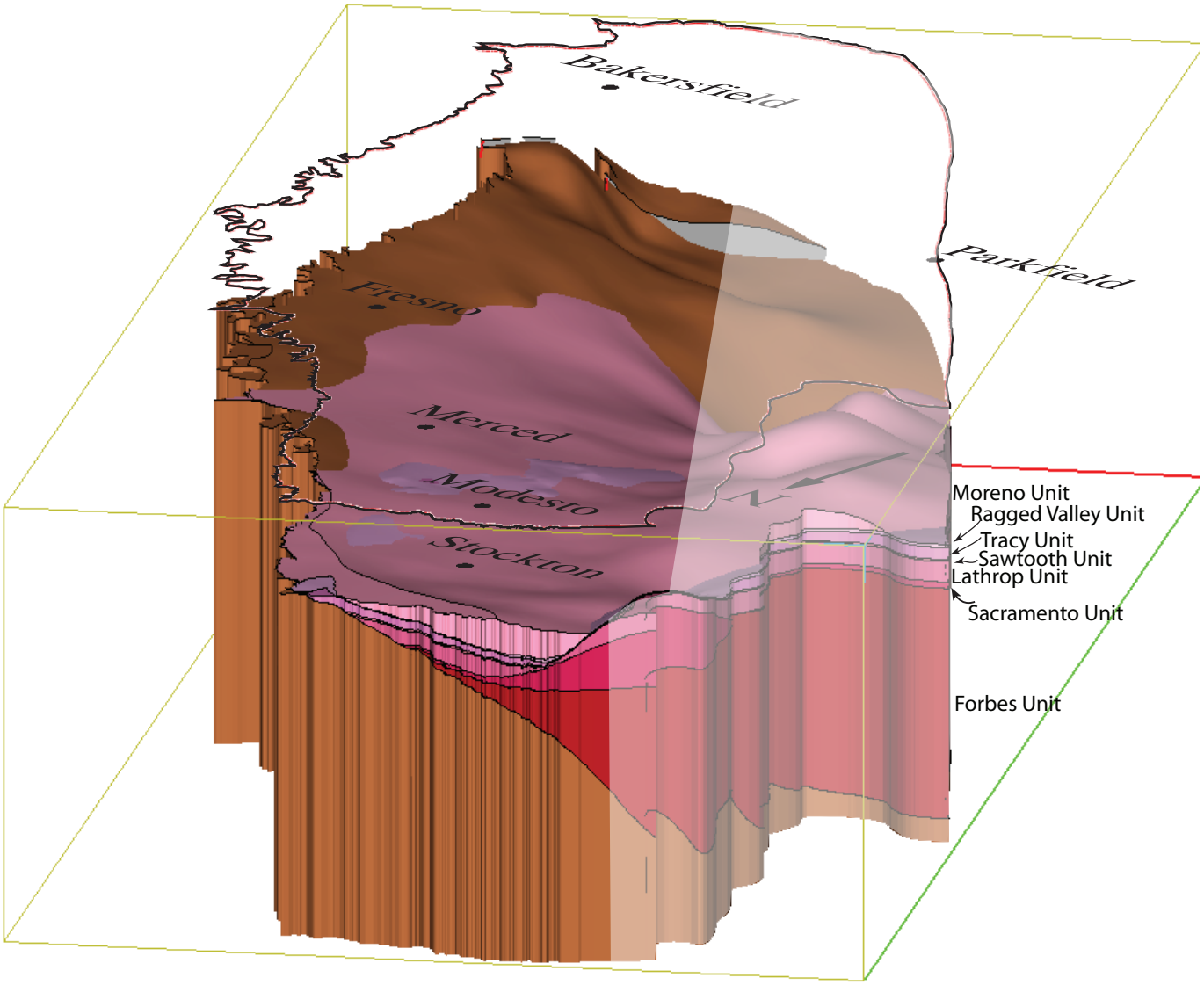

Figure 7.14. Oblique view of the model of the basement surface (brown) and the Cretaceous-aged units (shades of red). View is from 40° west of north at a 15° inclination angle. Informal unit names are italicized. Area of unresolved complexity, defined in the text, is indicated with transparent polygon.

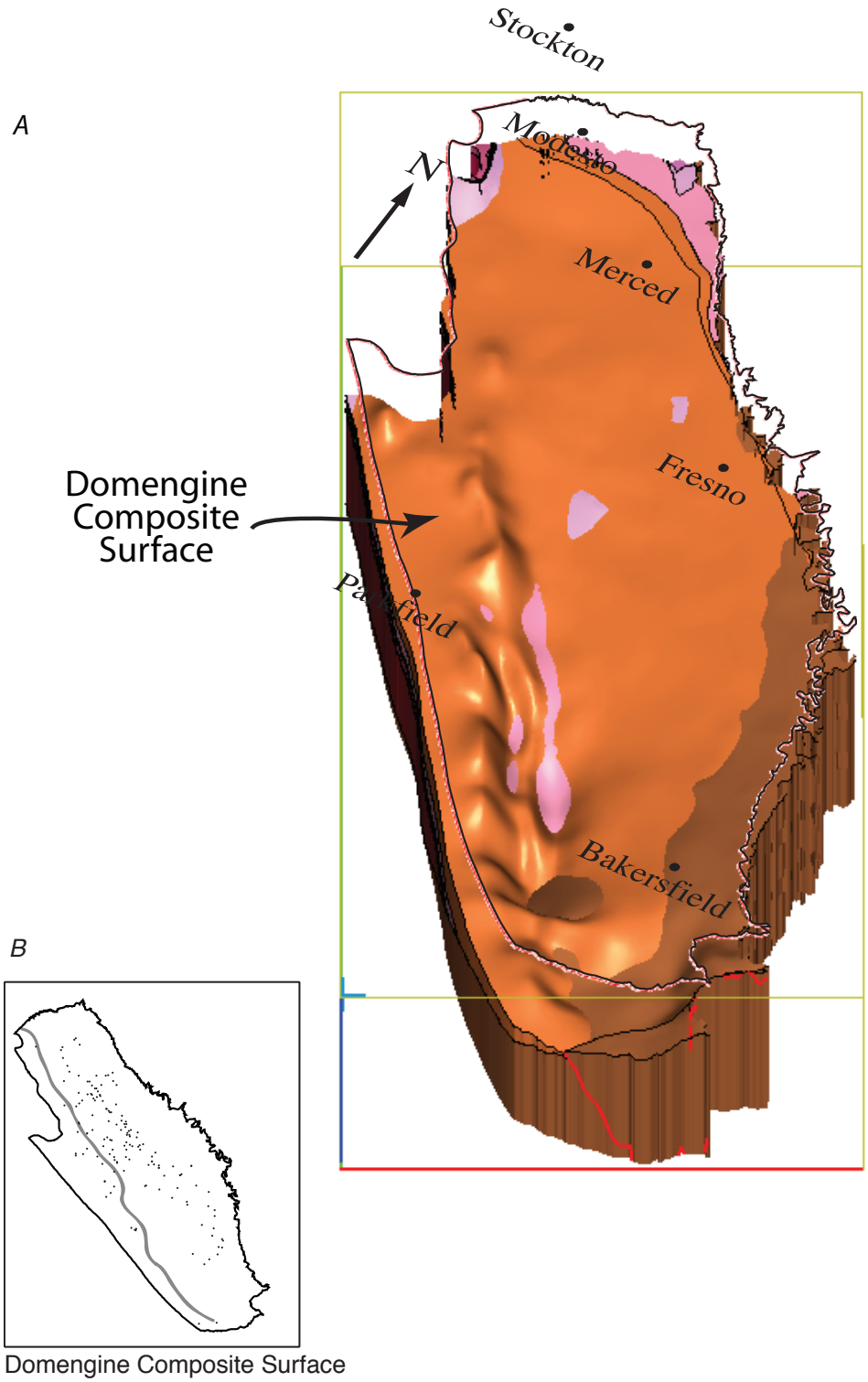

Figure 7.15. *A*, Oblique view of the Domengine Composite Surface. View is from 30° east of south (that is, aligned with the basin axis) at a 50° inclination angle. Grid resolution is 1 mile. *B*, Geographic distribution of observations; well picks can be viewed page-size in Hosford Scheirer and Magoon (this volume, chapter 5). In panels *B*, *C*, and *D*, heavy black line marks the province boundary and heavy gray line divides the area of correspondence (east) from the area of unresolved complexity (west). *C*, Structure contour map of the elevation of the Domengine Composite Surface. Contour interval is 2,000 feet. In panels *C* and *D*, thin gray lines mark county boundaries. *D*, Thickness of the unit bounded by the Domengine Composite Surface (top) and the Moreno Composite Surface (base).

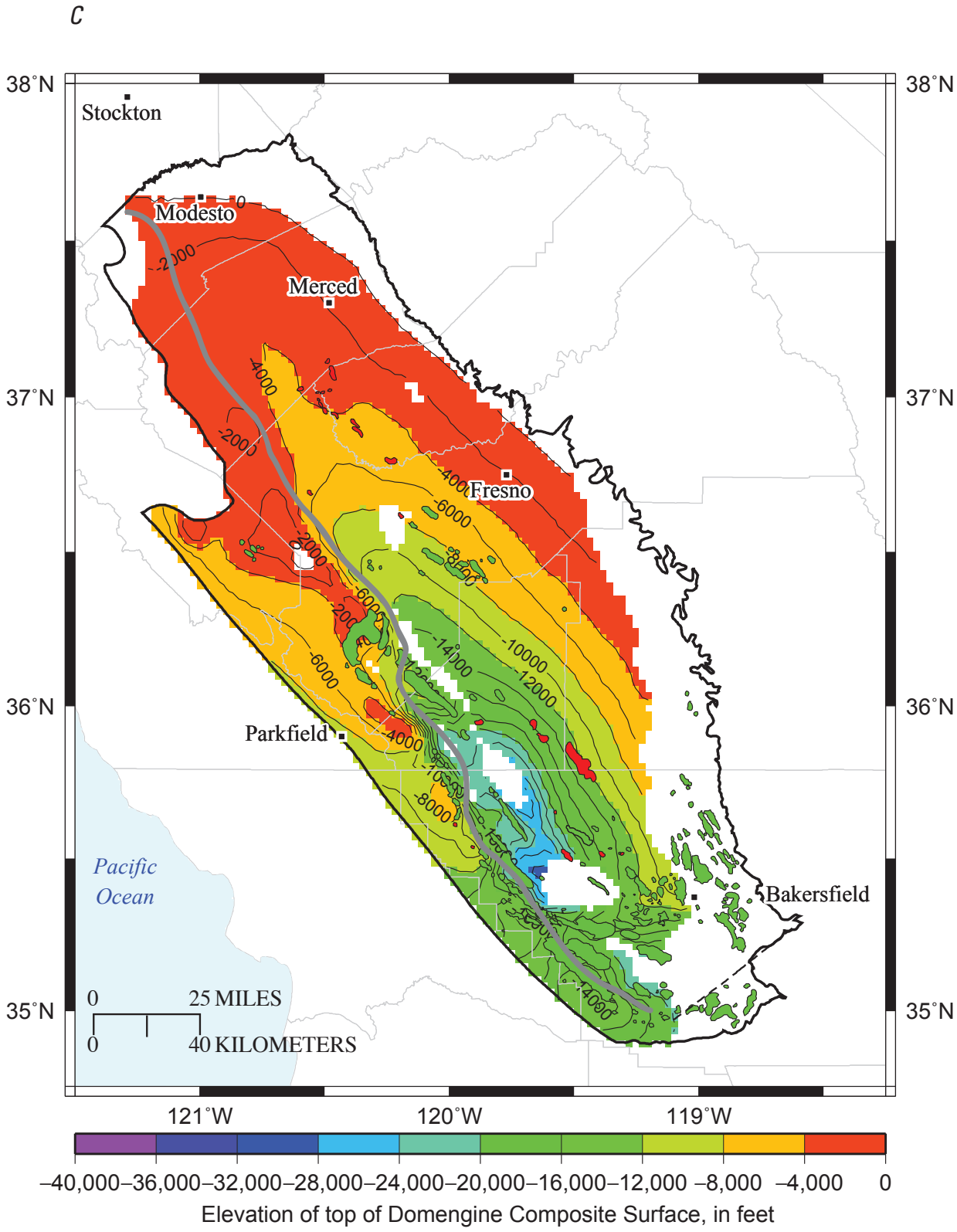

Figure 7.15.—Continued

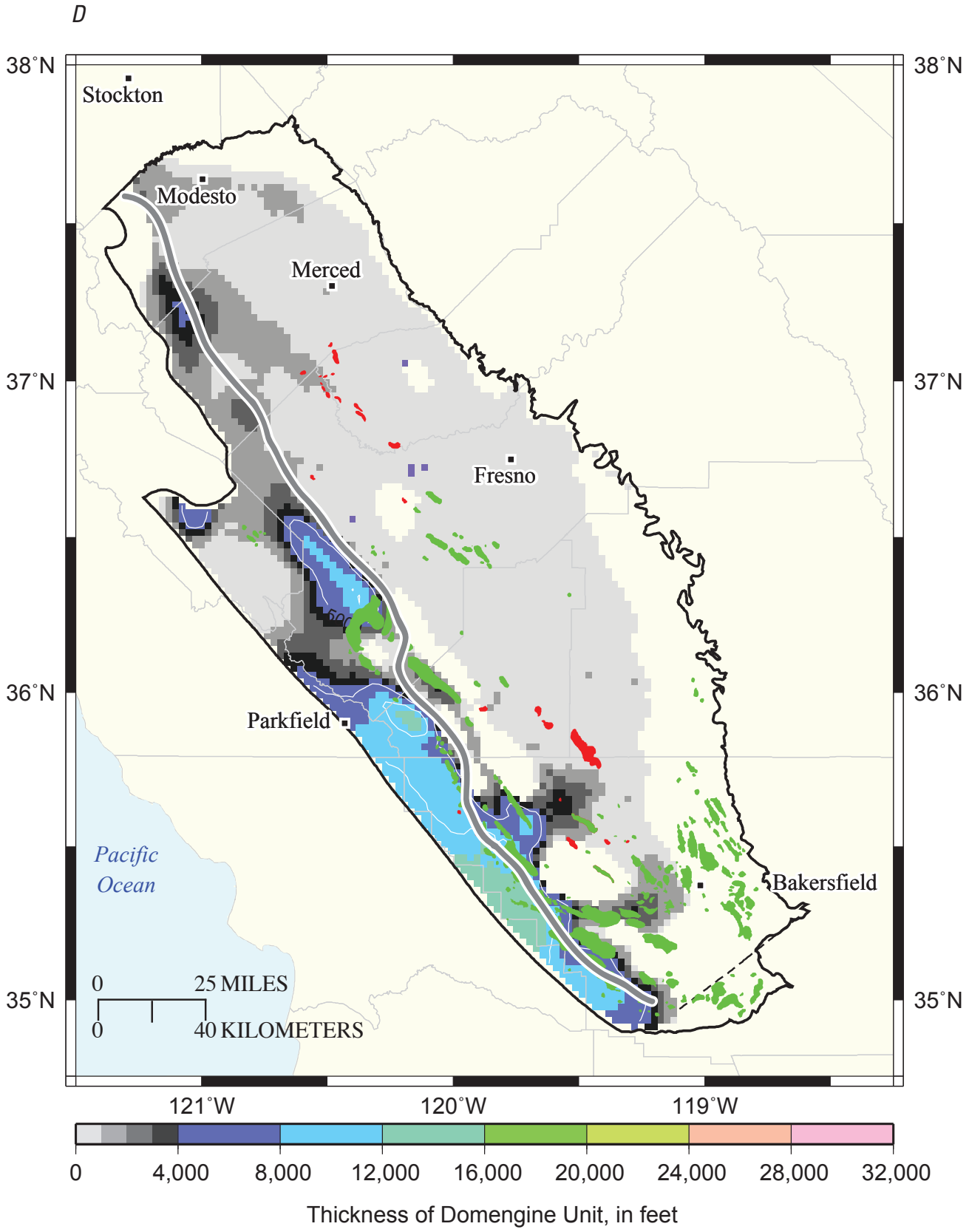

Figure 7.15.—Continued

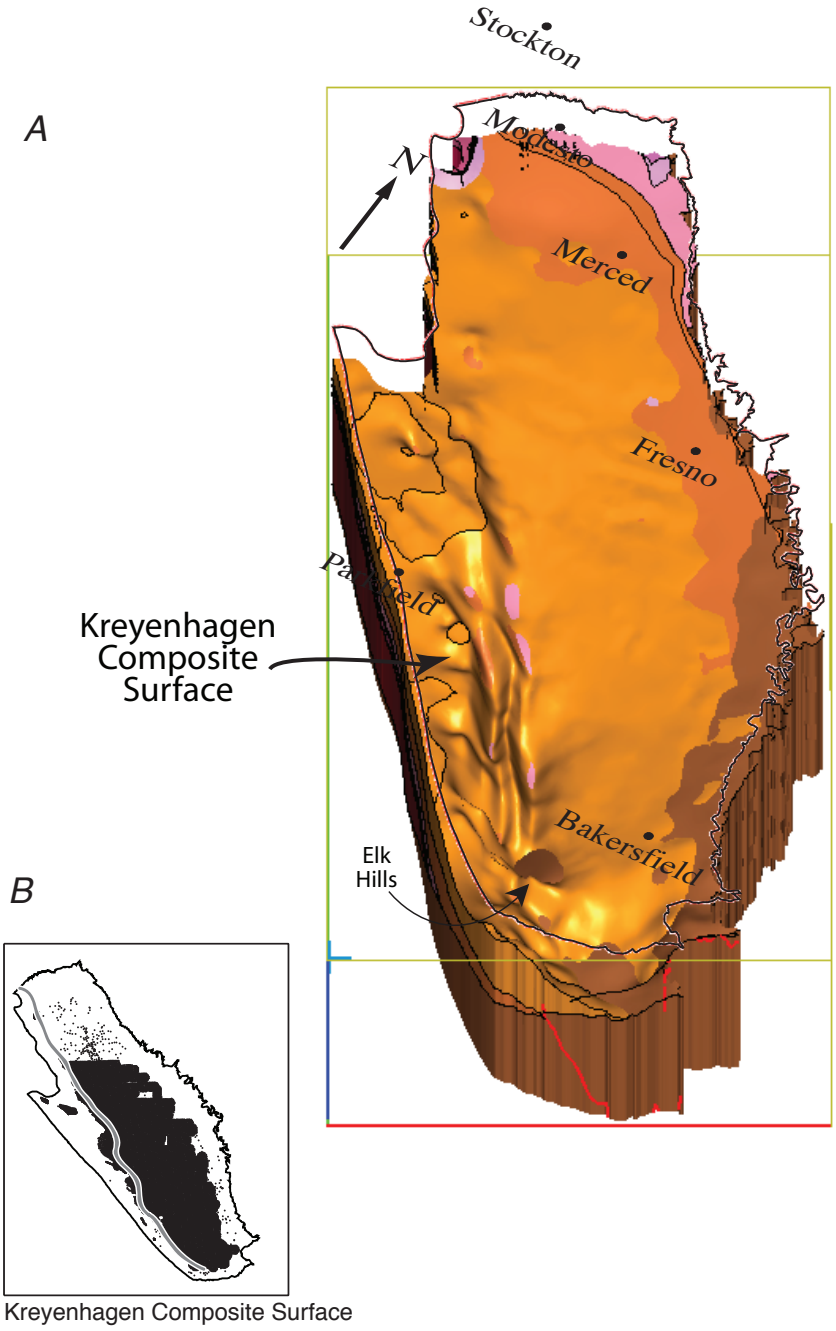

Figure 7.16. *A*, Oblique view of the Kreyenhagen Composite Surface. View is from 30° east of south (that is, aligned with the basin axis) at a 50° inclination angle. Grid resolution is 0.5 mile. *B*, Geographic distribution of observations; well picks can be viewed page-size in Hosford Scheirer and Magoon (this volume, chapter 5). Dark stippling indicates dense seismic grid. In panels *B, C*, and *D,* heavy black line marks the province boundary and heavy gray line divides the area of correspondence (east) from the area of unresolved complexity (west). *C*, Structure contour map of the elevation of the Kreyenhagen Composite Surface. Contour interval is 2,000 feet. In panels *C* and *D,* thin gray lines mark county boundaries. *D*, Thickness of the unit bounded by the Kreyenhagen Composite Surface (top) and the Domengine Composite Surface (base).

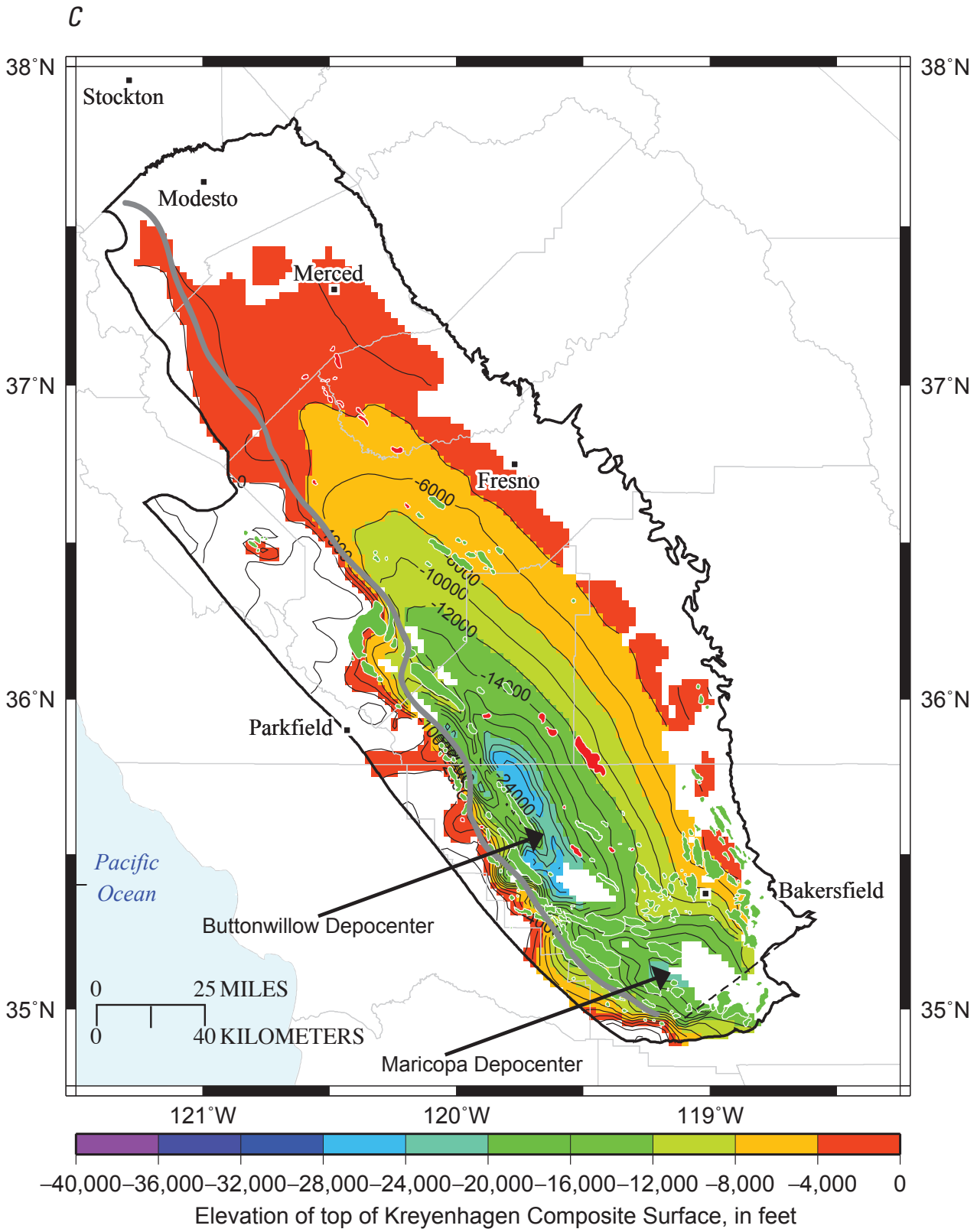

Figure 7.16.—Continued

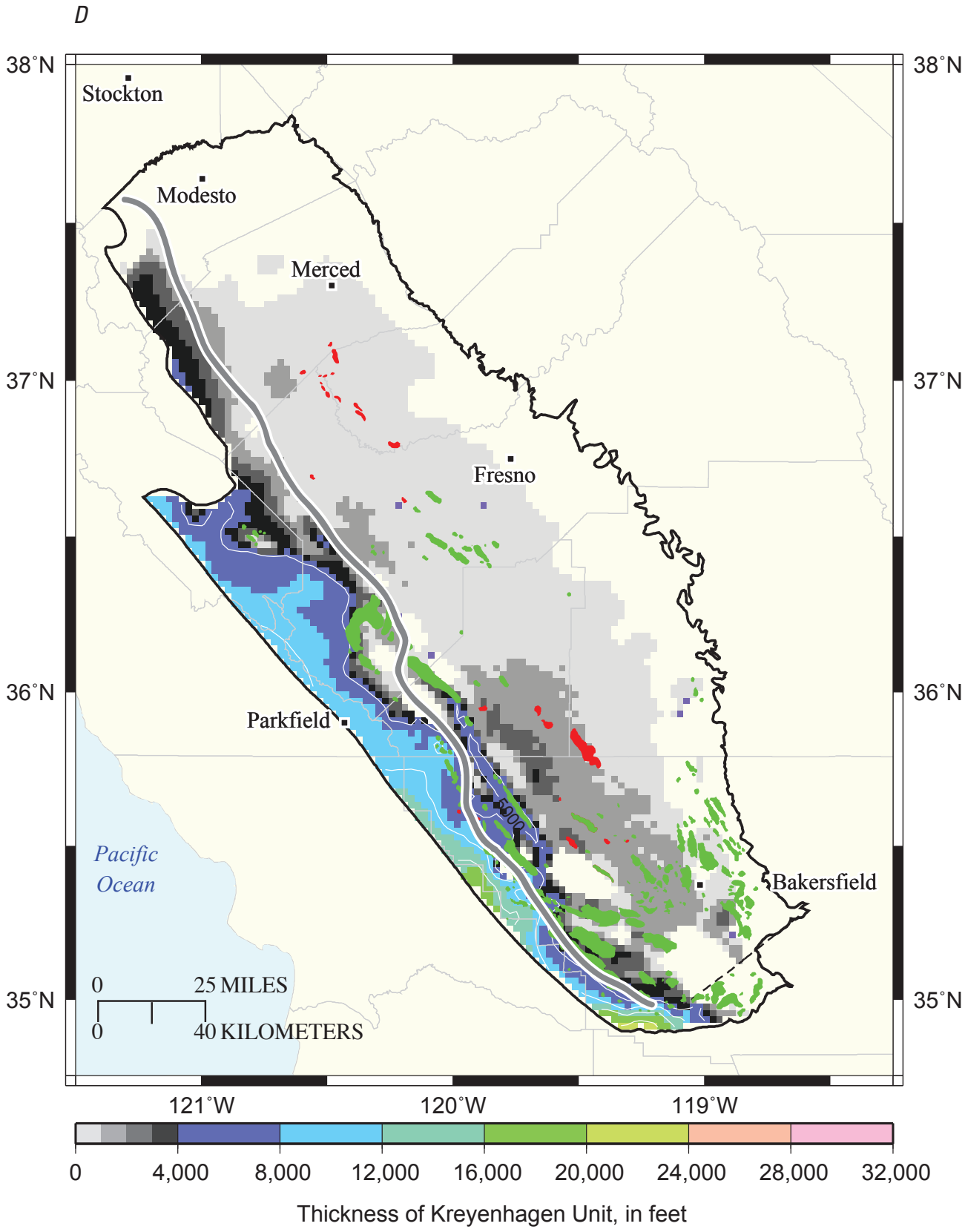

Figure 7.16.—Continued

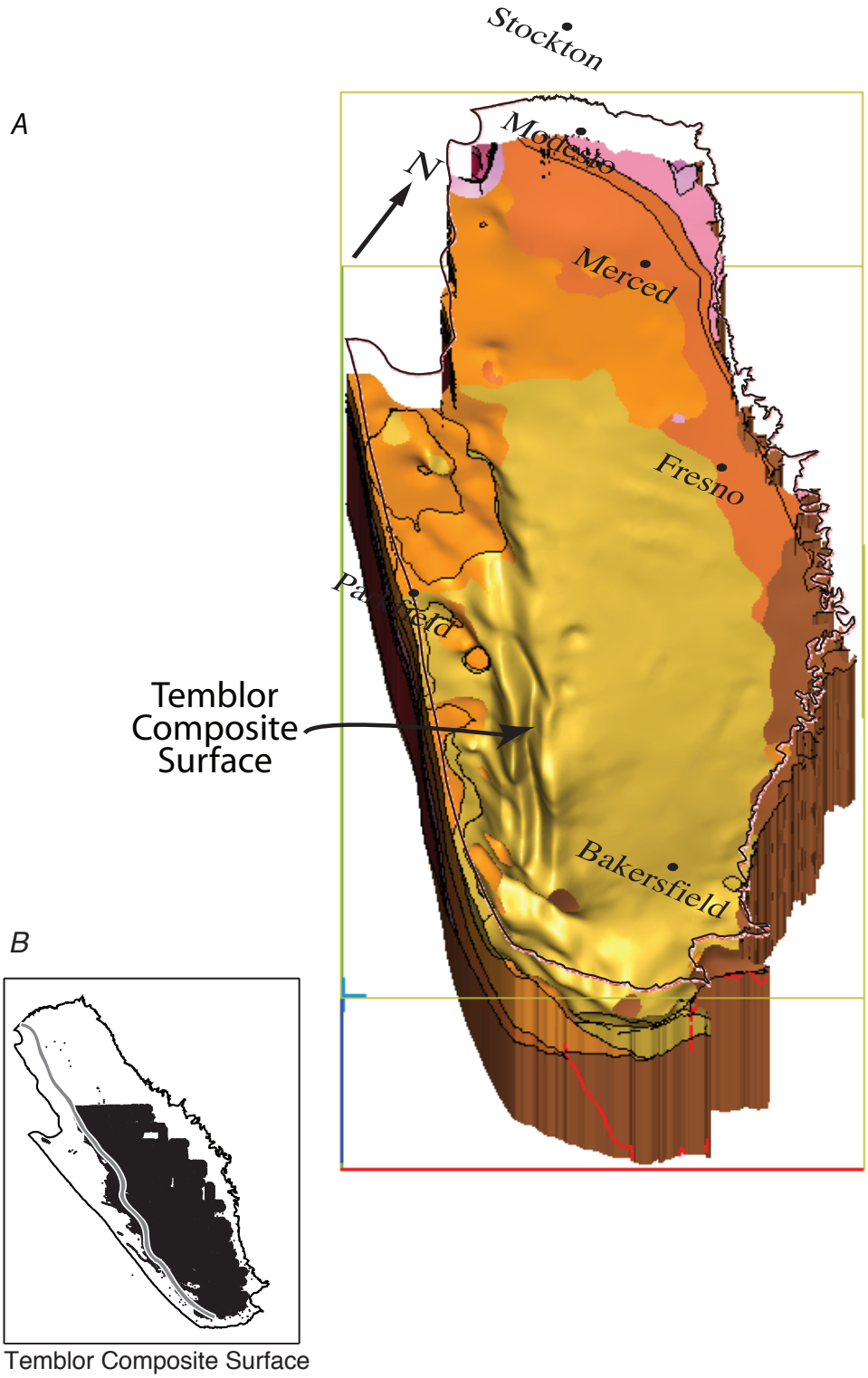

Figure 7.17. *A*, Oblique view of the Temblor Composite Surface. View is from 30° east of south (that is, aligned with the basin axis) at a 50° inclination angle. Grid resolution is 0.5 mile. *B*, Geographic distribution of observations; well picks can be viewed page-size in Hosford Scheirer and Magoon (this volume, chapter 5). Dark stippling indicates dense seismic grid. In panels *B*, *C*, and *D*, heavy black line marks the province boundary and heavy gray line divides the area of correspondence (east) from the area of unresolved complexity (west). *C*, Structure contour map of the elevation of the Temblor Composite Surface. Contour interval is 2,000 feet. In panels *C* and *D*, thin gray lines mark county boundaries. *D*, Thickness of the unit bounded by the Temblor Composite Surface (top) and the Kreyenhagen Composite Surface (base).

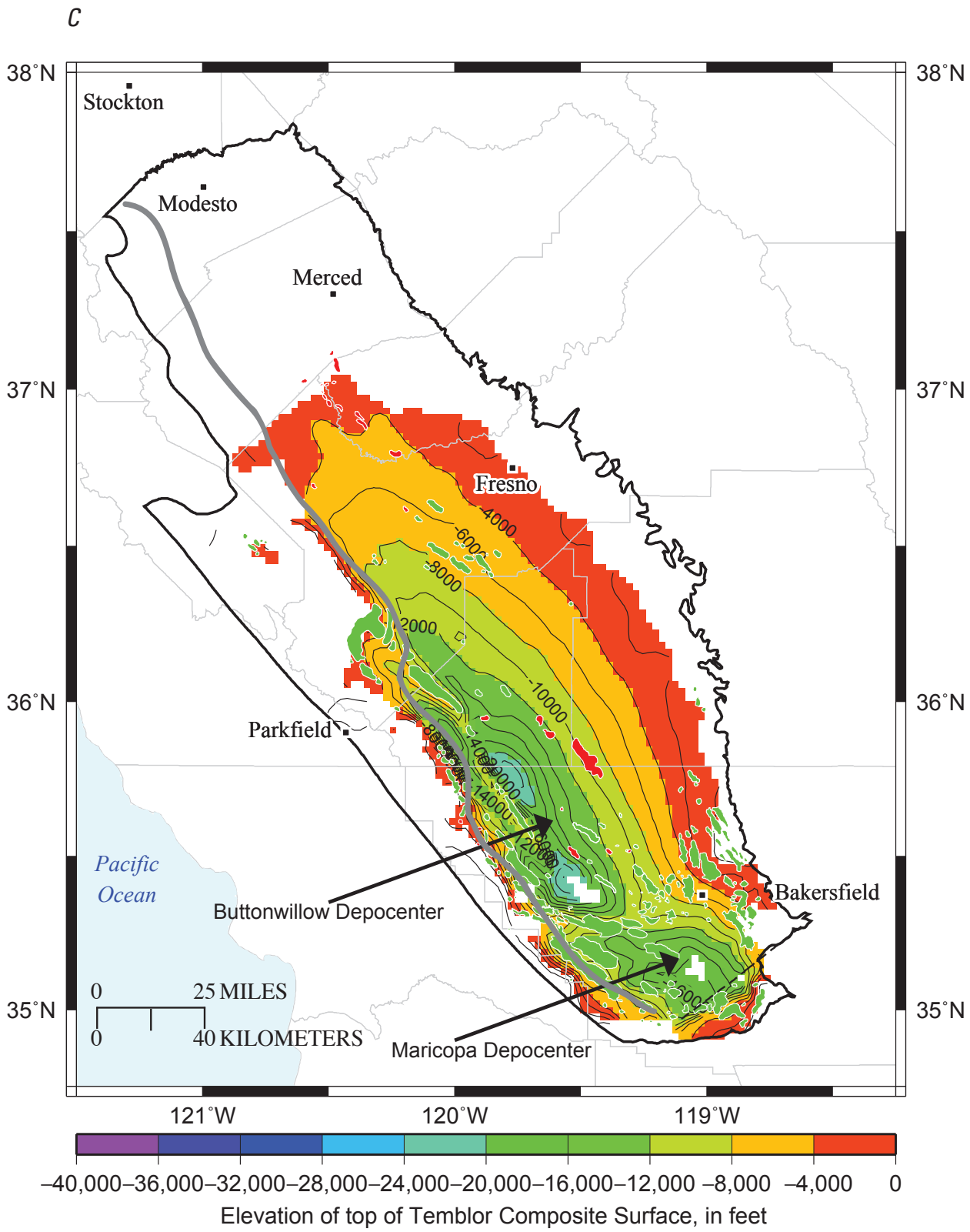

Figure 7.17.—Continued

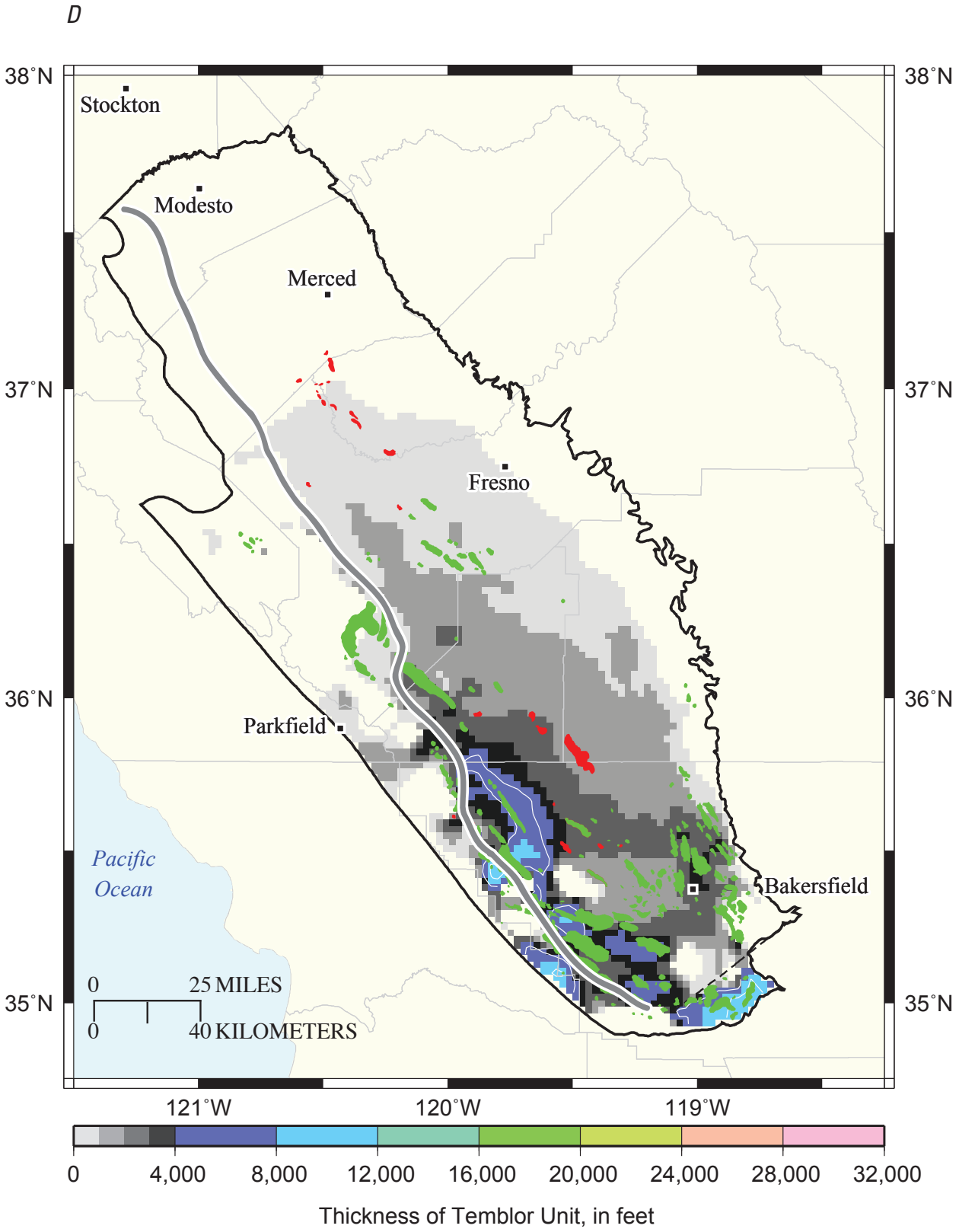

Figure 7.17.—Continued

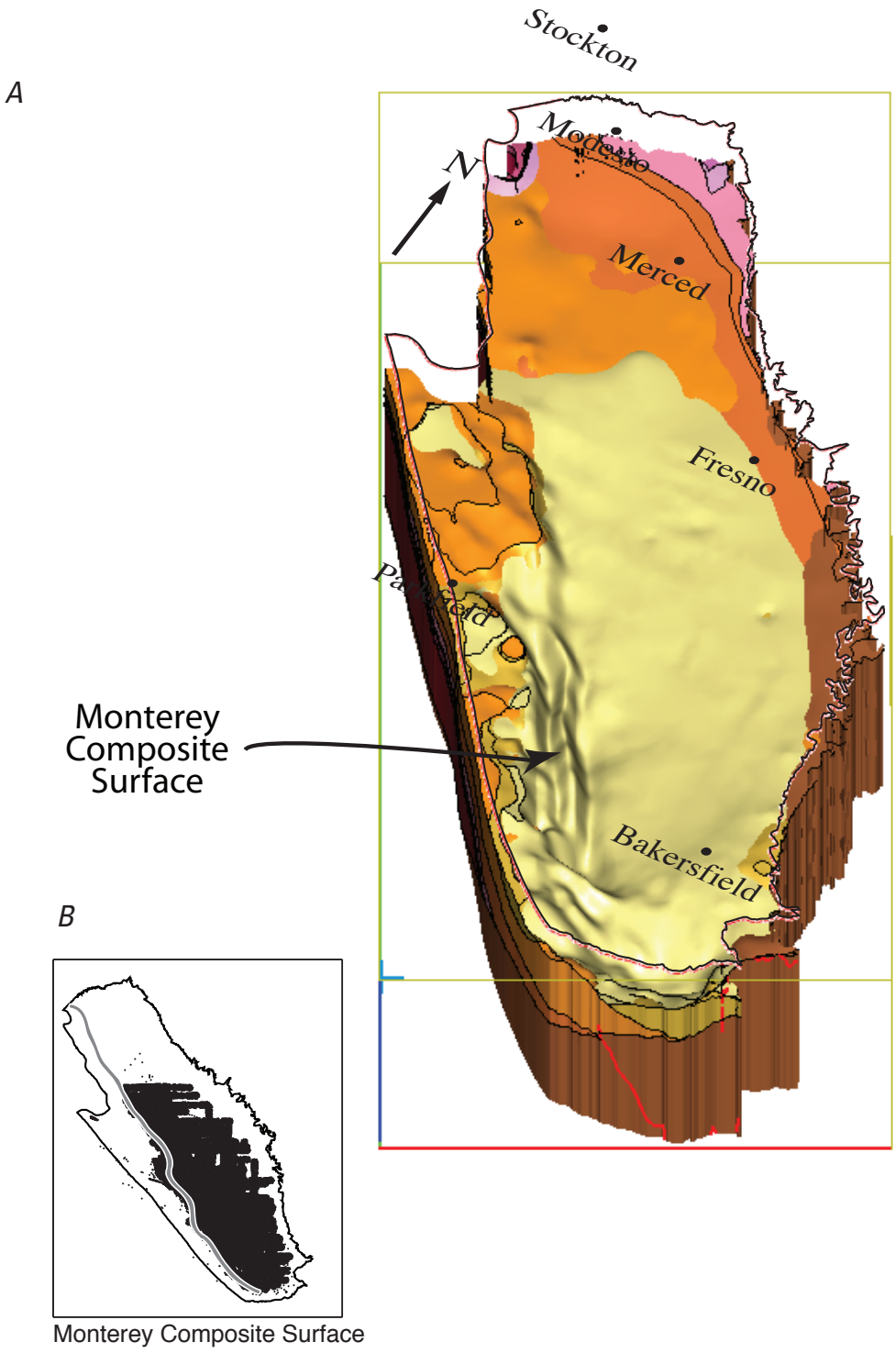

Figure 7.18. *A*, Oblique view of the Monterey Composite Surface. View is from 30° east of south (that is, aligned with the basin axis) at a 50° inclination angle. Grid resolution is 0.5 mile. (*B*), Geographic distribution of observations; well picks can be viewed page-size in Hosford Scheirer and Magoon (this volume, chapter 5). Dark stippling indicates dense seismic grid. In panels *B, C*, and *D,* heavy black line marks the province boundary and heavy gray line divides the area of correspondence (east) from the area of unresolved complexity (west) *C*, Structure contour map of the elevation of the Monterey Composite Surface. Contour interval is 2,000 feet. In panels *C* and *D*, thin gray lines mark county boundaries. *D,* Thickness of the unit bounded by the Monterey Composite Surface (top) and the Temblor Composite Surface (base).

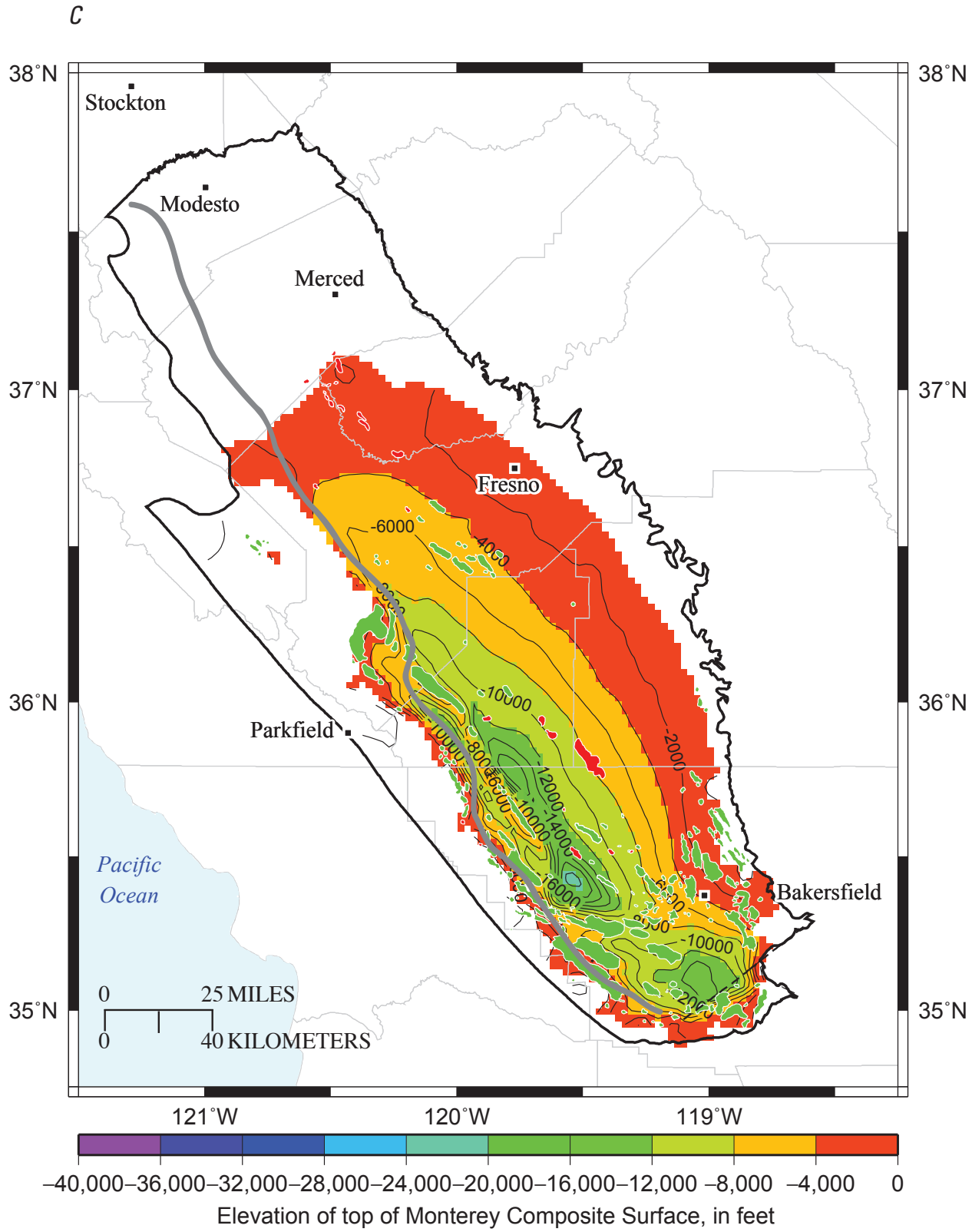

Figure 7.18.—Continued

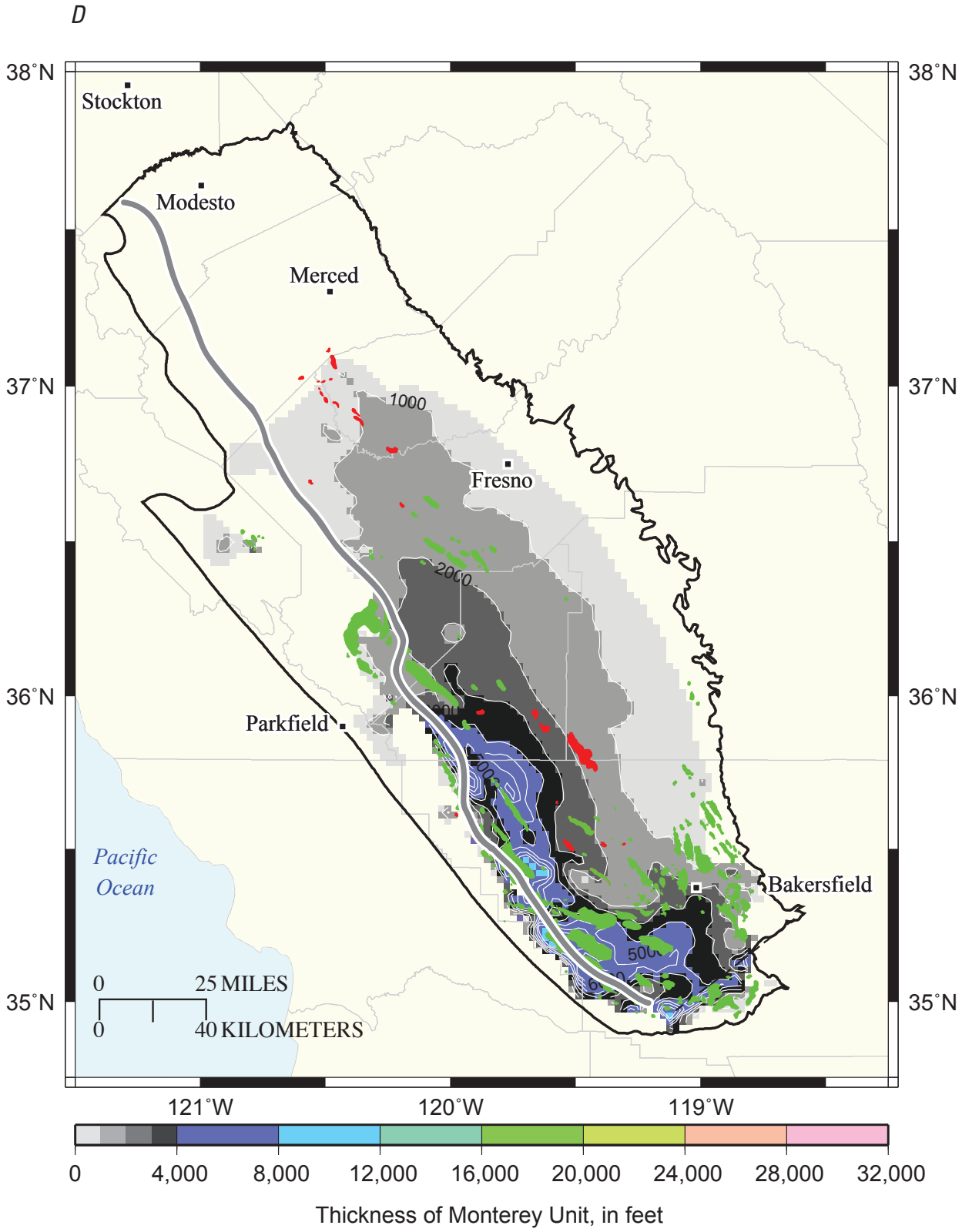

Figure 7.18.—Continued

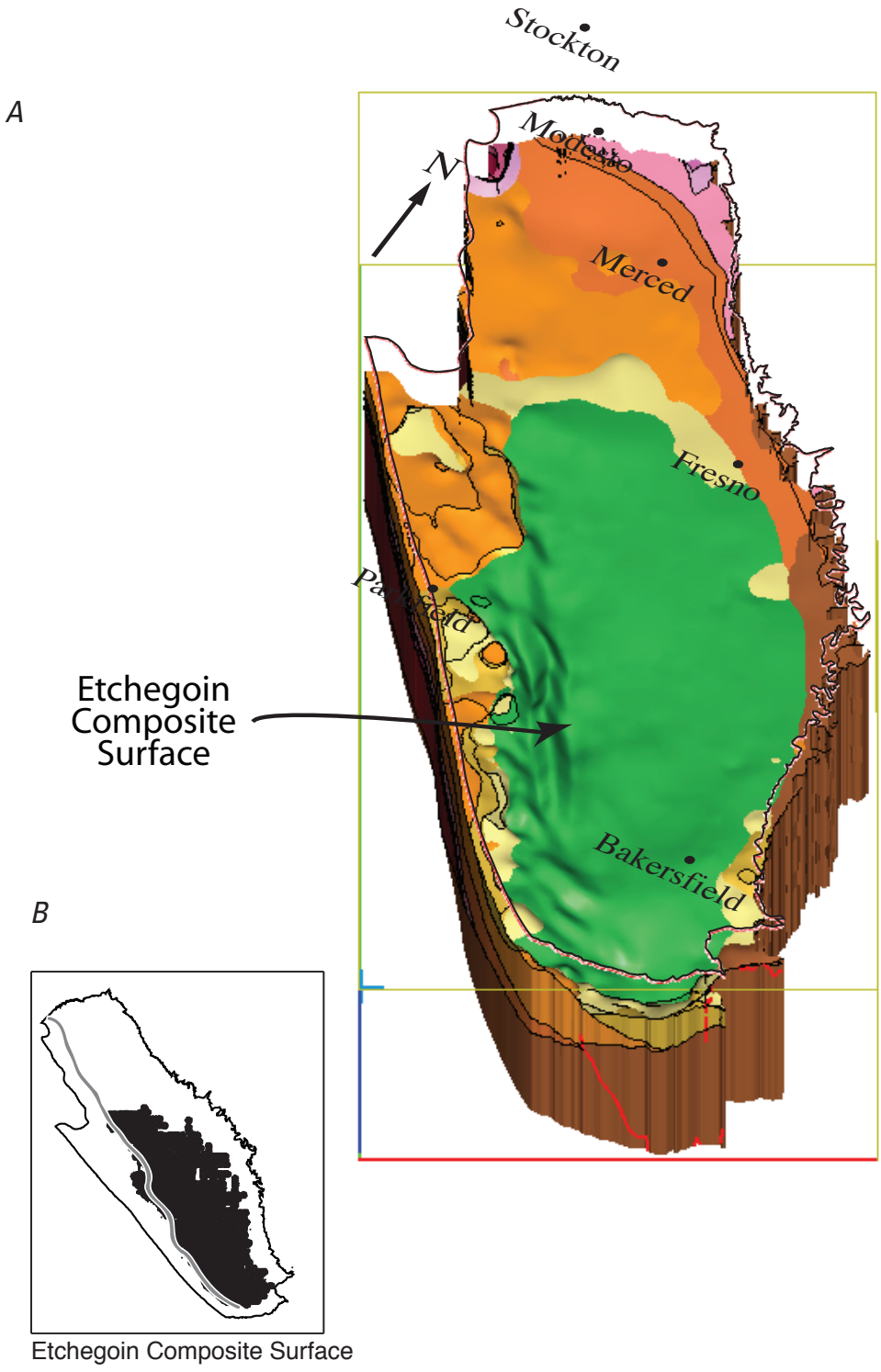

Figure 7.19. *A*, Oblique view of the Etchegoin Composite Surface. View is from 30° east of south (that is, aligned with the basin axis) at a 50° inclination angle. Grid resolution is 0.5 mile. *B*, Geographic distribution of observations; well picks can be viewed page-size in Hosford Scheirer and Magoon (this volume, chapter 5). Dark stippling indicates dense seismic grid. In panels *B, C*, and *D,* heavy black line marks the province boundary and heavy gray line divides the area of correspondence (east) from the area of unresolved complexity (west). *C*, Structure contour map of the elevation of the Etchegoin Composite Surface. Contour interval is 1,000 feet. In panels *C* and *D*, thin gray lines mark county boundaries. *D*, Thickness of the unit bounded by the Etchegoin Composite Surface (top) and the Monterey Composite Surface (base).

C

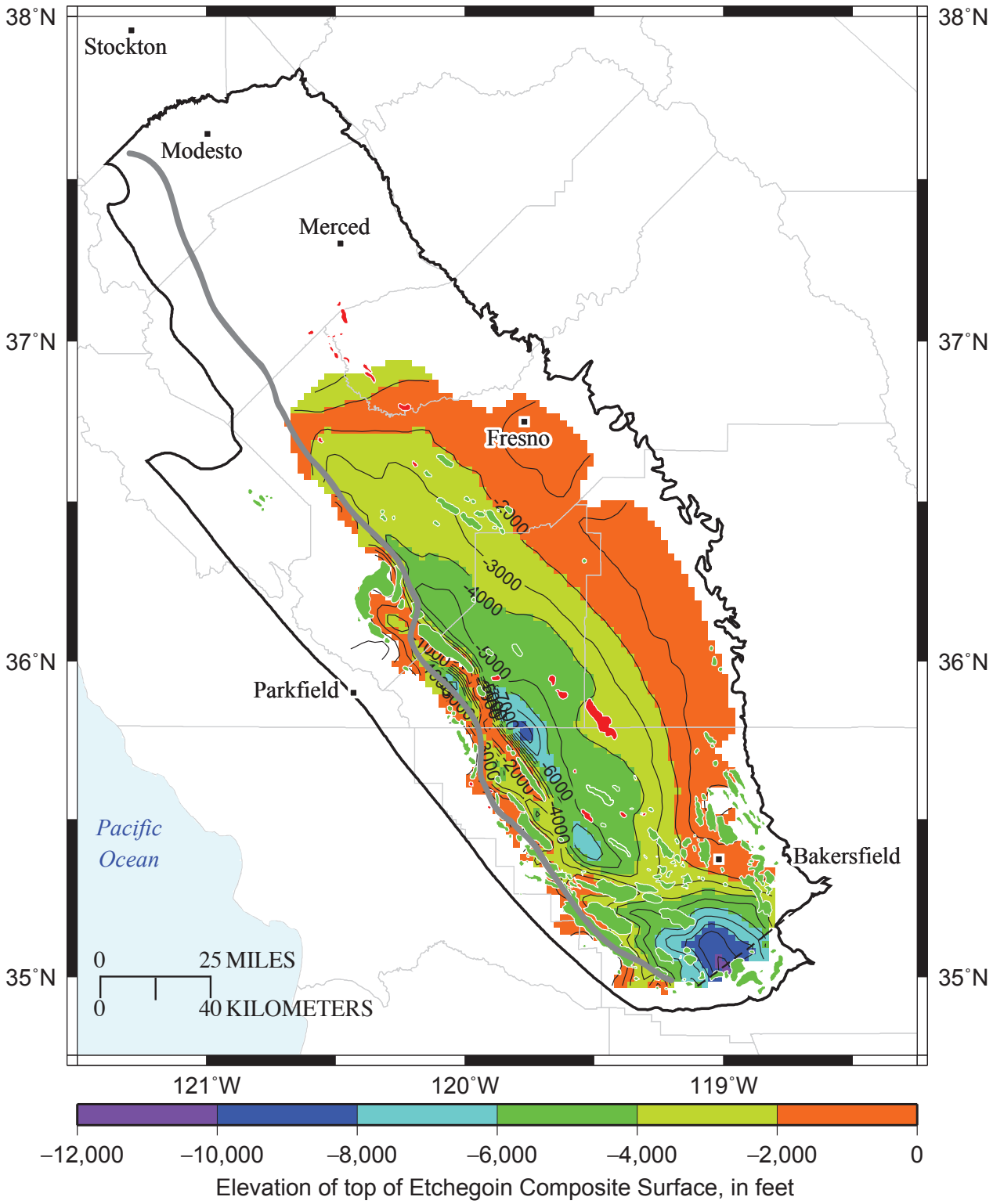

Figure 7.19.—Continued

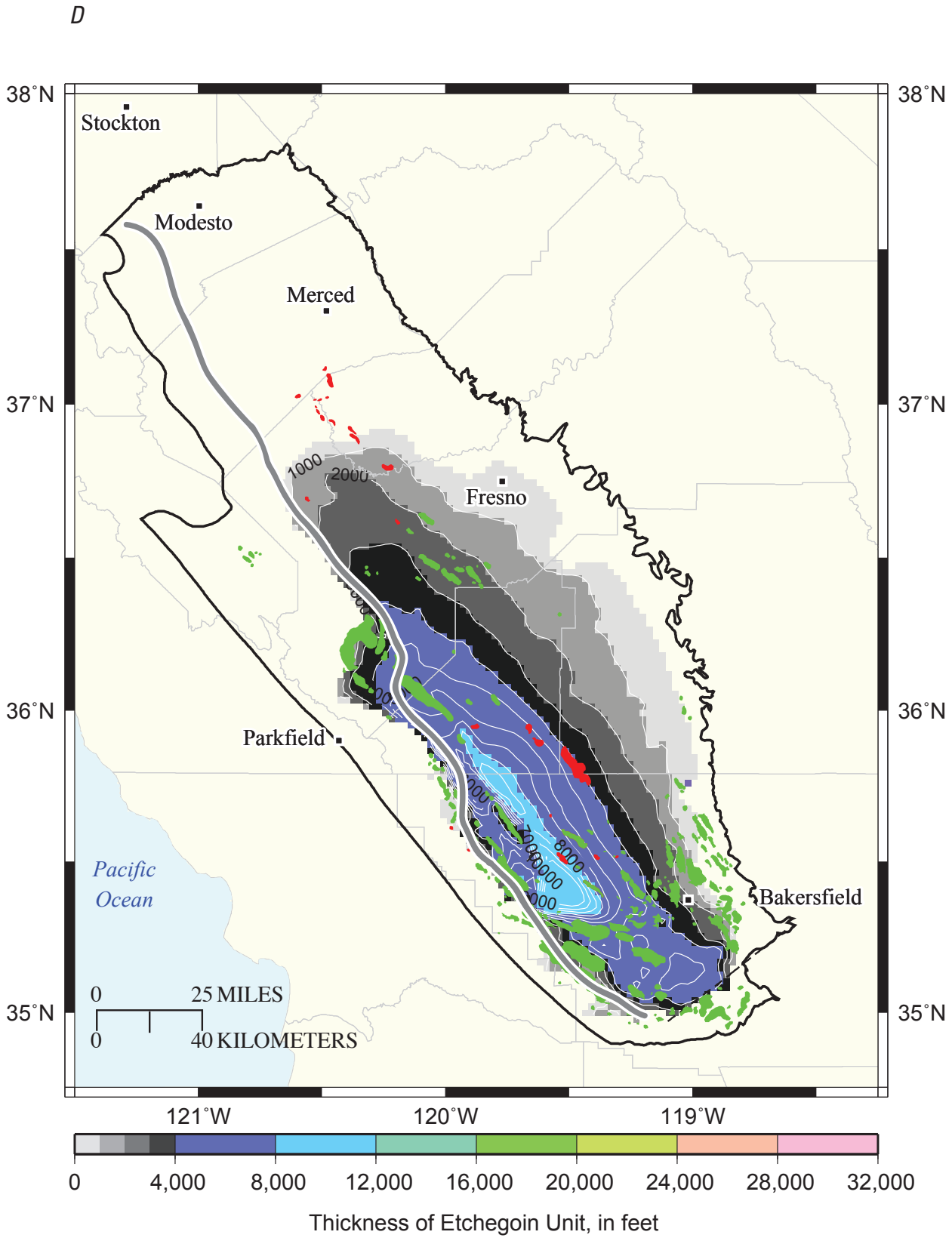

Figure 7.19.—Continued

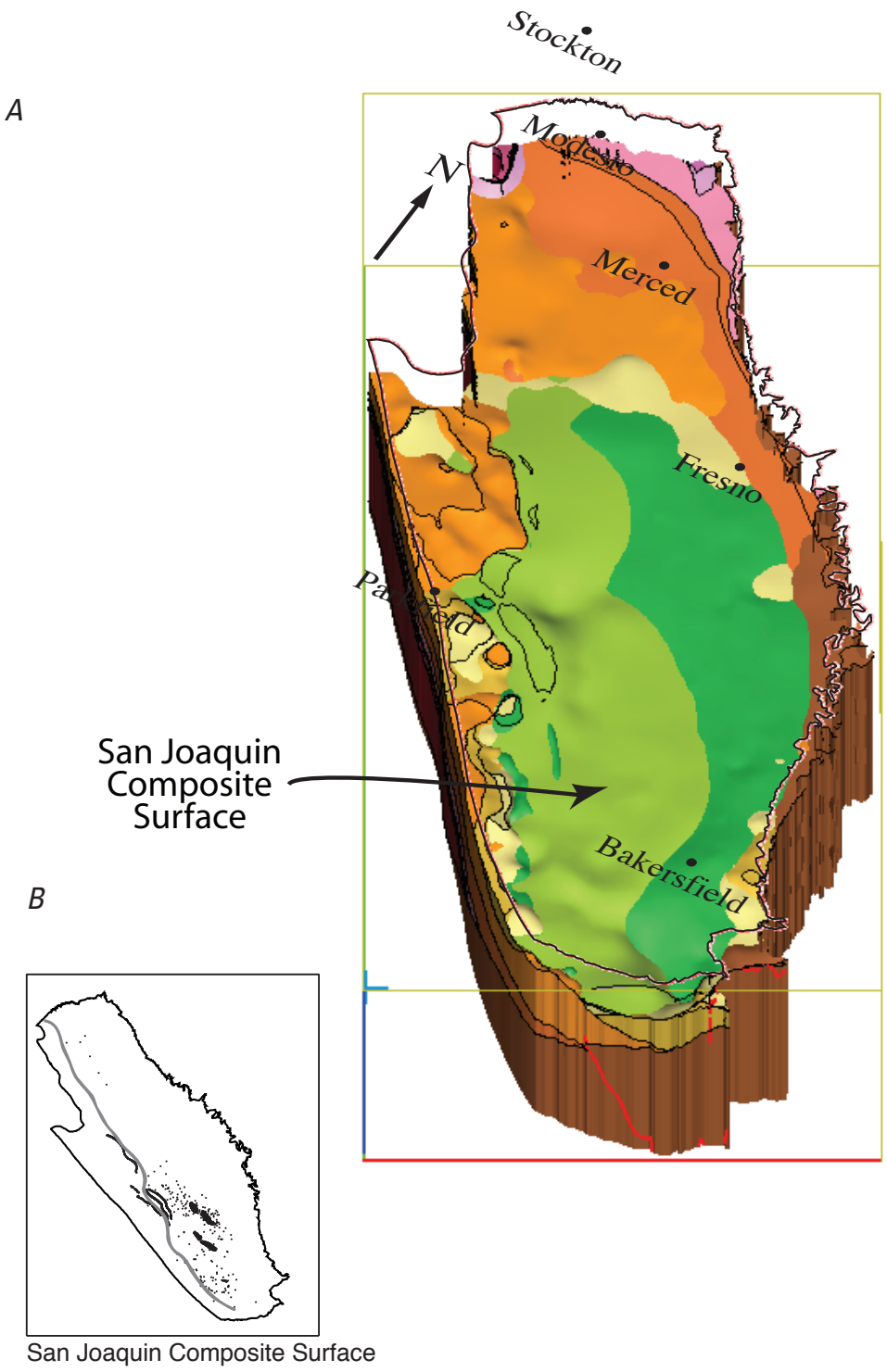

Figure 7.20. *A*, Oblique view of the San Joaquin Composite Surface. View is from 30° east of south (that is, aligned with the basin axis) at a 50° inclination angle. Grid resolution is 1 mile. *B*, Geographic distribution of observations; these can be viewed page-size in Hosford Scheirer and Magoon (this volume, chapter 5). In panels *B, C* and *D,* heavy black line marks the province boundary and heavy gray line divides the area of correspondence (east) from the area of unresolved complexity (west). *C*, Structure contour map of the elevation of the San Joaquin Composite Surface. Contour interval is 1,000 feet. In panels *C* and *D*, thin gray lines mark county boundaries. *D*, Thickness of the unit bounded by the San Joaquin Composite Surface (top) and the Etchegoin Composite Surface (base).

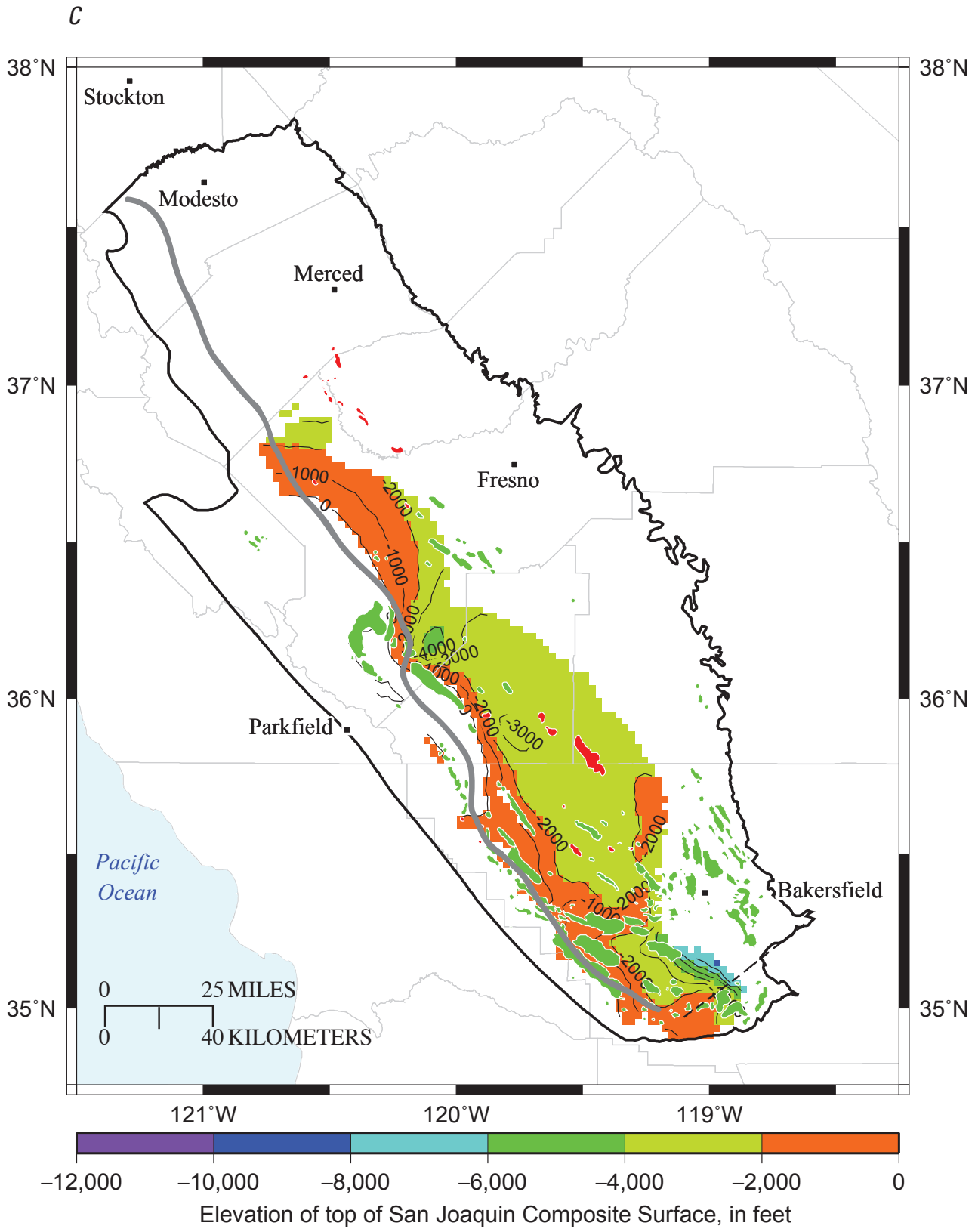

Figure 7.20.—Continued

D

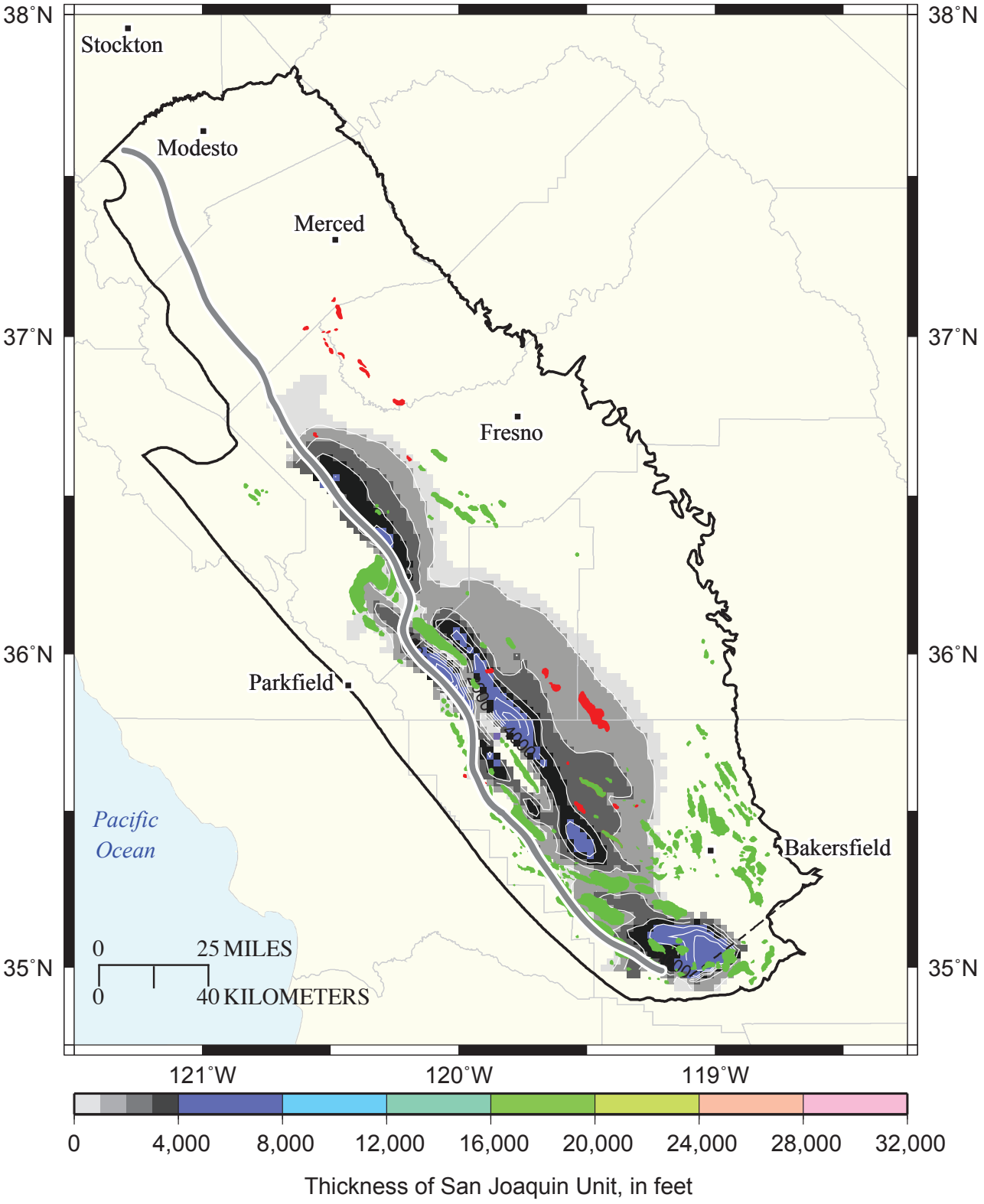

Figure 7.20.—Continued

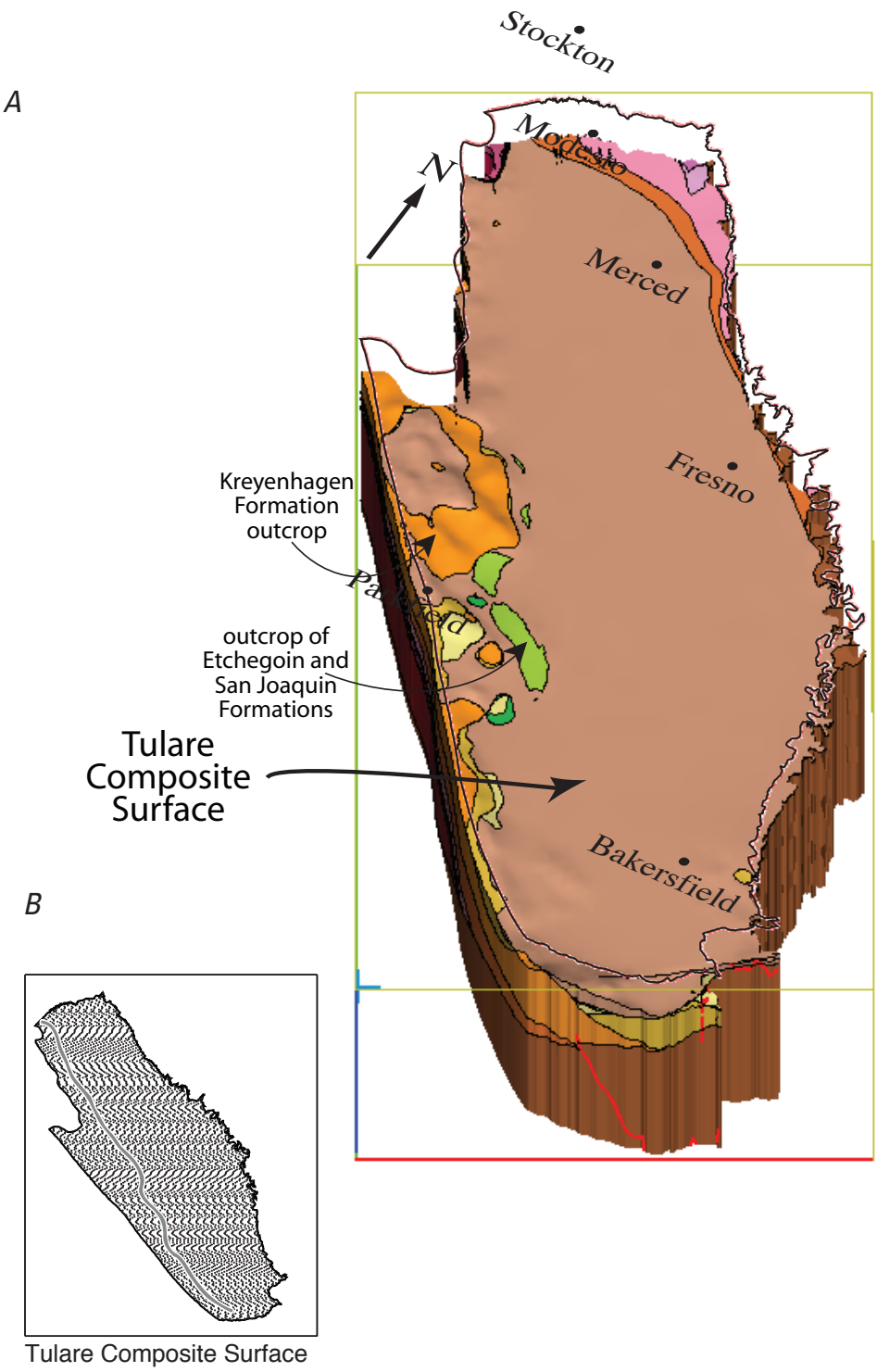

Figure 7.21. *A*, Oblique view of the elevation of the Tulare Composite Surface, which is equivalent to the topographic surface. View is from 30° east of south (that is, aligned with the basin axis) at a 50° inclination angle. Grid resolution is 0.5 mile. *B*, Geographic distribution of observations; dark stippling indicates dense topography grid. In panels *B, C*, and *D*, heavy black line marks the province boundary and heavy gray line divides the area of correspondence (east) from the area of unresolved complexity (west). *C*, Structure contour map of the elevation of the Tulare Composite Surface. Contour interval is 500 feet. In panels *C* and *D,* thin gray lines mark county boundaries. *D*, Thickness of the unit bounded by the topographic surface and the San Joaquin Composite Surface (base).

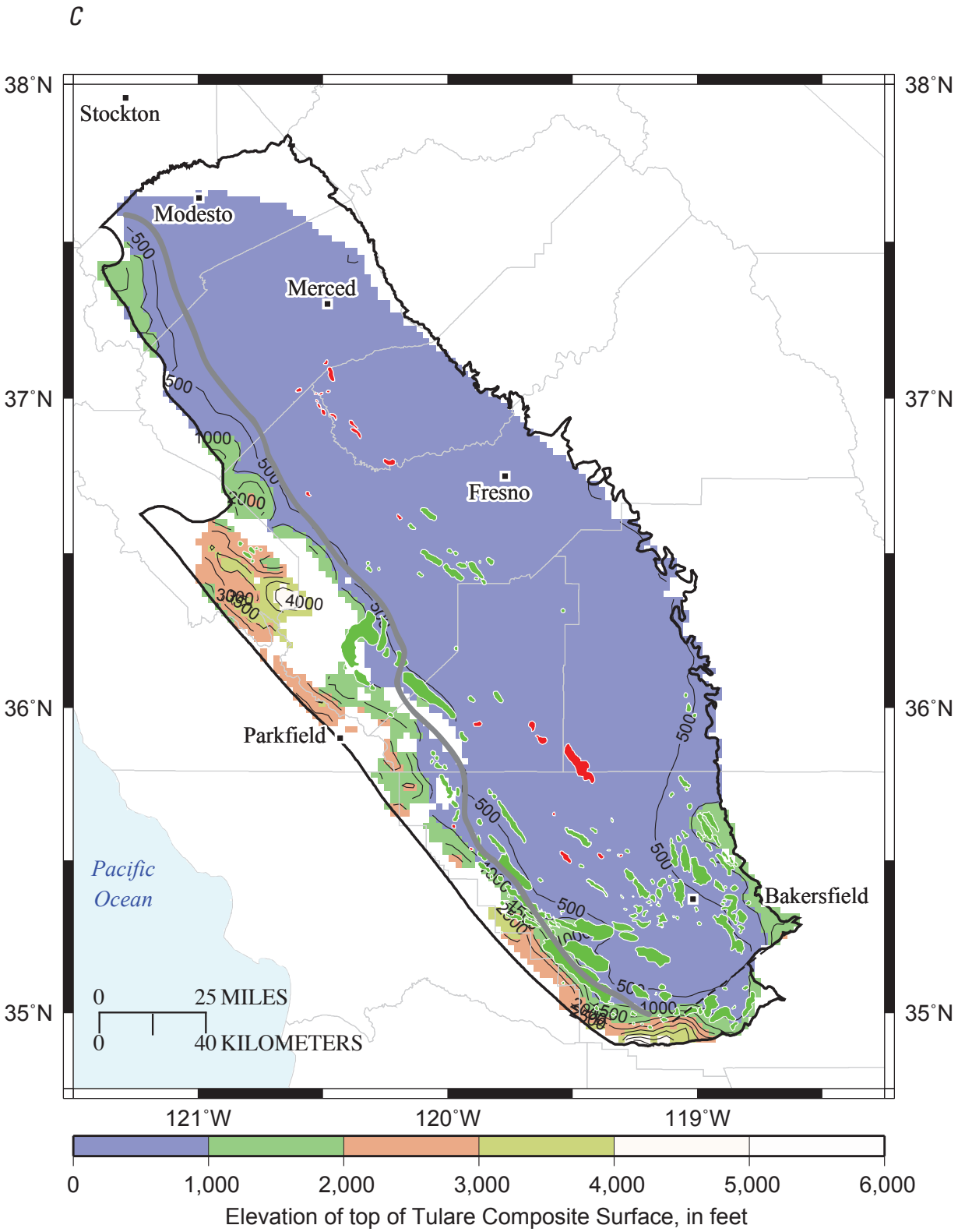

Figure 7.21.—Continued

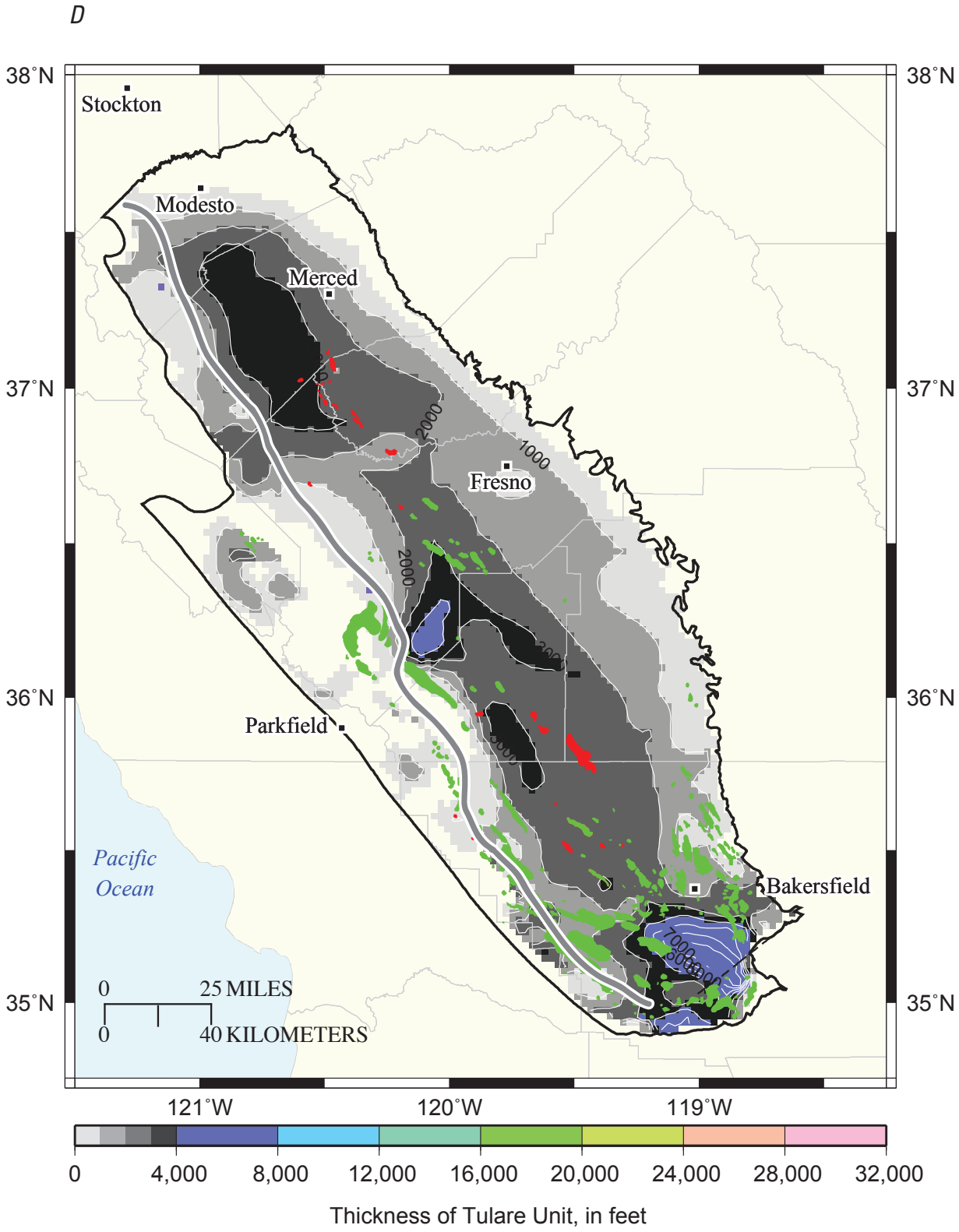

Figure 7.21.—Continued

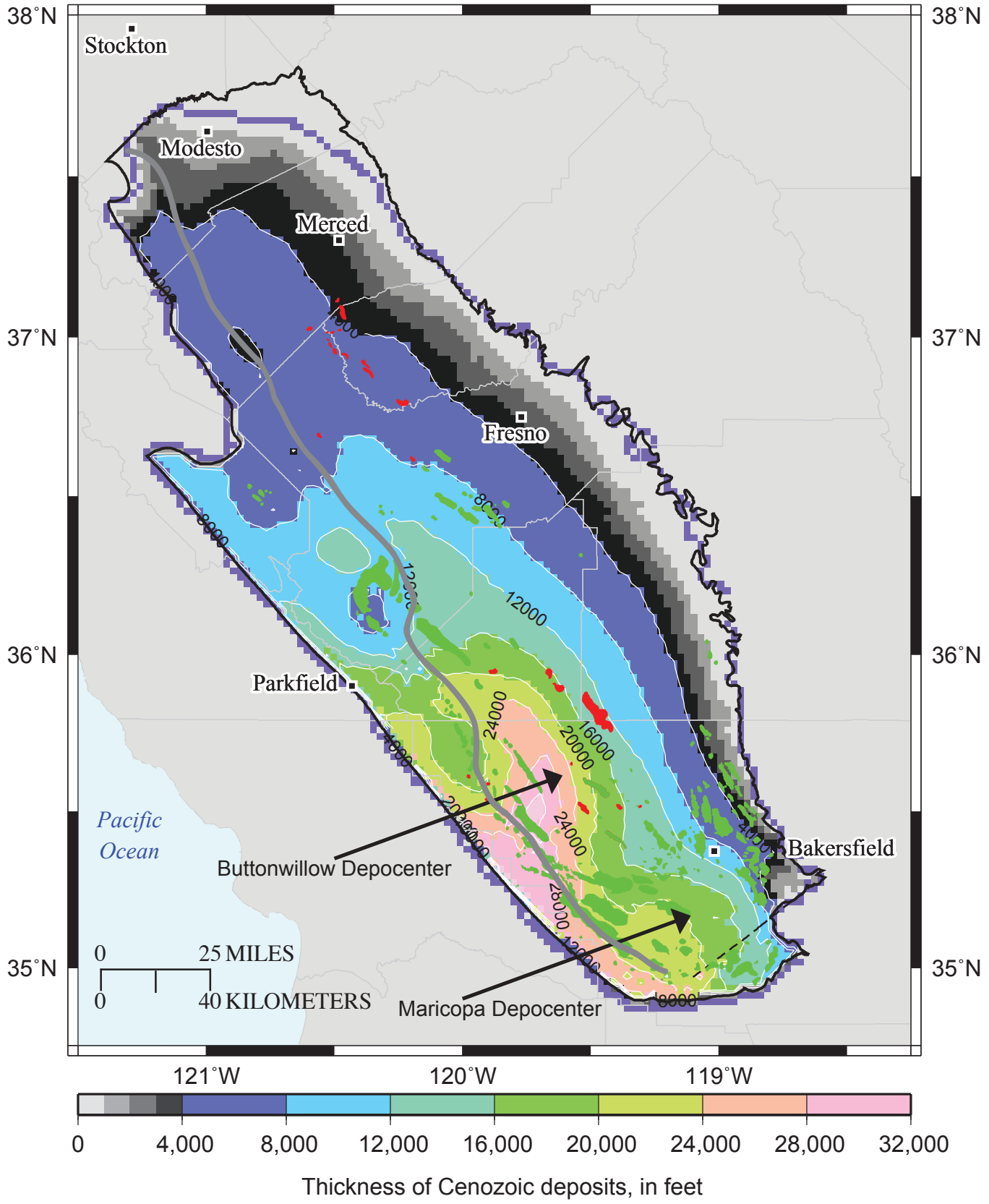

Figure 7.22. Thickness of Cenozoic and younger rocks, calculated by summing the thicknesses of all model layers above the Cretaceous section. Heavy black line marks the province boundary and heavy gray line divides the area of correspondence (east) from the area of unresolved complexity (west). Thin gray lines mark county boundaries.

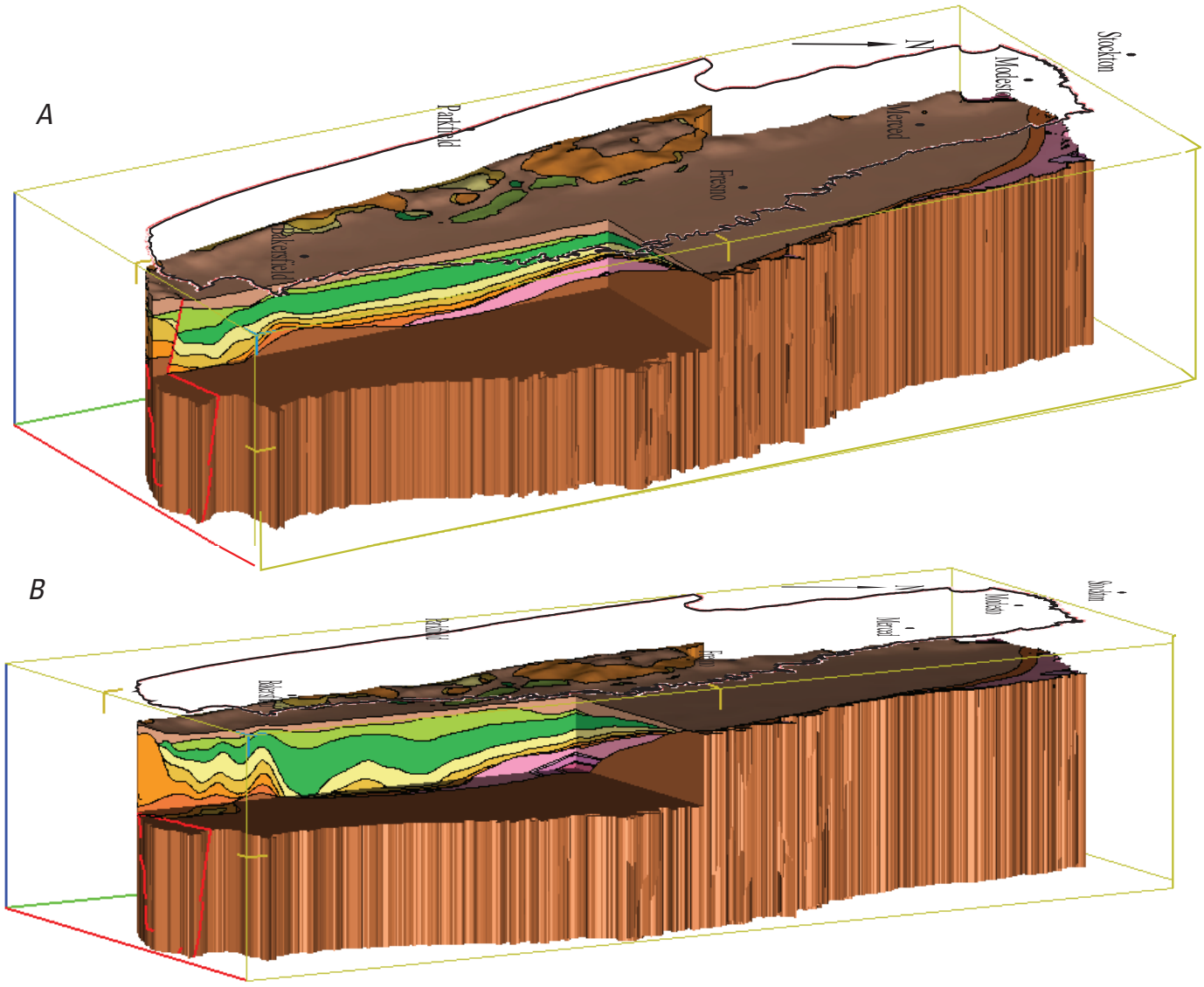

Figure 7.23. *A*, Oblique view of the San Joaquin Basin geologic model emphasizing the Maricopa depocenter and Bakersfield Arch. View is from due east at a 20° inclination angle. *B*, Three-dimensional view of the San Joaquin Basin emphasizing the Buttonwillow depocenter and west side fold belt. View is from due east at a 10° inclination angle.